UNIVERSITÀ DI PARMA

UNIVERSITA' DEGLI STUDI DI PARMA

DOTTORATO DI RICERCA IN

"Scienza e Tecnologia dei Materiali"

CICLO XXXVI

The Bioristor:
a novel in vivo sensor for plant phenotyping and variety selection

Coordinatore:

Chiar.mo Prof. Enrico Dalcanale

Tutore:

Dr. Andrea Zappettini

Dr. Michela Janni

Dottorando: Edoardo Marchetti

Anni Accademici 2020/2021 – 2022/2023

"*It is not the quantity of water applied to a crop, it is the quantity of intelligence applied which determines the result - there is more due to intelligence than water in every case.*"

Alfred Deakin (2nd Prime Minister of Australia)
in 1890 quoted during a speech to a conference of 'Irrigationists'

Abstract

Extreme weather events, water scarcity and excessive heat threaten agriculture management and food security. In the face of these challenges, the need for adaptive crops is urgent but it is slowed by traditional breeding programs, which are a major drag on the progress because of their cost and time required. In this work we demonstrate that the use of the OECT-based sensor called bioristor can accelerate the selection of improved genetic material for drought and heat stress resilience. To do so, the response of plants exposed to stress was monitored with the bioristor, allowing for the classification and identification of different responses belonging to different genotypes, in terms of tolerance and resilience to the stress. This demonstrated the feasibility to apply the bioristor in pre-breeding programs and its crucial role in deepening the knowledge on the dynamic of the response to drought and heat. Then, bioristor was integrated in a High-Throughput Phenotyping platform and its contribution validated in monitoring in real time, in vivo and in continuous plant growth and responses to drought. The exploitation of bioristor in frame of a climate smart agriculture approach in plant monitoring and water management automation in developing countries adds value to the ongoing research.

Summary

Abbreviation list

Analog-to-Digital Converter	**ADC**
Basal Sensor	**BS**
Crop Water Stress Index	**CSWI**
Control Unit	**CU**
Days After Stress	**DAS**
DodecylBenzeneSulfonic Acid	**DBSA**
3,4-EthyleneDiOxyThiophene	**EDOT**
Ethylene Glycol	**EG**
Electrolyte-Gated Field Effect Transistor	**EGOFET**
Electrolyte Gated Transistors	**EGT**
Electrical Impedance Spectroscopy	**EIS**
European Strategy Forum on Research Infrastructures	**ESFRI**
Greener Area	**GGA**
GreenHouse Gas	**GHG**
Geographic Information System	**GIS**
Global Navigation Satellite System	**GNSS**
Genomic Selection	**GS**
Genome-Wide Association Studies	**GWAS**
High-Throughput Phenotyping Platform	**HTPP**
Intrinsically Conductive Polymer	**ICP**
Introgression Line	**IL**
Internet of Things	**IoT**
Leaf Area Index	**LAI**
Marked Assisted Selection	**MAS**
Normalized Difference Vegetation Index	**NDVI**
Near InfraRed	**NIR**
Nuclear Magnetic Resonance	**NMR**
Normalized Response	**NR**
Organic Electro-Chemical Transistor	**OECT**
Organic Electronic Ion Pump	**OEIP**
Organic Field Effect Transistor	**OFET**
Precision Agriculture	**PA**
PolyANIline	**PANI**
Principal Components Analysis	**PCA**
Printed Circuit Board	**PCB**
Poly(3,4-EthyleneDiOxyThiophene) PolyStyrene Sulfonate	**PEDOT:PSS**
Precision Livestock Farming	**PLF**
PolyParaPhenylene	**PPP**
PolyParafenilenSulfide	**PPS**
PolyParaphenylene Vinylene	**PPV**
PolyPyrrole	**PPy**
PolyStyrene Sulfonate	**PSS**
PolyeThylene	**PT**
Quantitative Trait Locus	**QTL**
Response	**R**
Radio Frequency IDentification	**RFID**
Red Green Blue	**RGB**
Reactive Oxygen Species	**ROS**
Remote Sensing	**RS**
Relative Soil Water Content	**RSWC**
Single Nucleotide Polymorphism	**SNP**
Unmanned Aerial System	**UAS**
Unmanned Aerial Vehicles	**UAV**
Vapor Pressure Deficit	**VPD**
Variable Rate Application	**VRA**
Water Use Efficiency	**WUE**

1. Motivation and outlines

The discovery of agriculture, likely happened in the Fertile Crescent around 12000 years ago, represented one of the first consistent evolutions of the human species as, thanks to it, humanity changed its lifestyle, progressively leaving the hunting-gathering and embracing a more sedentary life (Rindos 2013); this change shaped the evolution of human culture, as people enlarged their community and developed languages, religions, arts, and sciences, and formed social hierarchies, laws, and institutions. Moreover, it implied a deep change in the human digesting apparatus as well as in body posture and in the progressive evolution of hands (Gowdy 2020). Over the centuries, as a result of population growth, agriculture has seen incessant improvements, from the development of the first irrigation systems to the domestication of animals and plants, from the use of fertilizers to the discovery of genetics and biotechnology; as a result, human dependence on it for food has also increased.

Nowadays, FAO estimates that about half of the population directly or indirectly depends on agriculture for their food supply, hence climate change, which is strongly impacting agriculture and therefore human beings' basic nutritional requirements, is considered a dangerous threat to human life on this planet. Nevertheless, as the rate of human population growth has soared, anthropogenic-related CO_2 emissions have also massively increased, in order to satisfy the higher need for food. In this sense, humanity is fueling a chain mechanism capable of rapidly bringing climate and human society to collapse.

Hence, a higher attention to the environment, in maximizing input use efficiency and preventing the simultaneous greenhouse gasses emission increase, will also be crucial. To this end, possible solutions can be the adoption of better agronomic practices, through the introduction of precision agriculture, or the improvement of breeding strategies, to accelerate the selection of more tolerant varieties.

Within this panorama, IMEM-CNR developed a new sensor named bioristor to enable real-time and in vivo monitoring. The sensor is based on the PEDOT:PSS organic semiconductor and its main strengths are the biocompatibility, which enables long-term operations, and the capability to lead in vivo and real-time monitoring.

The aim of this study is to address the need of identifying novel sources of drought tolerance through the use of innovative technologies and, in particular of bioristor, by accelerating the phenotypic selection.

Overall, this thesis deals with the use of the novel biosensor for plant phenotyping, both as novel tools for precisely selecting improved genetic material. To investigate this potential, genetic material ranging from

commercial varieties to introgression lines were analyzed with bioristor and classified according to their dynamic response to drought, drawing some conclusions on their potential tolerance or susceptibility.

Then, a case study combining both applications was carried out, taking advantage of the research project Maison Parma. This is an international cooperation project in view of a climate smart agriculture approach. The idea was to first test and select varieties with increased tolerance to adverse climate conditions suitable for the cultivation in Burundi, and then to apply the sensor as a tool for precision climate smart agriculture through the real time open field monitoring of tomato cultivation performed in 2023 the same place.

Finally, to fulfil the goal of developing a tool for in-vivo phenotyping, during this thesis the integration of the bioristor in a real phenotyping platform, thanks to the collaboration with ALSIA Metapontum Agrobios, was positively experimented.

Both approaches were successful in demonstrating the efficacy of bioristor in plant phenotyping and as a tool for plant monitoring in the field.

The thesis is organized as follow:

- Chapter 1 reports the work outlines and motivation.
- Chapter 2 provides an overall description of the state of the art on climate change, plant phenotyping, precision agriculture and plant sensors.
- Results are organized in 4 sections (Chapters 3, 4, 5 and 6, Fig. 1), structured with the aim of validating the use of the bioristor as an innovative tool for plant phenotyping.
- Chapters 3 and 4 report two experiments focused on commercial varieties during which bioristor was used to monitor the different responses of the varieties exposed to drought stress. The bioristor indices were compared with physiological based indices and the correlation between bioristor and the plant's physiological state analyzed. These indices were used to classify the different varieties in terms of tolerance to stress.
- Chapter 4 is dedicated to the application of bioristor in a case study in frame of an international cooperation project (Maison Parma). Here, bioristor serves as a selection tool for plant varieties. In a second instance, bioristor was used in open field in adverse environmental conditions as the Burundi environment.
- The purpose of Chapter 5, is the exploitation of bioristor to select complex tomato genomes as the tomato Introgression Lines (ILs), to demonstrate the ability of the sensor in detecting tolerant

genotypes. This part of the experiment was performed in the facility of Prof. Vicent Arbona in the Castellón de la Plana Universitat Jaume I.

- The last section (Chapter 6) is dedicated to the implementation of bioristor in a phenotyping platform; to this end, the chapter described the development of a control unit dedicated to the Phenotyping platform held by ALSIA Metaponto Agrobios.
- Overall conclusions in Chapter 7 shed light on the novel use of bioristor in plant monitoring and phenotyping applications.
- Chapters 8 and 9 show products of the research and bibliography, respectively.

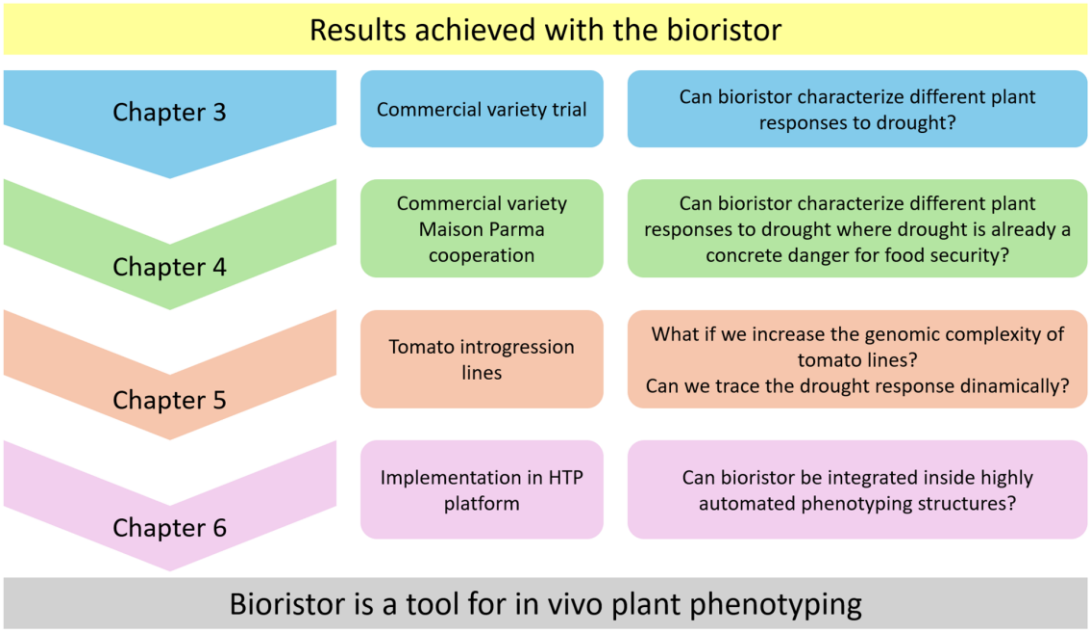

Fig. 1 - Scheme of the results of the thesis.

2. Introduction

2.1 Climate change, water shortage and drought events: being prepared for emerging threats

Climate change severely affects food security and agronomic practices due to the increasing severe weather events. (FAO 2022a), as a consequence, food safety emerges as a paramount and highly sensitive issue on a global scale facing continuous disruption (Yadav et al. 2021). Scientists express concern that the speed at which climate change events are occurring may leave some living things with no chance to adapt (Kemp et al. 2022). What if humanity is on that list?

The definition given for Climate change by scientists is a - *significant divergence in the average values of meteorological elements, as precipitation and temperature, for which data have been computed over a long period (Abbass et al. 2022)* -. This divergence is mainly reflected in the increased probability of extreme weather events.

Earth's history is populated by many of these events, such as ice ages, the last of which occurred during the Quaternary (Gamache et al. 2015); however, changes taking place at similar speed have never been reported before. Indeed, CO_2 levels as well as temperature are increasing vertiginously, with a speed ratio over 1:1000 compared with the last glaciation, see Fig. 2 (Nelson 2021).

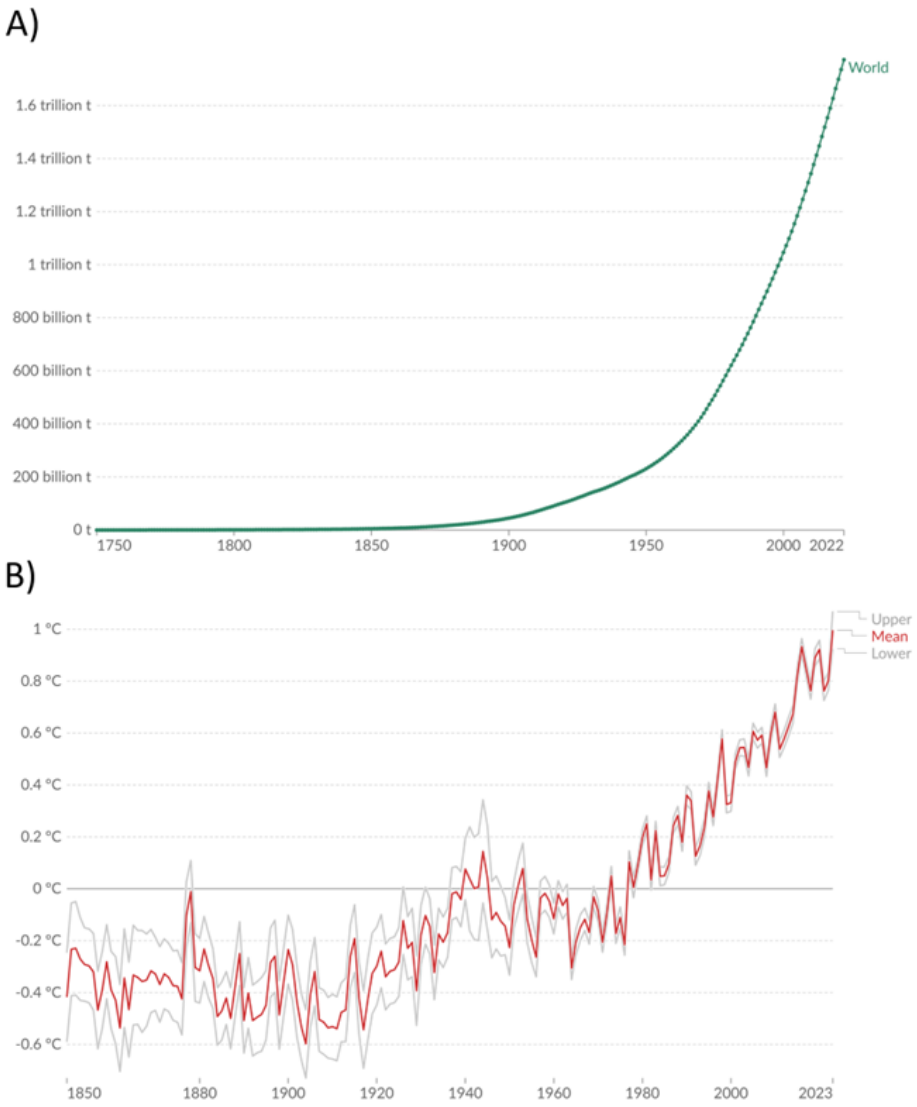

Fig. 2 - Evolution of two climate change indices: CO_2 and temperature (Morice 2021; GCB 2023). A) Total cumulative emissions of carbon dioxide, since the first year of available data, measured in tonnes. B) Global average land-sea temperature anomaly relative to the 1961-1990 average temperature.

Although there are multiple competing factors in the evolution of climate change, some of them natural such as changes in solar and volcanic activity as well as ocean circulation (Knutti and Rugenstein 2015; Holme and Rocha 2023), the major causes of this worldwide occurrence have to be identified in human activity as, since the beginning of the industrial era, anthropogenic activities on Earth have introduced a massive amount of gasses into the atmosphere (Stern and Kaufmann 2014). These include compounds such as carbon dioxide, methane and nitrous oxide, which are able to absorb infrared radiation naturally emitted from the planet's surface, preventing it from being scattered and emphasizing the so-called 'Greenhouse effect'. The accumulation of solar energy that is no longer allowed to disperse in the form

of infrared radiation, in turn, is responsible for the temperature increase and the triggering of extreme weather events (Bolin and Doos 1989).

Climate change generates considerable uncertainty about human life's future on planet Earth since, by affecting precipitation, runoff and snow/ice melt, with outcomes on hydrological systems, water quality and water temperature, as well as on groundwater recharge, it jeopardizes fresh water availability (some of these effects are summarized in figure 3). In many regions of the world, this issue will present a major challenge for climate adaptation, and will be aggravated by sea-level rise that will affect the salinity of surface and groundwater in coastal areas (FAO 2015).

Fig. 3 - Effects of climate change (NOAA 2021): among them, glacial ice melting, extreme thunders, excessive heat, whose consequences are fires and flooding as well as drought.

Considering agriculture's need for water, it is easy to see that the effects of climate change on water availability are immediately mirrored in this sector. To better distinguish and study them, a classification was proposed (Raza et al. 2019). Depending on their mechanism of action, three groups can be recognized, these are:

- Direct effects
- Indirect effects
- Socio-economics effects

Direct effects strongly impact on plants' morphological, physiological or phenotypic characteristics and yield. Indirect effects refer to the impact on the environment and in particular about soil fertility, irrigation availability, rise in sea level, pest aggressivity, and the well-known heat, flood and drought. Whether socio-economic effects are other consequences to be considered since they have negative impacts on global food security and safety, and they consist of food demand increase, farmer's response, cost, policy, trade and unequal distribution.

Another example of direct effect is the loss of biodiversity, which is specifically caused by the deep variation in precipitation and temperature (FAO 2022a, pp. 2022–2031; Habibullah et al. 2022). The latter not only impacts ecosystems' stability but in turn endangers crop breeding by eliminating possibly attractive genetic resources, and thus greatly reduces the effectiveness of this method in combating climate change itself (Prakash 2021). The International Union for Conservation of Nature (IUCN) is thoroughly studying the risks associated with it, and created the famous 'Red List' (IUCN 2023). The Red List tracks all the animal, fungus and plant species under extinction risk and, since its establishment in 1964, it represented an important starting point in the evolution of conservation plans as well as on their efficacy (Betts et al. 2020). Moreover, the list serves as a 'Barometer of Life', offering a continuous measurement of the pressures affecting species and providing insight into the overall health status of life on this planet (IUCN 2021).

Being agriculture the sector with the highest water needs among all industries, using approximately 70% of the available freshwater of the planet for irrigation (FAO 2022a, pp. 2022–2031; Vurro et al. 2023a; Kohli et al.), the most severe indirect effect of climate change is drought. To understand the impact of climate change in agriculture it must be considered that 12 million hectares are lost each year due to drought and desertification (23 hectares/minute), where 20 million tons of grain could have been grown (Azadi et al. 2018). In terms of water consumption, crops require different amounts of water for irrigation. The volume depends on the environment in which plants are grown and on their genome. In fact, tolerance and resilience to stress, as well as higher water use efficiency (WUE) can sensibly vary plants' water needs and productivity (Ozeki et al. 2022). See figure 4 for a comparison of water needs between some of the main crops.

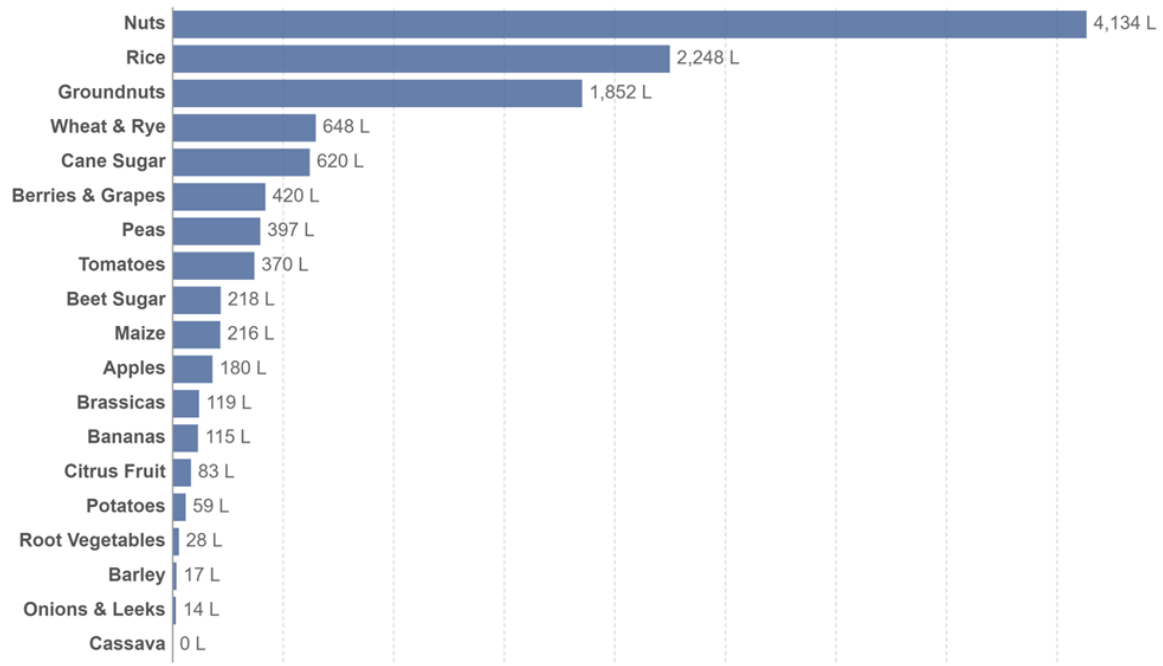

Fig. 4 - Freshwater withdrawals per kilogram of food product (Ritchie and Roser 2017): comparison between crops.

To understand how climate change can simultaneously exert its influence on many aspects related to the agricultural sector, including socio-economic, consider that coffee cultivation in Mexico, whose net revenue is drastically reducing, is forecasted to become unaffordable in the upcoming years (Gay et al. 2006).

Joint initiatives of several world states are in progress to globally reduce the effects of climate change. An example is the Paris Agreement (UNFCCC), for limiting the global temperature rise to well below 2 degrees Celsius, even though the continuous increases of greenhouse gas emission (GHG) are preventing most of the countries from reaching this goal.

Other important agreements are the famous Kyoto Protocol, adopted in 1997 (UNFCCC) and the COP28 Climate Change Conference, that took place in Dubai 2023 (UNFCCC). Overall, the objectives pursued are to address climate change by setting legally binding emission reduction targets for developed countries and establishing mechanisms to promote international cooperation in reducing greenhouse gas emissions, keeping the global warming limitation below 1.5 degrees Celsius, compared to pre-industrial levels, as a central goal.

The most recent one involved nearly 200 countries and focused on 4 paradigms shift: fast-tracking the energy transition and slashing emissions before 2030, transforming climate finance, by delivering on old

promises and setting the framework for a new deal on finance, putting nature, people, lives, and livelihoods at the heart of climate action and mobilizing to make next COPs more inclusive (UNFCCC).

Considering the ongoing increases in world population, new agriculture practices and new technologies will be needed soon to ensure food security, therefore the science community has a very important role.

2.2 Strategies to cope with climate change effects: drought stress, variety selection, improving growth techniques

Several strategies are adopted in agriculture to cope with drought stress, among them two main groups can be recognized; the first one regards the use of improved agronomic management, e.g, through the adoption of smart and digital agriculture, whereas the second one implies the selection and identification of novel genetic material, more adaptable to the ongoing climate change (Venkateswarlu and Shanker 2009).

Regarding the first, many approaches and new agronomic practices, including soil tillage, intercropping, increase the efficiency of nutrient management, and improve the efficiency of irrigation, have been suggested (Tyagi et al. 2020). Improvements in inputs use efficiency, in particular water use efficiency, has always been a major objective in agriculture, given the great impact on the environment. The application of fertilizer as well represents a major topic, since it is directly correlated with the increase of water use efficiency, as it determines greater yield in comparison with that of evapotranspiration (Sharma et al. 2015). However, the cost of these resources and the deriving need of maximizing their efficacy by providing fertilizer and water, where and when needed, led to the spread of the precision farming paradigm, a subject that will be discussed in the next section (Cammarano et al. 2023).

On the other hand, as previously cited, the identification of more adaptable crop varieties to address the needs of increased food production while improving food sustainability, represents another valid approach for climate change effect mitigation. In this scenario plant phenotyping is mandatory to achieve the characterization of novel genetic material; however, despite the big advances in other related fields like genomics, that lead to a faster production of novel material, phenotyping is still a bottleneck in the characterization of novel genetic material due to the limited number of phenotyping installation available, both in controlled conditions as well as in open fields (Song et al. 2021), and because it still relies on time-consuming and labor-intensive techniques, mainly performed by hand and heavily influenced by subjectivity. The discussion on the strategies to cope with climate change effects will be opened debating the newest agronomical practices first and plant breeding later.

2.2.1 Sensing technologies and precision agriculture

The Precision agriculture idea, also known as Site-Specific input Application, arose from the observation of inter and intra-field variability, consisting of soil texture, slope value, vegetation cover, etc., and is based on the integration of information and actuation technologies in a parcel's management (Meena et al. 2019).

The International Society of Precision Agriculture (PA) defined it as a *field management strategy that gathers, processes and analyzes temporal, spatial and individual data and combines it with other information to support management decisions accordingly to estimated variability for improved resource use efficiency, productivity, quality, profitability and sustainability of agricultural production* (Cammarano et al. 2023).

It is therefore evident that recognition and discrimination of parcels of different characteristics is crucial, for this reason, key factor in the emergence of precision agriculture has been GPS technology that, together with Geographic Information System (GIS) and Remote Sensing, help farmers to locate the exact position of field information, such as soil type, weed invasion, pest occurrence, boundaries, water leakages and obstructions, and to couple real-time data collection with accurate position (Meena et al. 2019): this process, that is the creation of maps using location-based data, is called Geo-mapping. Remote sensing and GIS will be further described in the next chapters.

In the last decade, the agriculture's challenge of improving agri-food products' quality and quantity while respecting human health and the environment (Coulibaly et al. 2022), which is achievable through the reduction of input employment obtained by maximizing their use efficiency, is the lever that has opened the debate on the crops' health status among scientists. Proximal sensors, e.g., enabling soil humidity, air temperature, and air humidity monitoring, as well as remote sensors, like figure sensors integrated on drones and satellites, are some of the results of these studies (Dobriyal et al. 2012; Aqeel-ur-Rehman et al. 2014; Krishna 2017; Bansod et al. 2017). In figure 5 are depicted the most commonly used technologies.

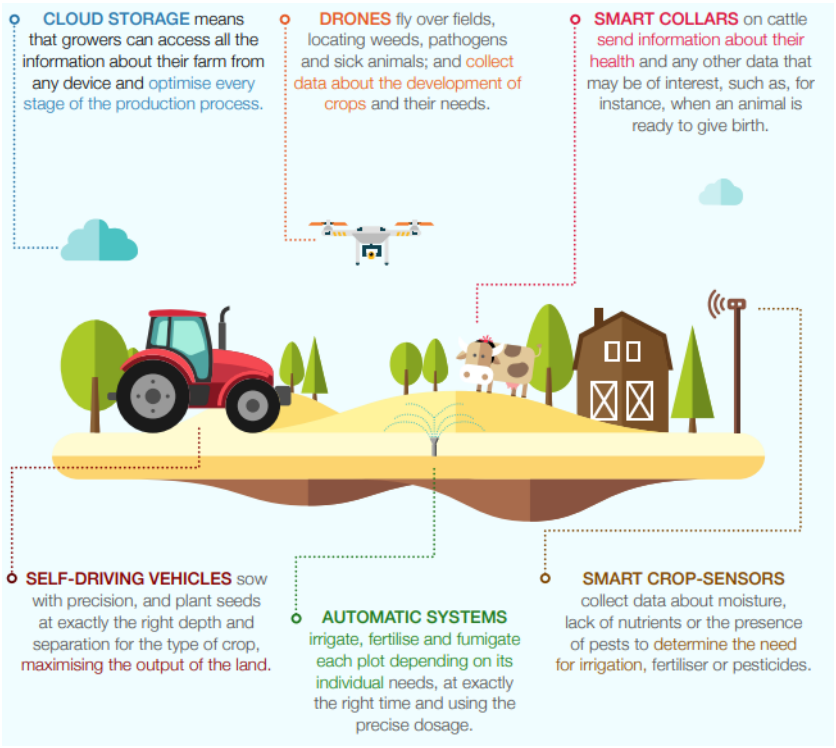

Fig. 5 - Overview of the main precision farming technologies: among them are recognizable cloud storage, drones, animal and plant sensors, together with the actuators like automatic irrigation systems and autonomous vehicles (Iberdrola 2024)

Sensing technologies play a crucial role in precision agriculture, upscaling the amount of information available as well as the precision and efficacy of the consequent decisions taken. The most used techniques are remote sensors, based on the use of satellite, airborne or unmanned aerial vehicles (UAV), platforms using multi- or hyperspectral imagery (Ranghetti et al. 2020), and proximal sensors, that are close to the object and usually installed on platforms ranging from handheld, fixed installations, or robotics and tractor-embedded sensors (Alexopoulos et al. 2023). Overall, the types of sensors involved include RGB or gray-level-cameras to multispectral and hyperspectral high-resolution imaging systems or even thermographic cameras. Associated with plant growth conditions and used for many phenotyping techniques, remote and proximal sensing enable the acquisition of information on nutrient deficiency, biotic stress, such as pests and diseases, as well as on abiotic stresses.

The main result in the processing of this information is the calculation of a Variable Rate Application (or VRA), a concept that refers to the variable distribution of the input in the field following the necessity of each field unit. Depending on how the application rate is modulated, two types of VRAs can be distinguished: a map-based VRA and a sensor-based VRA. In the former, the rate is adjusted on the basis of an electronic map; in the latter, no map is needed and the rate is calculated on the basis of data collected

by sensors (Grisso et al. 2011). The implementation of VRA has required the development of new tools, which in some cases resulted from the integration of advanced electronics into previous generation machines (Singh et al. 2023). One example is the Automated Steering System that enables self-driving machines, allowing to increase work cycles; these vehicles are essentially tractors modified to replace direct human control with computer-controlled actuators (Lange and Peake 2020). However, the need to perform new tasks in some cases has led to the design of completely new machines; consequently, it is not surprising that the revolution brought by precision agriculture is accompanied by a strong acceleration in the field of robotics (Botta et al. 2022). In fact, the use of robots may not only be intended to enable automation and relieve humans from doing labor-intensive tasks, but also to speed up weeding, planting, crop monitoring, fertilization, pest control, harvesting, pruning and thinning, soil sampling and analysis, data collection and mapping (Mahmud et al. 2020; Danton et al. 2020; Zhang et al. 2020b; Beloev et al. 2021; Botta et al. 2022).

The precision agriculture concept was extended to animal farming too, resulting in the so-called 'Precision livestock farming' (PLF) (Aquilani et al. 2022): PA and PLF belong to the 'precision farming' macrogroup. Recently, with the rapid development of electronic devices and their reduction in price, a new concept, called smart agriculture, is rapidly spreading, which can be seen as an evolution of precision agriculture, involving the widespread implementation of electronics in many aspects of the sector. The topic will be extensively treated in an ad-hoc paragraph, after the in-depth agriculture sensors analysis.

2.2.2 Plant breeding and variety selection

As mentioned, the use of more adaptable to climate change novel genetic material is a valid strategy to mitigate its effects on agriculture and to reduce the overall input and energy required; the identification of these variants can be obtained both through the selection of useful traits in the reservoir of genetic variability and through the production of novel material.

Genetic reservoirs consist of a group of individuals bearing, on the whole, a big number of alleles and genetic variations and storing the overall genetic diversity of a population; their composition is the result of many centuries of mutation and natural selection cycles (Yolcu et al. 2020). Since the beginning of domestication, crop selection has used these sources of variability to identify variants best suited to human needs (Purugganan 2019). Despite all these years of exploitation have resulted in a constant depletion, genetic reservoirs still represent useful resources that may help mitigating climate change effects on agricultural production (Ceccarelli et al. 2010; Pignone and Hammer 2013; Pignone et al. 2015), especially because the negative impact of climate changes on agriculture, and therefore on food production and quality, is aggravated by the greater uniformity existing in the agricultural crops of

developed countries, whose production generally relies on few closely related and genetically uniform cultivated varieties (pure lines and hybrids) (Pignone et al. 2015).

These crops mainly originated from the selection among previously produced élite lines, since landraces are seldom utilized in breeding programs; this is due to both lack of genetic uniformity, which makes it harder to make the best use of their potential, and to the difficulty of analyzing a large number of genotypes, which can be more than ten per each single landrace (Raman et al. 2010). For these reasons, landraces and traditional varieties have received very little attention by researchers, especially after the introduction of molecular tools, which have amplified the resolution of genetic studies. On the other hand, this method implied and is implying a gradual reduction of their genetic base.

Developing a new variety is a time-consuming process, which can take up to 11 years, so it is crucial to make it as efficient as possible. Nowadays, many techniques have been developed for this purpose (Schaart et al. 2016), among them, ideotype breeding is probably the most common breeding strategy and consists in the definition of an ideotype, i.e. an *a priori* defined traits set, to which the breeder is trying to get closer during the selection (Ahn et al. 2023). The identification of the selection traits drives the entire process and establishes the success of the selection, therefore it is usually the result of a deep market research that takes into account what consumers' personal preferences will be in the next decade (Lenaerts et al. 2019). Key factor of ideotype breeding is the identification of genes, strongly related with the focusing traits to produce desirable and predictable changes in the traits (Ahn et al. 2023).

Molecular markers are commonly used to trace the heritage of genes under selection in breeding programs (Hasan et al. 2021). The implementation of molecular markers for selection purposes is called marked assisted selection, or MAS, and was proposed for the first time by Soller and Beckmann in 1983 and by C. Smith and P. Simpson in 1986 (Altman and Hasegawa 2012). Marker-assisted selection, as well as Genomic Selection (GS), are the most common approaches used to follow useful traits during breeding programs, which is crucial to precisely select the individuals to be used for the creation of the following generation during the selection process. Genomic Selection, in particular, can significantly accelerate genetic gain and reduce generation interval enabling early and accurate selection based on the evaluation of individual reproductive value, called breeding value, which in turn is an estimation of the individual merit for a particular trait (Cappetta et al. 2020). This approach has become feasible thanks to the availability of numerous molecular markers, whose abundance led to a consistent increase of the estimation accuracy and the selection (Goddard and Hayes 2007).

The past decade has seen rapid development in genetic testing techniques and in the size of cultivated populations; indeed, advances in genetic analysis techniques, such as high-throughput sequencing and molecular tools, have enabled the rapid decoding of the genomic information of crops (Varshney et al.

2021). Simultaneously, there has been a significant increase in the scale and diversity of crop populations, driven by the demand for improved agricultural productivity, conservation efforts to preserve genetic diversity, and the integration of crop databases (Ahmar et al. 2020). However, in this climate of innovation, phenotyping has emerged as the main bottleneck limiting crop selection (Reynolds et al. 2021). The principal limitations linked with it are: manual labor and time-consuming, subjectivity and human error, limited throughput and scale, environmental variability, complex traits and multifactorial interactions, trait measurement precision and accuracy, limited trait coverage and resolution, technological and infrastructure constraints (Fiorani and Schurr 2013; Li et al. 2014; Costa et al. 2019; Haworth et al. 2023).

Drones, in particular UAVs, represented a revolution in this field, opening new opportunities for plant selection and in particular for tomato field phenotyping (Fullana-Pericàs et al. 2022). The implementation of such machines, equipped with remote sensing instruments as RGB, multispectral and hyperspectral cameras, quickened plant scoring by some orders of magnitude. Some of the most commonly measured traits through this kind of analysis are fresh shoot mass, fruit numbers, yield mass at harvest, biomass, height, leaf area index (LAI) and chlorophyll (Johansen et al. 2020). Among the image-based data, the normalized difference vegetation index (NDVI) is one of the most informative; being correlated with canopy reflectance and therefore with leaf's pigment composition, it is an indicator of plant physiological status (Enciso et al. 2019). For these reasons, the use of UAVs for abiotic stress detection, like the heat and drought, is experiencing increasing success. Compared with traditional methods, unmanned aerial system (UAS) based phenotyping is non-destructive, time-saving, high-efficient, low-cost, scalable and has high resolution data acquisition (Xie and Yang 2020). Although studies in recent years have focused on the analysis of the aerial part of the plant, root apparatus is getting greater attention, given its role in water uptake, in the reaching of deep reservoirs, and so in drought avoidance (Ilyas et al. 2021). Therefore, phenotyping is undergoing a rapid evolution, which is bringing it to have a wider and more complete vision of plant's traits.

In addition, along with phenotyping, an 'omics' approach was proposed to study the molecular function and the gene impact on the phenotype (Chaudhary et al. 2019), giving the opportunity to explore plant genetics and to detect even single nucleotide polymorphisms (SNPs). This approach was employed in the research of genes responsible for stress tolerance, in association with the use of novel genetic material, such as the introgression lines (ILs) (Bolger et al. 2014). Another application consisted in the identification of molecular markers associated with similar genes or directly in the identification of the trait causative genes for breeding program assistance (Sonah et al. 2011); to do so, the quantitative trait loci (QTL) mapping and genome-wide association studies (GWAS) has been utilized. These technologies aim to discover the genetic variants responsible for the studied trait, but with a different precision level.

The first mentioned can push the investigation resolution up to the chromosomal region while the second one can even identify the gene or genes involved (Cano-Gamez and Trynka 2020; Powder 2020). In both cases the working principle is based on the correlation between a specific trait manifestation with the presence of a given allele (Burton et al. 2007).

2.2.3 Plant phenotyping and variety selection

The challenge to develop sustainable and resilient agroecosystems with increased productivity is a key objective for the upcoming decades (Janni and Pieruschka 2022). Integrated solutions and new technologies to improve plant production, based on knowledge-driven innovations in the farming sector as well as in agricultural and seed industries, have been proposed on the way towards sustainable agriculture (Watt et al. 2020; Morisse et al. 2022; Janni and Pieruschka 2022). Moreover, with the rapid progression of functional genomics, an increasing number of crop genomes have been sequenced and a lot of genes influencing major agronomic traits have been identified (Hu et al. 2019), facilitating the research on the integration of genotyping and phenotyping for crop improvement (Xiao et al. 2022). Nevertheless, current genome sequence information has not been adequately exploited yet, due to a lack of phenotypic data and the consequent impossibility to understand the exact genetic contribution in trait determination. In fact, due to the link between genotype and phenotype, the latter being the result of the interaction of the phenotype with the environment, it is possible through the study of one to investigate the effect genes have on traits, such as the agronomic ones. In this sense, efficient, automatic and accurate technologies capable of capturing phenotypic data are crucial for crop improvement.

Plant phenotyping is an emerging science that combines multiple methodologies and protocols to measure plant traits (e.g., growth, morphology, architecture, function, and composition) at multiple scales of organization (Carvalho et al. 2021b). In more detail, it refers to a quantitative description of anatomical, physiological and biochemical properties, and generically to all the features deriving from the genome interaction with the environment (Dhondt et al. 2013; Watt et al. 2020; Morisse et al. 2022); these characteristics, by definition, compose the so-called phenotype. The chance of using phenotyping to understand environmental effects and to study genotype performance in a specific environment are two direct consequences of this link with environmental stimuli; moreover, although phenotyping is, currently, mainly used to monitor crops health status, to evaluate fertilization requirements and to detect the presence of weeds in the field (Chawade et al. 2019), many more are its possible applications. Phenotyping can be used for breeding as well as for growth monitoring but also to understand plant-environment interaction principles (see figure 6) and to individuate better agronomic practices.

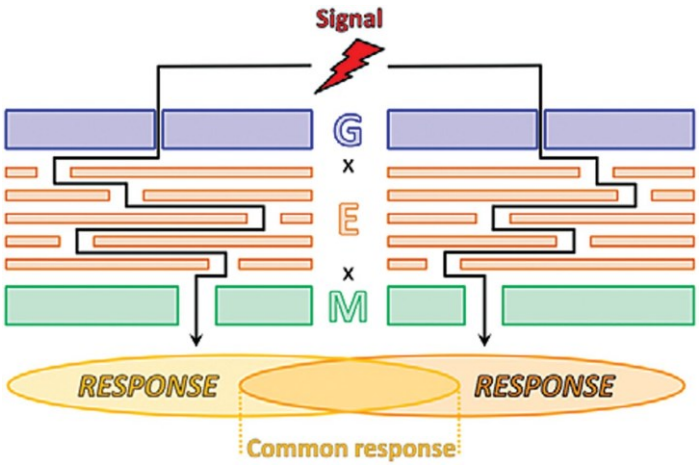

Fig. 6 - Scheme of the environment (E) and management (M) plant performance's (Response) modulation. Two plants having the same genotype (G) exposed to the same stimulus (Signal) can respond in different manners, bringing to the manifestation of two different responses (Großkinsky et al. 2015).

Given its potentialities and the increasing importance held by the phenotype, a discipline called "Phenomics" has been created; specifically, this term refers to the systematic study of an organism's phenotype and usually involves a wide range of analyses to achieve a comprehensive view of the plant phenotype (Großkinsky et al. 2015), this is because there is no holistic technique that can give a complete view of the whole plant at once. Each of these techniques has different execution methods and instruments, and focus on different part of the plant; for this reason, traditional phenotyping methods still largely rely on manual measurements, which are laborious, time-consuming, and hinder the acquisition of comprehensive phenotypic data from individuals in large populations (Chawade et al. 2019; Xiao et al. 2022). However, in recent decades, phenotyping has rapidly advanced since many scientists have become aware of its limitations to the advancement of crop breeding (Kumar et al. 2020; Song et al. 2021). This acceleration led to the development of new tools aimed at simplifying and speeding up data acquisition, and at extending the investigation traits range (Watt et al. 2020).

On the one hand, technological progress has led to the development of new sensing devices. As described in the figure below, these can be distinguished into two main groups depending on the distance between the plant and the sensor chosen (Tao et al. 2022). The 'Proximal group' includes all the technologies whose working principles require them to be in contact or in proximity with the analyzed individual; examples of these instruments are hand-helds, sensors array constituting networks, autonomous ground vehicles, tractor based, phenotyping towers and field scanning platform (Morisse et al. 2022). On the contrary, the 'Remote group' is composed of devices like UAVs, dirigible/fixed wings and satellites, capable of performing scans even kilometers away from the target (Impollonia et al. 2022; Tao et al. 2022;

Barbedo 2023). The technology used can substantially be the same applied for Smart agriculture, but with a different purpose.

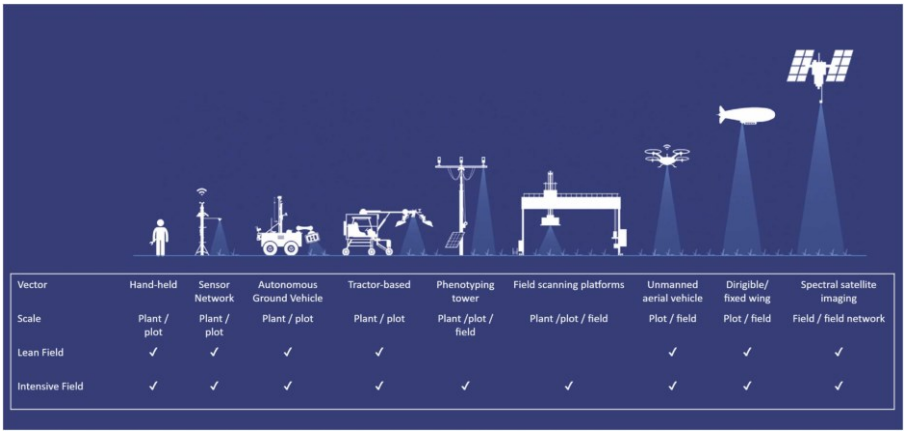

Fig. 7 - Phenotyping sensing technologies: from proximal to remote sensing (Morisse et al. 2022).

The main advantage shared by all of these technologies is the possibility to perform non-invasive quantification and function analysis of plant structure, as well as to investigate plant's interactions with the environment.

In parallel with the use of new sensors, the creation of artificial spaces with the ability to control environmental conditions has facilitated the study of the environmental contribution in phenotype determination and allowed the analysis of plants during unsuitable growing periods (Samantara et al. 2022). As a result, this led to the distinction of 'field phenotyping' and 'phenotyping under controlled conditions'; the former referring to the performing of phenotyping techniques in-situ, with plants growing in open field, whereas the latter considering all the applications of phenotyping performed inside these structures (Kumar et al. 2020).

Recently, due to the increased needs for screening big numbers of plants and for speeding up the process, the high-throughput phenotyping was conceived, enlarging inspection capabilities of phenotyping analysis by assimilating fast and large-scale automated systems originally designed for the industrial field, and exponentially increasing data reliability (Rebetzke et al. 2019). High-throughput phenotyping platforms integrate three essential elements: a control terminal, a data acquisition equipment and a data analysis computing unit (Cardellicchio et al. 2023); the second element usually uses non-invasive imaging and spectroscopy techniques whereas the third, consisting in a high-performance computing equipment, is able to deal with the large datasets generated and is adopted to rapidly analyze traits like plant growth activities and physiological status (Sarić et al. 2022). Compared with traditional phenotyping methods, high-throughput phenotyping facilitates simultaneous data acquisition for multiple traits in large

populations and dynamic observation of plants at different growth stages. Second, once again compared to traditional methods, such as visual scoring, which are prone to subjective interpretation, trait characterization based on spectra or images is more objective. High-throughput phenotyping facilities are in high demand among phenotyping operators such as scientists, prebreeders, and breeders as they can be used to study the phenotypic diversity of genetic resources and therefore to apply increasingly complex traits to crop improvement.

Phenotyping is another area that is strongly taking advantage of the rapid progress in automation and robotics, as the introduction of robots can not only allow the automation but also be a winning strategy to extend the high-throughput phenotyping concept to the open field (Xu and Li 2022). Robotic technologies are constituted by three essential parts: a sensing module, a computational module and an actuation module; this bone structure confers the ability to perceive plants and the surrounding environment, to interpret the data and make a decision, and to realize an operation respectively (Atefi et al. 2021). Unlike the traditional phenotyping, the application of robots in the field offers higher operational efficiency, precision, consistency and dynamic monitoring, but it also provides a great amount of data that can be extremely precious in the development and improvement of AIs and so in the evolution of the phenotyping itself (Yao et al. 2021). An example of a field phenotyping robot is the Field Scanalizer, visible in the figure 8.

Fig. 8 - A field phenotyping platform consisting of an automated structure moving on two rails. The sensing devices are embedded inside central tower, which is lifted according to crop's height, so that the operation can be conducted fully automatically (Sadeghi-Tehran et al. 2017).

2.3 Tomato

Tomato is the second most important vegetable crop next to potato, with a world production of about 100 million tons of fresh fruit with 3.7 million ha cultivated (FAOSTAT 2010), thanks to its adaptability to both field and greenhouse conditions. Italian tomato production is a good example to appreciate the cultivation trend and the success of this crop since, as in the rest of the world, the country's yield has been increasing unstoppably since 1961 (Ritchie et al. 2022). The overall evolution is clearly visible in figure 9.

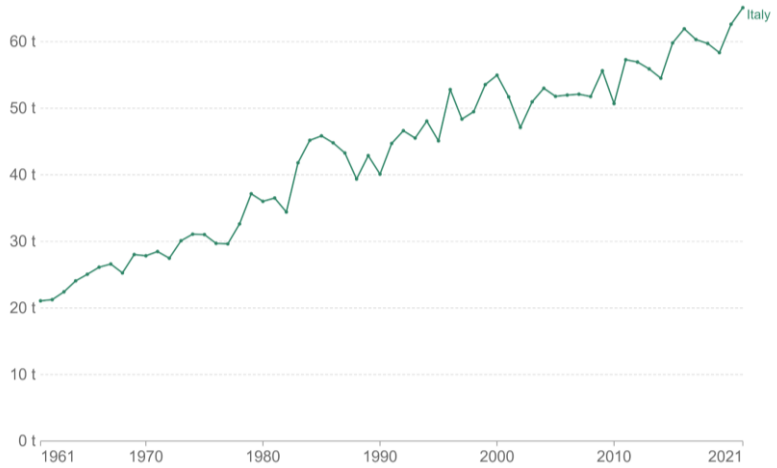

Fig. 9 - Average tomato yield per hectare in Italy. Our World in Data (Ritchie et al. 2022).

Regarding production, the entire Italian territory, considering both the productive district of the North and the South-Central Italy, produces about 5 million tons, equivalent to 50% of what worked in the European Union. Italy as a whole is the first producer of tomato for European industry ahead of Spain and Portugal (OI Pomodoro da Industria Nord Italia).

The Italian National Register of Varieties counts around 350 tomato varieties, among them 65 are considered traditional. Data from 2010 confirmed that the entire production of Italian tomatoes reached 660 thousand tons, mainly represented by processing varieties (Sardaro et al. 2013). In Italy, the processing tomato's principal cultivation is the Southern Capitanata plain (Giuliani et al. 2019), whether the North Italy tomato district includes Emilia Romagna, Lombardia, Piemonte and Veneto regions accounting for over 36000 ha of industry tomato. This district covers 2000 producers and 25 factories for the processing of about 2.5 million tons of tomato (OI Pomodoro da Industria Nord Italia).

Tomato (*Solanum lycopersicum)* is a member of the *Solanaceae* family which also includes potato, pepper and aubergine. Its center of diversification is the Peruvian and Ecuadorian regions of South America,

where the tomato ancestors *S. pimpinellifolium*, *S. lycopersicum* var. *cerasiforme* and *S. pennellii* can be found (Bolger et al. 2014; Mata-Nicolás et al. 2020; Takei et al. 2021). Tomato originated from Latin America at the beginning of the XVI century, however, as a consequence of the different pedoclimatic, cultural, and political environments, the tomato found in Italy a secondary center of diversification (Farinon et al. 2022). The distribution of this crop is almost worldwide, moving from east to west over many latitudes and altitudes and involving many countries, such as China, India, European Union, Turkey, United States, Egypt, Mexico, Brazil, Nigeria and Iran (Costa and Heuvelink 2018; FAO 2022b).

In general, for all crops, the domestication process occurred in prehistoric times and aimed at reducing the growth habit, increasing earliness, preventing seed dispersal and dormancy, and emphasizing morphological diversity in the more interesting portion of the plant (Frary and Doganlar 2003). In tomato, the process led to a profound modification of the wild relative characteristics, resulting for example in a massive increase in fruit size, see the figure below (Bai and Lindhout 2007).

Fig. 10 - Comparison between the fruit of the cultivated tomato (on the right) and that of its ancestor *Solanum pimpinellifolium* (Doebley et al. 2006).

Despite the substantial advantages gained in terms of yield and ease of cultivation, domestication reduced tomato's tolerance to stresses and its adaptability to the environment, increasing plants' dependence by human management and strongly narrowing the crop's genetic background (Jaiswal et al. 2020).

Cultivated tomatoes varieties offer a wide range of alternative forms; examples are the vegetative apparatus, having a determinate, indeterminate, semi-determinate, and dwarf growth habit, depending on the duration of the production of new leaves and branches, the fruit color, which can oscillate between

red, yellow, orange, pink, orange-red, and brown, and the time for fruit maturation, having a range of more than 25 days among the earliest and the latest genotype (Nankar et al. 2020; Islam et al. 2021).

The variability observable around tomato's principal diversification center remains even more pronounced, reporting morphological differences in leaves, fruit (shape, size and color) and flower. Moreover, the tomato's wild relative *S. lycopersicum* var. *cerasiforme*, praises a high phylogenetic relatedness with the cultivated one, making its genetic resource available for tomato breeding too (Mata-Nicolás et al. 2020).

Within the available genetic variability of tomato germplasm, several levels of drought tolerance were recognized among germplasm accessions; examples are the high tolerant "*Lycopersicon pennellii*" and "*Lycopersicon chilense*", the moderate "Punjab Chuhara", "Pusa Ruby" and "Ailsa Craig", and the sensitive "Roma", "Avinash-2" and "Ratan" (Shamim et al. 2014; Ilakiya et al. 2022; Pessoa et al. 2023). Summarizing, these genetic reservoirs represent a valuable resource for crop improvement, demonstrating an enormous variability yet to be exploited and the presence of stress-associated genes contained in closely related species, useful for counteracting the effects of climate change.

In tomato improvement programs, breeders pursue the objective to enhance species' majors traits such as yield, water use efficiency, fruit sugar content as well as biotic and abiotic stresses tolerance; among them, the latter are assuming a particular relevance with the upcoming climate change (Causse et al. 2020). For this purpose, the newest technologies have been applied in the field to accelerate the selection for such traits (Conti et al. 2021). The genomic selection is widely diffused in tomato breeding, solving issues like increasing the selection efficiency for traits with polygenic inheritance as well as simplifying the improvement for all the traits with low heritability in general (Xu et al. 2020). This is possible thanks to a genome-wide distribution of the markers, which in turn is capable of explaining all the genetic variance (Voss-Fels et al. 2019). However, in order to take advantage of this approach, a good calibration of marker density, population structure, phenotyping, and statistical model reliability has to be made (Heslot et al. 2015). In this scenario, many different phenotyping methods have been tested, ranging from the use of phenotyping platforms to the application of sensors (Janni et al. 2019). Genomic selection can be particularly useful for complex traits like disease tolerance as well as drought, salinity and heat tolerance, representing a difficult task for breeders (Cappetta et al. 2020). In recent years, a methodology to associate complex traits and phenotypes, coupling modern sequencing technology and high throughput phenotyping, has been developed; its name is genome wide association mapping and consists in a comparison of the genomes of many individuals which have a certain trait with those which do not, looking for the small variations in DNA responsible for this phenotypic difference (Tibbs Cortes et al. 2021).

Apart from its importance as a total amount of food produced, tomato has interesting nutraceutical properties too (Carvalho et al. 2021a); its fruit provides a valid protection against oxidative stress, as a consequence of the rich phytonutrient and antioxidant content, such as retinol, ascorbic acid, potassium, folate, carotenoids (lycopene, β-carotene and phytoene), polyphenols, and glycoalkaloids (Chaudhary et al. 2018; Yong et al. 2023).

In this thesis work, tomato has been chosen as a reference crop, not only for its world-wide distribution, its centrality in human nutrition and its nutraceutical role, but also for its cultivation ease and growth speed, that allowed experiments to be performed with minimal equipment, as well as for its anatomy. Indeed, the distribution and abundance of the vasculature proved to be crucial aspects in achieving the goal of the thesis, this topic will be later clarified in the course of the following chapters.

2.4 Bioelectronics

Bioelectronics is an interdisciplinary field that combines biology, electronics, chemistry and physics to create new devices that interface with biological systems (Simon et al. 2016). This in-vivo and in real-time interfacing can be aimed at the study of the biological, biochemical and biophysical mechanisms or at their regulation (Liao et al. 2019; Bernacka-Wojcik et al. 2019). For these reasons, bioelectronics is a rapidly growing field with significant potential for future development.

Some of the main topics in bioelectronics are biosensors and implantable devices: biosensors are devices that detect and measure biological signals or molecules in living beings' bodies. They can be used for diagnostic purposes or for monitoring physiological parameters like heart rate, blood glucose levels and plant sap composition (Contardi et al. 2021). Implantable actuators, instead, are devices that are implanted into the host's body to perform specific functions, such as drug delivery and cell stimulation, triggered by biological stimuli (Srinivasa Rao et al. 2020).

Interfacing electronic devices with biological systems represents a huge challenge since the establishment of a connection between these apparently incompatible fields is not straightforward. In fact, among the number of obstacles to overcome, the availability of biocompatible materials with appropriate physical and chemical characteristics is surely one of the main bottlenecks in this field (Li et al. 2022). Moreover, despite electronic devices almost completely rely on electron currents, biological systems usually prefer ions as charge transporter (Simon et al. 2016); the reason is that ion form is privileged because, depending on the cross section of membranes' pores and molecular dynamics, it is able to migrate through organic soft materials more easily (Simon et al. 2016).

Recently, the synthesis of innovative polymeric materials capable of mimicking living tissues reduced rejection risks simplifying the interfacing issue (Berggren and Richter-Dahlfors 2007); among them, PEDOT:PSS is worth a citation. Additionally, these polymers offered high signal transduction and amplification, which led to the improvement of device sensitivity. Other consequent innovations have been the enhancement of electro-active characteristics, the substitution of oxide with organic materials and the increased efficiency of ionic movement between device and living tissue, which led to the development of innovative, low cost and easy to use devices (Simon et al. 2016; Berggren et al. 2019). Among them there are organic electro-chemical transistors (OECTs), organic field effect transistors (OFETs), electrolyte-gated field-effect transistors (EGOFETs), organic electronic ion pumps (OEIPs) and ionic diodes and circuits (Rivnay et al. 2018).

2.4.1 Conductive Polymers

Research on conductive polymers began in 1977 when Shirikawa, Heeger and MacDiarmid discovered the possibility to dope polyacetylene by using arsenic pentafluoride (AsF_5) and obtaining an organic material with a conductivity level similar to the metal semiconductor. The basic skeleton of a conducting polymer is a carbon chain consisting of conjugated double bonds with hybridized sp^2 carbon atoms. Three of the electrons in the carbon's sp^2 hybrid orbital form three σ bonds, while the remaining electrons in the p_z orbitals form a π bond, permitting the electrons relocation along the polymer spine.

Thanks to their properties, semiconductors are conventionally described as materials with intermediate characteristics between conductors and insulators (Garrett and Brattain 1955).

As shown in figure 11, insulators exhibit a relatively substantial energy gap that impedes the movement of electrons from the valence band to the conduction band, resulting in the non-conductivity of these materials. Conversely, metals feature overlapping conduction and valence bands, which facilitate the unhindered passage of electrons between them, thereby determining their conductive nature.

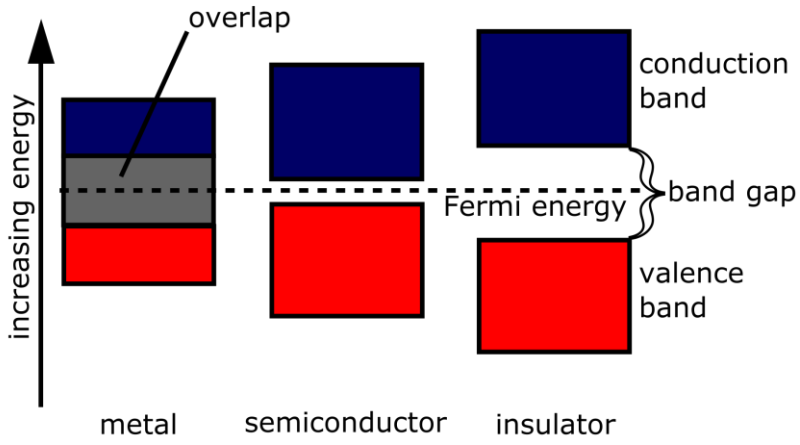

Fig. 11 - Energy gap in conductor, semiconductor and insulator (Wikipedia 2006).

The distinctive attribute of semiconductor materials lies in the presence of two non-overlapping bands separated by a narrow gap. The reduced gap width permits the transit of some electrons from the valence band to the conduction band, determining in this way the presence of electron vacancies in the valence band and electron mobility in the conduction band. These electrons in the conduction band and the vacancies in the valence band are key contributors to the material's conductivity (Zhang et al. 2020a).

The conductivity of neutral conjugated polymers is closer to insulators than to metal semiconductors therefore, in order to increase the conductivity of polymers, doping techniques is mandatory, but a larger fraction of the material must be affected if compared to metal semiconductors (Kar 2013). In fact, in the doping of crystalline semiconductors (e.g. silicon and germanium), the doping atom replaces an atom of the crystalline lattice establishing a covalent bond with the surrounding atoms. The doping of conjugated polymers instead leads to ionic bonding. Moreover, polymer doping can be induced through two distinct mechanisms: oxidation of the polymer chain, resulting from the substitution of electrons by the π system (p-type), or reduction of the π system, which introduces negatively charged units into the conjugated system (n-type) (Kar 2013).

The most commonly employed methods for doping conjugated polymers include:

- chemical doping: occurs through redox reactions between the polymer to be doped and the doping species. In case of oxidation, doping is p-type, in case of reduction it is n-type. This doping, however, leads to the formation of a non-homogeneous material (Lu et al. 2021);
- electrochemical doping: doping atoms are accelerated through an electrical field, an electrode is polarized to produce an ion flow moving from the polymer under doping, the process tends to maintain neutrality in the polymer itself (Bargigia et al. 2021);

- photodoping: photo-absorption induces the oxidation and reduction of the polymer resulting in a consequent separation of the charges which produce electron-gap pairs and thus free carriers (Ghini et al. 2021);
- charge injection: consists in the injection of electrons and gaps through a metal contact, reducing or oxidizing the polymer. Unlike chemical or electrochemical drugs, no counter-ions are needed.

Polymers subjected to these treatments may vary their conductivity from 103 S/m to 1011 S/m, essentially assuming the characteristics of an insulator, a semiconductor, or a metal.

The discovery of these 'synthetic metals', also known as 'intrinsically conductive polymers' (ICPs), worthed the attribution of the Nobel prize in chemistry to Alan J. Heeger, Alan G. MacDiarmid and Hideki Shirakawa in 2000. Thanks to their excellent processing and electronic properties, ICPs have been the subject of many studies; among them, a particular consideration deserved polyparaphenylene (PPP), polyparafenilensulfide (PPS), polyparaphenylene vinylene (PPV), polyaniline (PANI), polypyrrole (PPy), polyethylene (PT) and polyethylenedioxythiophene (PEDOT).

2.4.2 PEDOT:PSS

The poly(3,4-ethylenedioxythiophene) (PEDOT) is one of the most successful conducting polymers ever studied (Groenendaal et al. 2000). Its primary structure is composed by a sequence of partially cationic ethylenedioxythiophene and anionic styrenesulfonic acid monomer units (Fig. 12 A); the interaction of these two elements, held by electrostatic forces, causes the polyion complex to assemble (secondary structure). Since it is usually sold diluted in water, the polymer rearranges in the form of a colloidal gel particle (tertiary structure, Fig. 12 B); among these particles, numerous groups with diameters of several tens of nanometers can be observed (Fig. 12 C), these densely packed aggregates form the pristine (Fig. 12 D, quaternary structure).

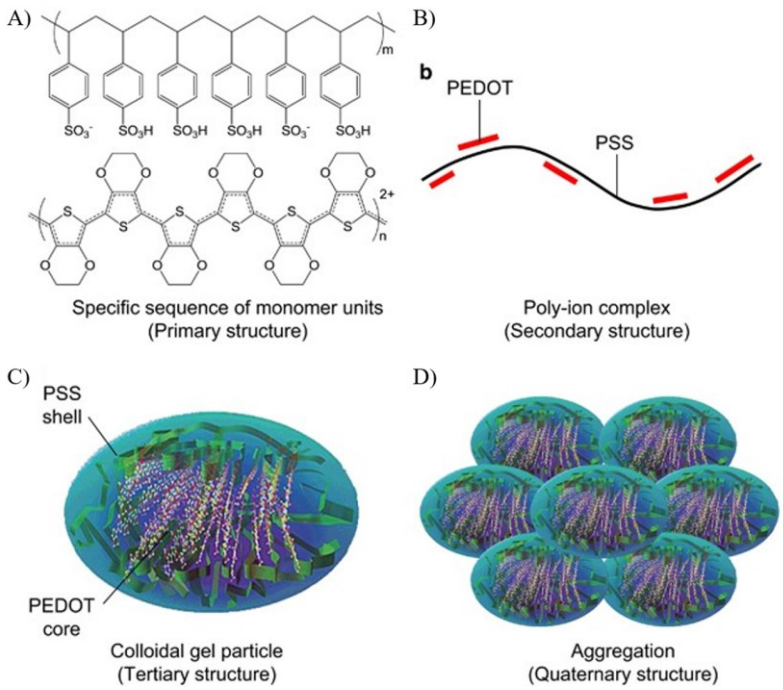

Fig. 12 - PEDOT:PSS arrangements: A) primary structure, B) secondary structure, C) tertiary structure, D) quaternary structure (Horii et al. 2015).

PEDOT:PSS belongs to the class of p-doped semiconductors and is characterized by (Nikolou and Malliaras 2008; Wang 2009; Shi et al. 2015; Strakosas et al. 2015; Sun et al. 2015; Kim et al. 2019b):

- high conductivity: PEDOT's band gap is around 1.5-1.6 eV and can be further reduced if doped; the resulting electrical conductivity is about 550 S/cm;
- drug state reversibility: the polymer can be turned back to its initial state many times after subsequent doping events. Furthermore, PEDOT's optical properties can be changed behind doping treatments, making it suitable for optical applications;
- structural regularity: the regular structure characterizing the polymer is a consequence of its short chain composition;
- stability: PEDOT has an excellent thermal stability, in fact, film temperature can be rise up to 100 °C for over 1000 h with only minimal changes in electrical conductivity. Moreover, it shows high chemical stability levels;
- electrochemical stability: electrochemically synthesized PEDOT films show low reduction and oxidation potentials as well as excellent doped state stability.

Some of the properties previously mentioned can be tuned choosing different dopants, in any case the polystyrene sulfonate (PSS) is the preferred dopant. Its link with the polymer gives a considerable increase

in conductivity (up to 100 S/cm) and allows its dispersion in water (Groenendaal et al. 2000; Nikolou and Malliaras 2008). The PSS, being a polyanion, is able to compensate for the PEDOT backbone's gaps, thanks to its negative charges. Moreover, PSS affects polymer transparency and the effortless preparation of high-quality films, making it widely available on the market.

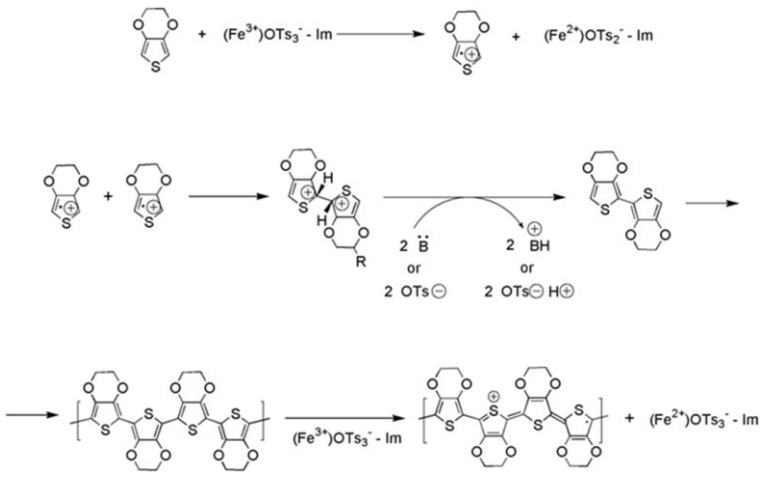

Fig. 13 - PEDOT polymerization mechanisms considering the interaction with a positively charged metal ion (in this case Fe^{2+}) (Kim et al. 2019a).

PEDOT:PSS polymerization can be carried out chemically or electrochemically, figure 13 summarizes a generic polymerization process. Electrochemical polymerization implies the use of a three-electrode electrochemical cell in which the metal electrode oxidizes 3,4-ethylenedioxythiophene (EDOT) monomers in presence of PSS sodium salt. Chemical procedure uses iron (III) chloride or nitride and peroxydisulfates as oxidizing agents, inducing EDOT monomers oxidation; the role of PSS is crucial in both the procedures since it stabilizes the process and solvates the PEDOT. In order to prevent the aggregation of the highly conductive PEDOT:PSS particles, an excess of PSS is also imperative for the formation of protective shells around them. Further, the addition of some extra components can be used to modulate PEDOT characteristics and its degree of doping; among them, ethylene glycol (EG) and dodecylbenzenesulfonic acid (DBSA) are the most common. The first one improves polymer conductivity, the second one changes suspension viscosity and increases substrate adhesion (Dimitriev et al. 2009).

Once synthesized, PEDOT:PSS can be subjected to different deposition methods, the most common two are coating and printing. The term "coating" refers to the complete coverage of a substrate's entire surface, as opposed to "printing", which implies the application of "'ink" onto selected portions of the substrate.

Deposition techniques can be selected depending on various aspects of the material under study as:

- volume and viscosity of the solution
- shape, homogeneity and adhesion of the substrate
- process speed

Here is a brief list of the most used deposition techniques (Deegan et al. 2000; Nguyen 2012; Islam and Islam 2013; Kaliyaraj Selva Kumar et al. 2020; Wang et al. 2021, 2023; Karami et al. 2022):

- drop casting: is probably one of the simplest deposition techniques. The procedure consists in the casting drop-by-drop of a solution on the substrate's surface, and waiting for the evaporation of the solvent. The deposition generates a thin film however, being a fast and cheap method, it results in uneven deposition rates, convex regions and denser deposits
- spin coating: together with drop casting is usually included among the easiest deposition techniques. The process begins by diluting the material in a solvent and distributing it on the entire substrate surface. The plate is then spun at high speed provoking the removal of the exceeding material. Spin coating leads to the formation of a sufficiently planar surface whose thickness can be controlled by varying angular velocity, acceleration chosen for spinning, surface tension and viscosity of the solution, as described by the relation $d = k\omega\alpha$ (ω is the angular velocity of spinning, k and α are constants depending on the solvent and the substrate chosen). The technique is applied to sol-gels and various ceramics deposition as well as for fotoresist transferring during photolithography
- ink-jet printing: is a 2D printing technology with industrial and scientific applications (e.g. electronics, biosensors, catalysts, and bio-cells). The use of this technique serves to mitigate solution wastage, but necessitates the implementation of precise measures during its preparation. Specifically, ink-jet printing involves the precise injection of ink onto the substrate, which propels solution droplets under the influence of an electric field. To facilitate this propulsion, the droplets must be endowed with an electric charge. In contrast, the formation of these droplets entails the application of heat, achieved using a needle. Consequently, the solution must exhibit high surface tension and low viscosity. Inkjet printing is a reliable, affordable and feasible method for high-quality thin films development;
- electro-deposition: is an economic and effective method to process conductive materials and implies the immersionion of the substrate in an electrolytic solution containing the material to be deposited. Electrodeposition is achieved by imposing a constant or variable voltage between two electrodes. One of these electrodes is in direct contact with the substrate, while the other, termed the counter electrode, polarizes the surrounding solution. This electrochemical process unfolds within an aqueous electrolytic solution containing precisely measured quantities of EDOT and

PSS. Electro-deposition is commonly used with different methodologies like cyclic voltammetry, potential step deposition and double pulse. Deposit characteristics, such as its component, phase and microstructure, can be modulated by varying parameters like current density, electrolyte composition and temperature.

2.5 Organic electrochemical transistor

An Organic EleCtrochemical Transistor (OECT) is a transistor in which the electrolyte constitutes an integral part of the device; transistors of this class are also called EGT (electrolyte gated transistors). A direct consequence of this characteristic is the pronounced affinity with water and consequently with biological environments (Strakosas et al. 2015). Moreover, this configuration implies the pumping of ions into the transistor's channel, that is the key factor conferring OECTs the ability to realize large amplification even in subvolt regimes (Khodagholy et al. 2013; Strakosas et al. 2015). Interest around OECTs is rising during the last years, since their characteristics make them suitable for many research applications like cell culture, biomedical diagnosis and electrophysiological stimulation (He et al. 2022).

Other remarkable characteristics of such a device are:

- reduced production cost
- ease of use
- miniaturizability
- low voltage requirement
- high sensitivity
- high trans-conductance

Two of the most interesting applications of OECTs are the ones in biomedicine and agriculture. In these particular sectors, OECTs can work as sensors for saliva, sweat, plasma and sap monitoring (Coppedè et al. 2014, 2017; Keene et al. 2019; Moudgil and Leong 2023).

Main components of an organic electrochemical transistor are two electrodes (called channel and gate) and the electrolyte solution. The channel is composed of an organic semiconductor and is the heart of the device as the behavior of the whole transistor mainly depends on it. The gate electrode can consist of a metallic or an organic conductive material additional layer. An OECT has three terminals called source, drain and gate; drain and source are located at the opposite sides of the channel, whereas the third terminal is located at the extremity of the gate electrode. The role of the terminals is to ensure the connection of each OECT component to the electronic circuit needed for powering the device and reading its parameters.

The last essential part of the transistor is the electrolyte solution that links the two electrodes and can be represented by a solid, a liquid or a gel containing electrolytes (see Fig. 14).

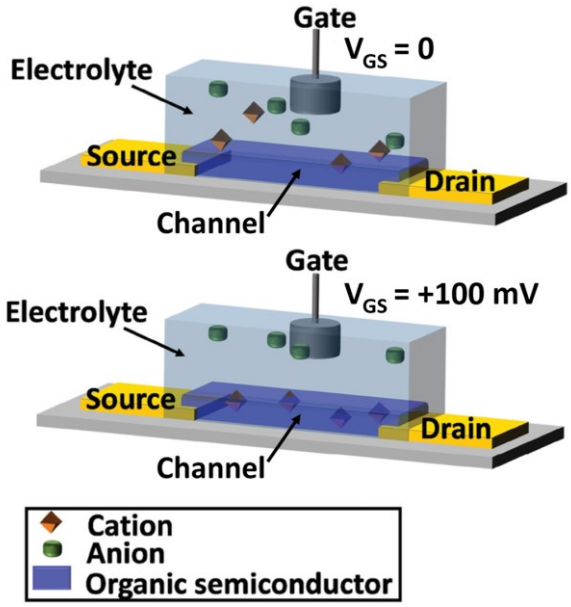

Fig. 14 - Anatomy of an OECT and response of the electrolytes in the solution when a positive voltage is applied to the gate (Friedlein et al. 2016).

OECT's operation modes are distinguishable into depletion-mode and accumulation-mode (Ohayon et al. 2023). In depletion-mode, the positive bias, applied to the gate terminal, pushes the cations into the channel, resulting in a decreased number of holes in the channel (de-doping). On the contrary, in accumulation-mode a negative bias is applied, pushing anions inside the channel and increasing the number of holes (doping). The resulting doping and the de-doping of the channel led in turn to decrease and increase of its electrical conductivity (Khodagholy et al. 2013).

Seen PEDOT:PSS' importance in the OECT's landscape (Liao et al. 2019), to describe the physics and chemical principles governing OECTs a focus on the depletion-mode operation is proposed here.

The polarization of the OECTs, similarly to the inorganic transistors, is indispensable for the device to work correctly. As a convention, the source contact is grounded and a positive voltage and a negative voltage respect to ground are applied to the drain (V_{ds}) and gate (V_{gs}) contacts, respectively. A physical model of the transistor has been proposed by D.A. Bernards and G.G. Malliaras, who supposed the combination of an electronic and a ion circuit (Bernards and Malliaras 2007a). The electronic circuit illustrates the transport of holes inside the channel, while the second one describes the transport of charged

ions in the electrolyte. This model allows to study transistor transcharacteristic, explaining the dependence of I_{ds} on V_{gs}.

The electronic circuit can be described using the generalized Ohm's law:

$$J(x) = q\mu\rho(x)\frac{dV(x)}{dx}$$

where μ indicates the mobility of holes, $\rho(x)$ represents holes concentration in the semiconductor, and x stands for the coordinate of the axis on which the channel is placed longitudinally. As previously mentioned, despite V_{ds} to be fixed, I_{ds} current is a time varying variable because of the effect of the cation interaction with the channel polymer. When an ion is added to the chain, a hole is removed from the source (de-doping) without altering its electroneutrality. This process is described in the following formula:

$$\rho = \rho_0 \left(1 - \frac{Q}{qV\rho_0}\right)$$

here ρ_0 stands for holes concentration at $V_{gs} = 0$, V for semiconductor volume, and Q as electrical charge of the cations injected into the polymer film. These two parameters are inversely correlated, as expected.

The ionic circuit describes the migration of cations within the electrolyte toward the channel and can be conceptualized as a combination of a capacitor and a series-connected resistance. The resistance characterizes the electrolyte's conductivity and gauges its ionic strength, while the capacitance accounts for polarization at the channel-electrolyte and gate-electrolyte interfaces. Depending on the trend of V_{gs} over time, transistor behavior can be distinguished in static and dynamic.

The static behavior consists in applying a fixed V_{gs} and evaluating I_{ds} according to V_{ds}. In the dynamic behavior instead, the transistor works under constant V_{ds}, varying V_{gs} for repetitive cycles from 0 to a positive value.

The static mode involves a uniform de-doping process in the channel, and its working principle is described in this equation:

$$J(x) = q\mu\rho\left[1 - \frac{Vg - V}{Vds}\right]\frac{dV(x)}{dx}$$

The equation must be solved considering that its result varies depending on V_{ds}.

Assuming that $V_{gs} > 0$:

at $V_{ds} > 0$ and $V_{ds} < V_{gs}$, the de-doping affects the entire film;

at $V_{ds} > 0$, $V_{ds} > V_g$ and $V(x) < V_{gs}$, the de-doping reach the emptying condition;

at V_{ds} 0 and $V_{ds} \leq V_{ds,sat}$, $V_{ds,sat}$ is defined as the critical drain voltage at which the polymer doping is completely undone. This state, called "saturation", is characterized by the lowering of the injected cations local density, down to the same level of the semiconductor's intrinsic doping. When the channel is in saturation, the I_{ds} current is called saturation current.

This state assumes particular interest because it allows the study of the so-called "Characteristics"; this curves family (shown in the figure below) represents the function linking the output with the input and, in this sense, supplies fundamental information for sensors and transductors analysis (Fig. 15).

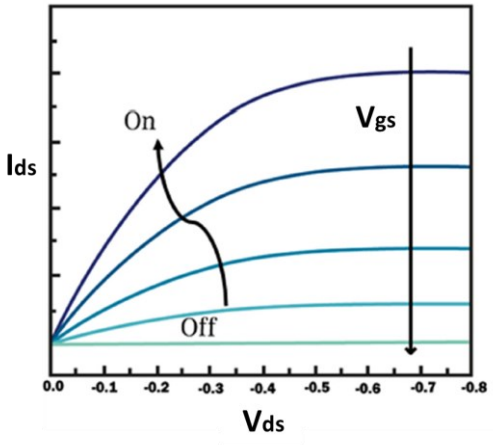

Fig. 15 - Characteristic of a generic OECT: each curve resulted by maintaining V_{gs} constant and varying V_{ds} (Marquez et al. 2020).

The OECT dynamic behavior implies continuous cycles of doping and dedoping as a consequence of V_{gs} changes; as previously mentioned, during all these measurements V_{ds} is maintained at a fixed value. In figure 16 the resulting I_{ds} (figure 16 A) and I_{gs} (figure 16 B) trend is shown. This regime was conceptualized to analyze variations in the electrolyte solution such as in ion concentration; the OECT is able to respond to a similar stimulus with a signal variation since the presence of ions in the electrolyte solution deeply affects transistor's working parameters (Khodagholy et al. 2013).

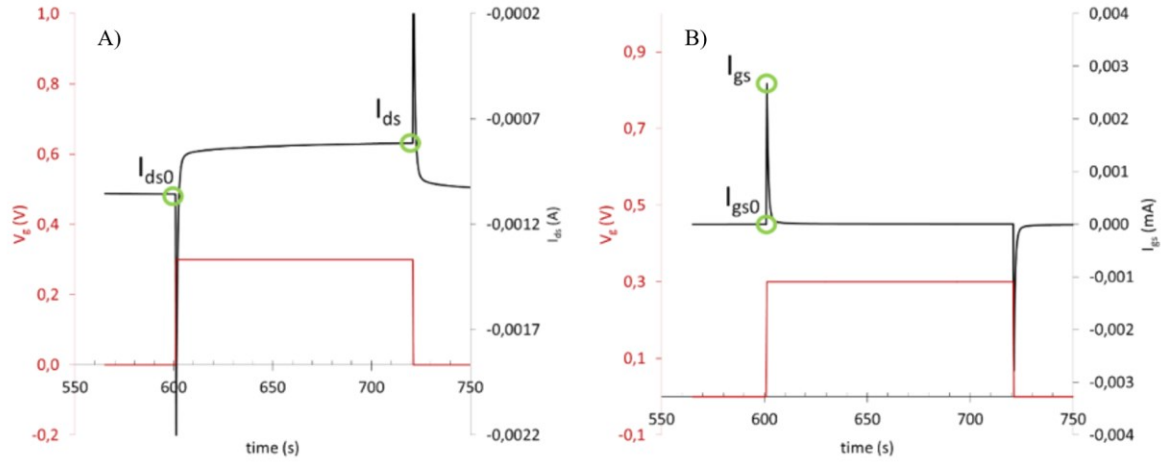

Fig. 16 - A) I_{ds} modulation occurring when gate voltage is applied in OECT. Green circles indicate the drain-source current when V_{gs}=0 (I_{ds0}), and the drain source-current when $V_{gs} > 0$ (I_{ds}); B) I_{gs} behavior when gate voltage is applied in OECT. Green circles indicate the gate-source current when V_{gs}=0 (I_{gs0}), and the gate-source current when $V_{gs} > 0$ (I_{gs}).

In fact, the increase in ion concentration results in greater reductions of channel conductivity because a higher amount of ions are available to enter inside the polymer realizing a faster and more intense conductivity reduction in each cycle. To take into account this feature, a new variable called the 'Response' (R) has been introduced. The response is calculated as:

$$R = \frac{|I_{ds} - I_{ds0}|}{I_{ds0}}$$

This kind of analysis shows a fundamental relation between OECTs parameters, which is the "Modulation". The modulation is an adimensional value defined as the ratio between on-state (I_{ds}) and off-state (I_{ds0}) of the channel current (figure 17 A).

Other essential variables used to characterize dynamic behavior of these transistors are I_{gs} and the time constant τ. After applying a positive gate bias, a current begins to flow through the solution from the gate electrode to the main channel, denoted as I_{gs}. As noted by (Gentile et al. 2020), the effect is also a function of the moisture status of the OECT.

The time constant τ is determined through curve fitting of the I_{ds} (Fig. 17 A) and I_{gs} (Fig. 17 B) currents, the parameter expresses the time to reach the steady state.

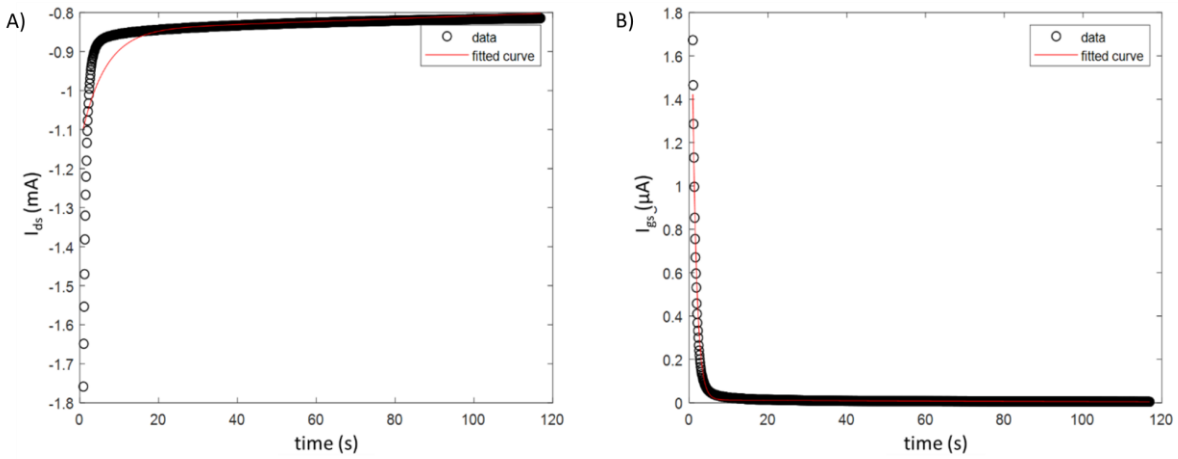

Fig. 17 - Exponential curve fitting for τ calculation operated on I_{ds} (A) and on I_{gs} (B).

The formula used for describing τ_{ds} (τ referred to the I_{ds} current) is:

$$\tau_{ds} = A\ (1 - e^{-t/\tau}\ )$$

where the exponent $-t/\tau$ determines the speed at which the plateau is reached. The possible effect determined by different ion species overlapping is not taken into consideration. Fitting the I_{gs} curve with the same approach gives τ_{gs}:

$$\tau_{gs} = A * \ e^{-t/\tau}$$

τ_{ds} and τ_{gs} are linked to the time required for ions to penetrate the polymer, and to the ion diffusion within the solution respectively.

PEDOT is one of the most used semiconductors for OECT applications and is normally employed in its doped state (PEDOT:PSS). The low voltages required for the transistor to work, together with the following tiny currents determined, strongly limit the power consumption of these OECT. But most importantly, thanks to the intrinsic affinity with water, conferred by the architecture of the device, OECTs are capable of detecting solute concentration variation in an electrolyte solution, making them perfect biosensors.

2.6 IoT and Smart farming

The Internet of Things (IoT) approach dates back to 1980 and refers to the integration of technology capable of exchanging information relatively to the surroundings in everyday life (Atzori et al. 2010). Primary goal of IoT is to enhance the efficiency, productivity, and functionality of various sectors by enabling seamless communication and data sharing between devices. In an IoT ecosystem, common use objects become "smart" as they acquire the ability to sense, analyze, and communicate information (Atzori et al. 2014). These devices can include many different items such as household appliances, wearable gadgets, industrial machinery and city infrastructure; other examples are depicted in figure 18. The deployment of this innovative concept owes its feasibility to the existence of an extensive telecommunications network, ensuring connectivity for all the nodes, and the deployment of a large number of sensors, serving for the connected devices as a window to the physical world (Sikimić et al. 2020).

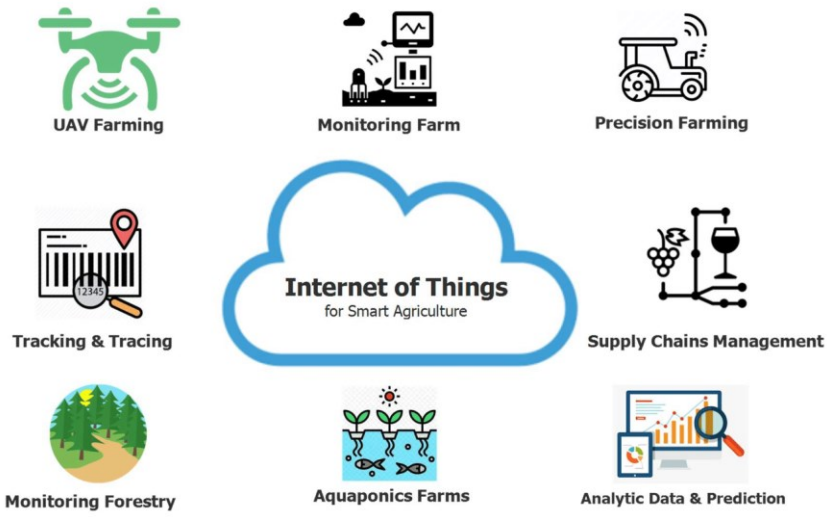

Fig. 18 - Internet of Thing application in smart agriculture (Ansar et al. 2023).

IoT architecture is structured in three parts: the hardware, the middleware and the presentation layer (Shafique et al. 2020).

- Hardware: is represented by the sensors and all the electronics needed for interfacing them to the net;
- Middleware: consisting in the data analysis and elaboration;
- Presentation layer: aims at providing the elaborated information to the users.

The concept of Smart Agriculture, or Smart farming, arose as an application of the IoT technological approach for the promotion of precision farming with modern, sophisticated technology, not only for enabling remote monitoring of the plants (Dhanaraju et al. 2022), but also for the control of agricultural processes and the contrast of agricultural emergencies (Xu et al. 2022). Central to this framework are sensors, which assume a critical role in capturing data related to diverse elements such as soil characteristics, meteorological conditions, water utilization, and overall plant status. Smart agriculture, more than many other IoT applications, has required significant technical and engineering efforts to establish a robust and well-managed network infrastructure with the aim of facilitating communication between individual nodes frequently located at considerable distances from each other and from the access point; similar attention has been taken to avoid congestion, which is a concrete risk in highly ramified nets (Poonia et al. 2023).

Nowadays, the most used communication protocols are Wireless WAN (GPRS/4G/5G), WiFi, Bluetooth, ZigBee and LoRaWAN (Çorak et al. 2018; Kassim 2020; Bayılmış et al. 2022). The diverse characteristics of these technologies make them suitable for a wide range of applications and environmental conditions. Regarding net congestion avoidance, it is intuitive that a wide number of nodes generates a huge amount of data that need to be managed, therefore a new approach called Cloud Computing has been proposed as a possible solution; the latter is considered the most advanced computing paradigm and has the ability to lighten on-site hardware from storage, calculation and processing tasks (Kalyani and Collier 2021; Xu et al. 2022). Of equal importance is network node geolocation, as each data provider would become unusable if not referred to a specific site; on the other hand, spatial information can be particularly useful, as such data can be exploited to monitor the spread of diseases and prevent hydrogeological disasters.

In Smart agriculture two advanced and widely diffused technologies deserve to be mentioned: radio frequency identification (RFID) and 3S. Their targets are completely different since the first one is used for animal, equipment tracking as well as food tracing, transportation and logistics (Rayhana et al. 2021), whereas 3S enables the monitoring, geolocation and visual analysis of field information (Xu et al. 2022). RFID is a technology lying at the base of the data generation process which consists in powering antenna-equipped systems and receiving their readings using electromagnetic waves. Essentially, unpowered devices (tags) are installed in the site of interest and consulted when needed using a reader, supplying energy via electromagnetic waves and receiving the replying information. Most of the RFID technologies require proximity during the reading process so these devices are particularly used in the perishable food supply chain tracing, implementation in which the reader is usually stuck and devices are moved close to it (Alfian et al. 2020). 3S, on the other hand, refers to the combination of Remote Sensing (RS), global navigation satellite system (GNSS), and Geographic Information System (GIS). RS includes a branch of technologies whose aim is to obtain data through distance monitoring, hence is not surprising its focus on

electromagnetic waves as source of information. This task is realized thanks to a broad range of transducers capable of analyzing a wide electromagnetic spectrum fraction, however the main importance is taken on light closer radiation like infrared, far-infrared, and microwaves (Xu et al. 2022). GNSS, instead, is capable of providing global three-dimensional position in all weather conditions with high precision allowing RS readings to be corrected. In closing, GIS is a technology that integrates, analyzes and visualizes spatial data and can therefore be used to merge the data obtained from the previous two and display them in the form of overlapping map layers.

Summarizing, smart agriculture can be seen as an Iot application, evolved to optimize resource utilization, reduce wasting and facilitate farm management by encouraging data-driven decisions (Xu et al. 2022). The resulting new farming approach enables increased yields and enhanced crop quality, representing a promising strategy for climate change contrast; at the same time, cost reduction positively impacts farmers' economy, contributing to the sustainability of the whole agriculture industrial sector (Farooq et al. 2020). In this scenario, it is crucial to remember sensors' role, which lie at the base of the information cycle, since they act as information extractors, allowing an automatic reading of the surrounding world (Raj et al. 2021).

2.7 In vivo plant sensing and monitoring

In the landscape of sensors available for monitoring plants, whether in the open field or in controlled environments, the ability to monitor their health status and needs in real time and directly from the inside was missing. In the last 5 years, IMEM-CNR developed a novel sensor named bioristor that enables *in vivo* and in *real-time* monitoring.

2.7.1 The bioristor's state of the art

The bioristor is an OECT consisting of two electrodes, the channel and the gate, functionalized with PEDOT:PSS and immersed in an electrolyte solution. Being an OECT, the role of this electrolyte solution is crucial for the well-functioning of the device; the distinctive trait of the bioristor is that its peculiar architecture allows for its insertion in plants. This, in turn, let to cross plant's vascular bundles, replacing the so-called electrolyte solution with plant's internal fluids, as the sap (see figure 19 A), and conferring the possibility to analyze plant's physiological conditions and making the transistor to act as a sensor. Hence, by inserting the bioristor in the plant stem it is possible to continuously monitor the plant health status.

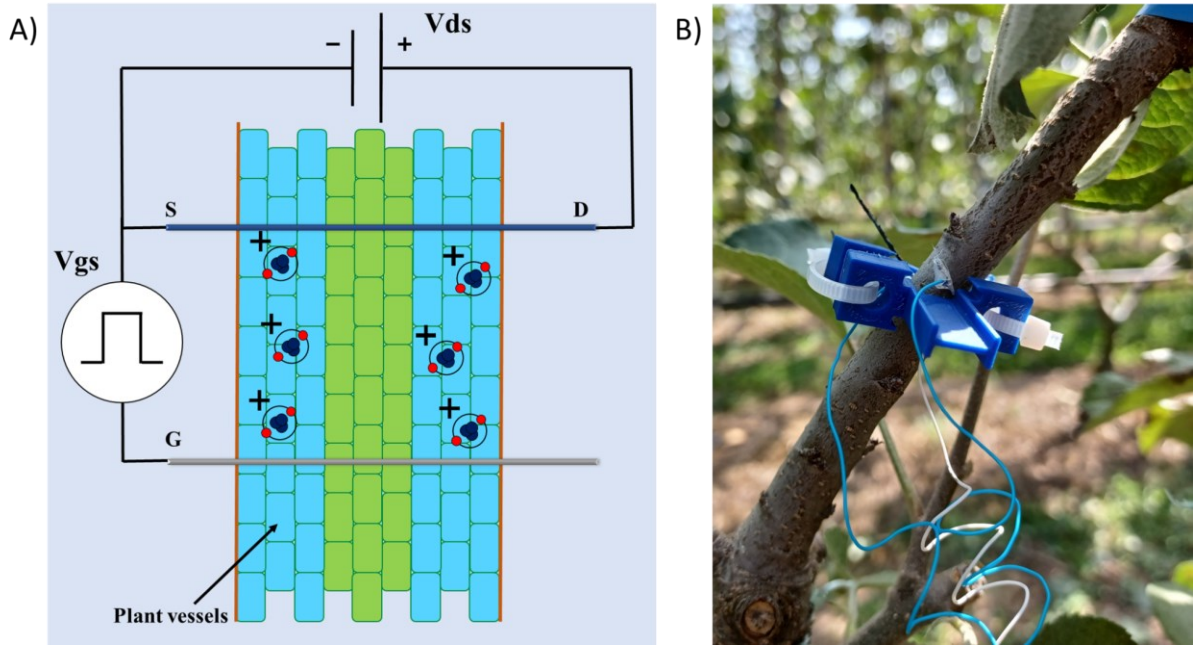

Fig. 19 - A) Bioristor working principle schematized, here is introduced the bioristor polarization circuit which consists of a constant voltage and a square wave generator, B) demonstration of bioristor implementation in *Malus domestica*, the connection blue and white wires are shown together with the holder.

The working principle of the OECT was previously described in Gentile et al., 2022, Coppedè et al., 2017 and is schematized in Fig. 19. The sensor is shown in figure 19 B. Upon application of a positive voltage to the gate, anions react at the gate electrode through a redox process and cations are forced towards the channel, which is the active part of the OECT device (Fig. 19 A). The sensor device measures a current of electrons flowing in the channel from the drain to the source, which is modulated by the current of cations that run from the plant to the channel. For this reason, the bioristor as well as the OECTs, can be considered an ion-electron transducer (Simon et al. 2016). Remarkably, the entire process is reversible: when the voltage between the gate and the source drops ($V_{gs} = 0$), ion diffusion from the channel to the electrolyte solution increases the number of conducting holes and, consequently, I_{ds} (Bernards and Malliaras 2007b). In this configuration, the gate and the drain are the cathodes, and the source is the anode, thus positive charges move in the plant from the gate to the source, and in the channel from the drain to the source.

The most frequently analyzed bioristor indexes are: I_{ds}, I_{gs}, R, τ_{ds} and τ_{gs}.

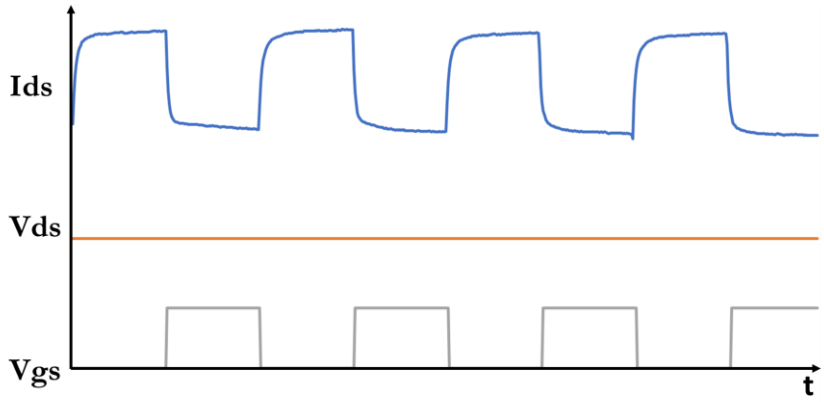

Fig. 20 - Dependence of I_{ds} on V_{ds} and V_{gs} waveforms: I_{ds} oscillations follow V_{gs} ones, maintaining the same frequency.

I_{ds} is the current flowing across the channel, from the drain to the source terminal; despite V_{ds} to be constant, the former has a typical double exponential shape because V_{gs} oscillates as a 50% duty cycle square wave (Fig. 20). This leads to an alternating ion flux that regularly inverts its direction, entering and exiting outside of the polymer. The main parameter returned by the sensor is the response (R), which is a dimensionless unit obtained dividing $I_0 - I_1$ by I_0, where I_0 is the current flowing across the channel at $V_{gs} = 0$ whether I_1 is the current flowing across the channel at $V_{gs} \neq 0$. The imposition of V_{gs} causes a second current to flow, namely I_{gs}, that is the current flowing across the gate electrode, plant sap and channel electrode. In contrast to I_{ds}, I_{gs} direction is continuously alternating. The shape of I_{ds} and I_{gs} curves don't resemble the V_{gs} one, as ions flow across the sap, and their recombination with the polymer, determine a shifting in the two currents. The parameters τ_{ds} and τ_{gs} were introduced to take into account this delay, which can be examined to find indication about the solution characteristics.

2.7.2 Bioristor and functional phenotyping

As previously mentioned, the bioristor has been applied in plants to sense their physiological status, precisely, the first application was performed in tomato, demonstrating its ability to trace changes occuring in the plant sap during night-day circadian rhythms. During this test, it was demonstrated that sensor response R decreases during the day and increases during the night (Coppedè et al. 2017); the observation strongly links R with plant physiology, as a direct consequence of transpiration oscillation and of the photosynthesis circadian regulation (Coppedè et al. 2017).

Tomato was also used to demonstrate bioristor biocompatibility, since no monitoring could be possible without a high affinity between plant's and sensor's constituents. Hence, stem sections surrounding the sensor's insertion points were cut and stained to distinguish its constituents. The experiment reveals the complete absence of damages in the vascular tissues and slight necrotic lesions in correspondence of the silver gate electrode (Coppedè et al. 2017), suggesting the need to replace the material; after this experience, both the channel and the gate were made of PEDOT:PSS (Janni et al. 2019). Another important discovery resulting from the experiment was the substantial morphological identity between plants equipped with bioristor and control plants in absence of the sensor (Coppedè et al. 2017), demonstrating that woundings induced by sensor insertion were easily recovered by the plants and caused no excessive damages.

The study continued by analyzing the link between bioristor parameters and the physiological state of the plant; to this end, the variation in sensor parameters was studied along with changes in the humidity of the plant's surroundings. Consequently, a strong increase in sensor response was detected upon the increases in the relative air humidity (RH%) and a decrease in Vapor Pressure Deficit (Vurro et al. 2019). The bioristor showed a similar trend with the transpiration rate enabling to trace the plant transpiration throughout the measurements of the ions dissolved in the plant sap in the transpiration stream (Janni et al. 2021).

After these initial tests, essential to verify the usability of the transistor as a sensor for plants, the application of the bioristor in phenotyping was evaluated (Janni et al. 2019). In this context, our research group coupled bioristor measurements with high-throughput scanalizer image based platform (Lemnatech, Aachen, Germany) analysis of plants subjected to drought stress, envisaging the relevance of this tool in plant breeding and variety selection (Janni et al. 2019). The first study in the field was published in 2019 by Janni *et al*. and involved the use of tomato plants. The application of the bioristor showed its efficacy in detecting the ongoing stress and demonstrated sensor response's correlation with the stomatal conductance as well as with the digital biovolume (Janni et al. 2019).

Bioristor's efficacy in detecting plant stress conditions was demonstrated under saline stress conditions too (Janni et al. 2021). The study, performed in *Arundo donax*, allowed to increase the knowledge around the dynamics of saline stress response (Janni et al. 2021). In particular, an increased R in both basal and apical sensors, as well as a linear correlation between R and the concentration of cations, clearly indicated that the bioristor can effectively sense presence and changes of cations in the plant sap. The R trend observed is consistent with the daily transpiration trend due to light-driven stomatal opening and the consequent onset of transpirative passive flux from the soil to the air. Overall, the results support a positive ion compartmentalization, namely of Na^+, in the basal portion of the plant during the early phases of the saline stress, following the addition of NaCl to the substrate. Moreover, the ion transport was described

by the NR as follows: the basal sensor (BS) continuously detected a different and higher number of positive ions at lower rate, whereas the upper leaves showed that higher values of ions occurred at a later stage of salinity stress (14 days post insertion).

The bioristor was applied in the field as a first use case as well, enabling the continuous monitoring of the plant health status during the entire tomato plant growth and development. The application of different water regimes led to the hypothesis that a water saving of 40% could be achieved if a bioristor was used (Vurro et al. 2023a).

The feasibility of bioristor as a tool for plant monitoring was demonstrated also for fruit trees (Vurro et al. 2023b). In this study, the biosensor was applied to continuously monitor fruit tree crops, demonstrating its ability in analyzing physiological plant status and the changes in the physiological processes, such as the transpiration rate and environmental conditions; moreover, it reported the occurrence of water stress in a timely manner. The sensor response showed a trend in accordance with previously reported data in kiwi, where the fruit transpiration rates are generally high during early fruit growth but decline to much lower values towards maturity (Montanaro et al. 2012). As previously seen for herbaceous plants, sensor response inverse correlation with stomatal conductance was demonstrated in trees too, proving that the reduction in transpiration is triggered to prevent the loss of water (Janni et al. 2019). The fact confirmed its usefulness in deficit irrigation regimes, in which the stress level has to be carefully monitored; the deficit irrigation strategy is a water management practice born to reduce water usage as well as to manipulate fruit size and sugar content for a premium price in specific markets (Romero et al. 2022).

Under drought, the R circadian pattern showed a decrease in the slope that is pronounced in apple and kiwi, while the flattening of the R is reduced in grapes, indicating an increased tolerance to drought. A difference among and within the fruit species' transpirational water losses, which is responsible for a reduction in the fruit water balance, was also observed; this confirmed that there is a positive influence on the fruit's ability to attract xylem and phloem flows, since they reduce fruit pressure potential, thus potentially increasing stem-to-fruit water potential and supporting the trend of the sensor response (Rossi et al. 2022).

Sensor parameters prove sensitivity to rainfall events too, since, because of leaves wetting, it causes a strong increase in the R values, which in turn causes a block in the transpiration process. The strong increases in R value can thus be used to exactly calculate the overall time of leaves wetting and to correctly plan actions to avoid the development of fungal diseases (Jindo et al. 2021).

Bioristor technology is patented in Europe, USA, and Mexico (published as EP3559647A1; IT201600130803A1; WO2018116149A1).

Due to its features and novel capabilities in plant phenology, all the information learned so far paves the way to a possible application of bioristor in plant phenotyping.

2.7.3 Sensor assembling and readout

The bioristor assembling procedure consists of 3 conceptual phases: sensor insertion, connection and securing. The first one is realized by employing a needle, required for the PEDOT:PSS functionalized fibers to be placed inside the plant. The phase can or not be preceded by a hole drilling pre-phase (⌀ 0.5 mm), taking place just for tree species. Next, the textile fibers are physically and electrically connected to copper wires tying them to each other and surrounding the contact points among the two wires with conductive paste (RS Components Ltd., Northants, UK). The operation is completed by securing the entire structure with a holder, employed to reduce the weight of the wires on the plant. Sensor insertion's last step is the sealing with some hot glue drops, this operation is done when needed. The result is visible in the photo below.

Fig. 21 - Bioristor implementation in *Malus domestica.* The T-shaped blue part is the holder, fastened around the plant branch. On the right, the sensor's label, use to ease its identification.

The two electrodes composing the bioristor are prepared soaking a textile fiber in the PEDOT:PSS - DBSA solution and later inserted inside the plant.

The channel electrode protrudes outside of the plant at both the sides and is connected at the extremities with two copper wires whereas the gate is connected only at one end, in correspondence with the gate terminal.

The three wires transmit the signal acquired to an Arduino based control unit designed by the authors leading the information to be recorded on-site and sent in real time at the server.

The control unit reads and supplies the power to the sensors providing a fixed voltage across the channel electrode (V_{ds}) and an alternate voltage between channel and gate (V_{gs}). The V_{gs} square wave oscillates between 0V and 0.5V with a period of 30 minutes and a 50% duty cycle. Each sensor is driven at low voltages (V_{ds} = -0.1V, V_{gs} = 0.5V) in order to reduce plant rejection phenomena and to maximize the duration of the device itself (Manfredi et al. 2023).

The control units utilized for sensor data acquisition have been custom-developed in our laboratory to fit in two distinct usage scenarios, the first one involves conducting experiments in open field conditions, while the second one within controlled environments. Both the control units share the core circuit designed for Bioristors reading, involving some analog-to-digital converters (ADCs), and powering as well as the two used to save data locally and send them wirelessly to the CNR server.

Specifically, the control unit designed for field experiments is optimized for situations where plants under observation are spread across significant distances. To address this, the unit has only four channels for data acquisition (Fig. 22 A, B, C, D, E), moreover to ensure uninterrupted measurements in remote locations, this unit is equipped with a 12 Ah lead battery, a solar panel and a charge controller (Fig. 22 F, G, H). This configuration enables an IoT approach and a continuous data collection.

The second control unit, planned for controlled environment experiments, reads 15 channels simultaneously (Fig. 22 I); each reading channel is connected to a bioristor. The unit doesn’t require extensive autonomous power equipment and is connected to the power grid, allowing for 24/7 operation.

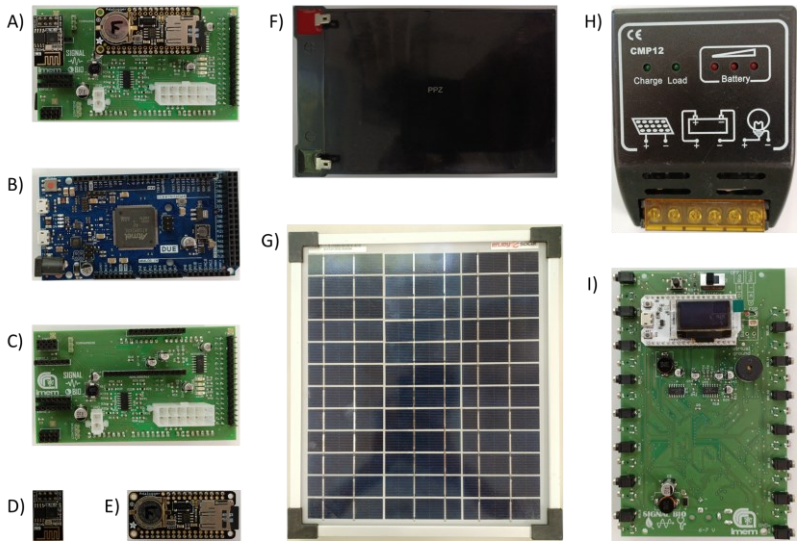

Fig. 22 - A) Field control unit fully assembled, B) Arduino DUE (providing the microcontroller for the field control unit), C) Arduino DUE shield for sensor reading, D) WiFi module (field control unit), E) RTC + SD slot (field control unit), F) lead battery for field monitoring, G) 10W solar panel for lead battery charging, H) charge controller, I) controlled environment control unit.

Bioristor is read in real time using a data analysis script written in Matlab programming language (https://uk.mathworks.com/).

2.7.4 Sap measurements sensors

The sensor adopted in this thesis is original and, as far as we know, there are on the market a number of sensors enabling the measurements of sap flow but no previously reported sensors enable the detection of the ion's concentration and changes within the plant sap.

Within the sap flow sensors, heat-based sensors are the most common and commercially available, they use a heat pulse or a heat balance method to estimate the sap flow rate by measuring temperature difference between two or more probes inserted into the plant's body (Dix and Aubrey 2021). Dye-based sensors instead use colored or fluorescent dye to track the movement of sap in the plant; they can provide high-resolution images of the sap flow distribution and velocity, but they are usually invasive (Swanson et al. 2011). NMR-based (nuclear magnetic resonance) sensors use a magnetic field to measure sap flow by detecting the spin of the hydrogen atoms in the water molecules. Although non-invasive, they provide accurate and continuous measurements of the sap flow and the stem water content.

However, they are expensive, complex to operate and hardly scalable (Kumar et al. 2022). In the field, most techniques focus on the flow of sap rather than its content, which gives the bioristor a strong advantage over all others.

A second approach is the pH measurement. The procedure consists in the measurement of the sap pH and it normally implies destructive techniques to extract plant sap and plant samples. Thus, it does not involve in vivo measurements, however it can be used to measure plant stress level and metabolic activity (de Menezes de Assis Gomes et al. 2023).

Recently, Electrical Impedance Spectroscopy (EIS) as described in Jócsák et al. 2019 has also been used as a method for plant measurements. EIS works in alternate current mode, using external electrodes placed on the leaves to measure impedance and its correlation with water and salt stress.

The following table shows some commercial tools used for plant monitoring, with a focus on their biocompatibility, capability of performing in-vivo monitoring, real-time monitoring, analytical sap measurement and environmental monitoring.

Tab. 1 - Comparison between the bioristor and some commercial plant monitoring instruments.

	Biocompatibility	In-vivo	Real-time	Analytical sap measurement	Environmental monitoring
Bioristor	X	X	X	X	X
ICT INTERNATIONAL		X	X		
NAelettronica NEW AGROTECNOLOGY			X		X
Dynamax			X		X
AERMATICA3D KEY FROM THE SKY					X

Summarizing, bioristor represents a novel approach to analyze plant sap and to monitor the plant physiological status. Its innovative features concern not only the type of information that can be collected, but also the possibility of using it in vivo, in real time, non-invasive, with minimal stress to the plant and the possibility of rapidly scaling up the number of plants monitored. Moreover, it allows to extract more precise information about the composition of plant sap.

3. Commercial Variety experiment

To demonstrate the efficacy of bioristor in classifying plant material more adaptable to climate change and adverse conditions, our approach covers the monitoring under drought stress of increasing genomic complex tomato material.

We started using commercial varieties, developed with the aim of increasing yield and improving quality features. As previously explained, the ongoing selection approach leads to a depletion of the genetic background and variability of crops, strongly reducing their adaptability to the ongoing climate change.

Two varieties developed in Emilia Romagna by a breeding company (ISI sementi), Mariner and Faber, as well as a reference variety called Red Setter, were identified as targets in this controlled condition experiment.

Mariner is an elongated hybrid tomato variety with a medium-early cycle, with a compact plant, well covered, healthy and very productive, while Faber is a tomato hybrid with vigorous and healthy plants. The prismatic fruits have high consistency and hold, thick pulp, intense red color and excellent Brix. Red Setter is a processing tomato variety that completes its reproductive cycle within 110 days, it is a highly productive variety and its architecture permits mechanical harvesting.

The experiment was conducted in the Parma University campus, inside a greenhouse under natural photoperiod (13/11 day/night).

3.1 Material and Methods

Plant material

Three controls and three stressed plants for each variety were grown in a greenhouse. Twenty seeds for each genotype were sterilized in 70% ethanol solution for 5 minutes followed by a wash with 10% (v/v) sodium hypochlorite for 5 minutes. Seeds were placed in 9 cm petri dishes on wet filter paper and left for germination in a dark environment for 7 days at room temperature. Seedlings were then transferred to seedbed in a growth chamber at 18/6 h light/dark photoperiod at 25 °C and, at the fourth leaf stage, were moved to a greenhouse at 25 °C and potted into 0.6 L pots.

Drought treatment

Plants were grown up to the fourth leaf stage under full irrigation conditions then, the biorsitor was inserted in the plant stem. After 6 days of sensor stabilization, the drought stress was imposed on half the plants (the stressed) by water withholding for 8 days (from 0 to 8 DAS) whereas controls were kept fully hydrated for all the duration of the experiment. Due to severe drought stress effects on stressed plants, an emergency irrigation occurred 4 DAS, hence 50 ml of water per pot was restituted to them. At 6 and 7 DAS, 15 ml of water was also restituted to the stressed to avoid irreversible damages (Fig. 23).

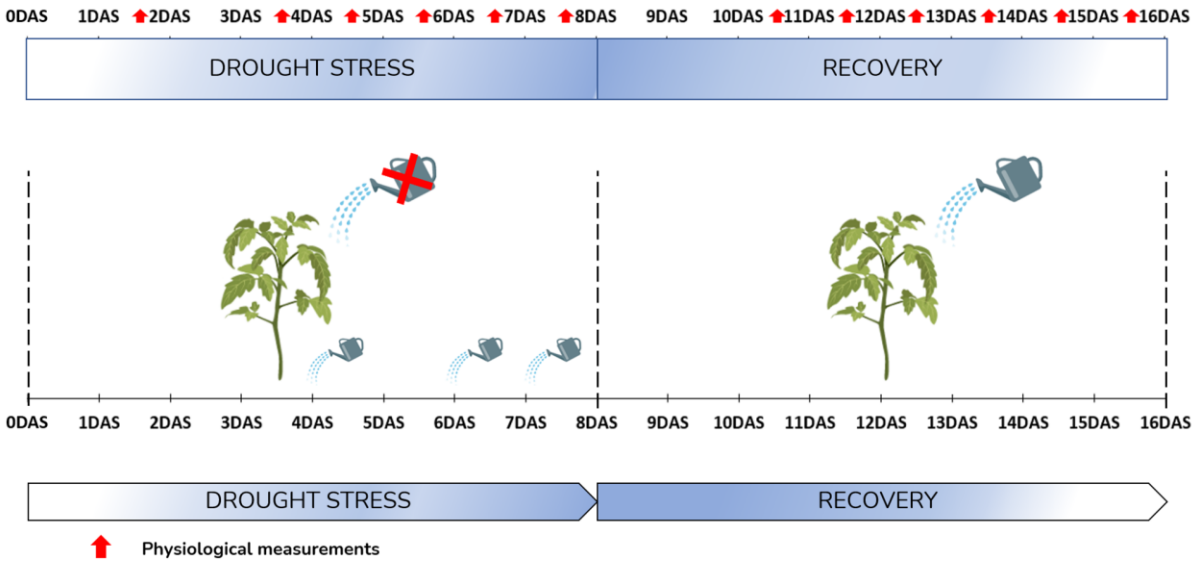

Fig. 23 - Experimental design of trial. DAS, Days after stress; red arrows indicate the physiological measurements. Watering cans visible during drought stress and red arrows mark the days during which irrigations and measurements respectively occurred.

Sensor response analysis

The main parameter returned by the sensors (sensor response) was extracted from the raw data acquired by the control units through a MATLAB script and analyzed using Excel (Microsoft Excel 2016) allowing the data to be cleaned, trends smoothed using 24 hours moving average and thesis curves to be merged. The normalized sensor response was shown. Bioristor sensor indices R, I_{gs}, τ_{ds}, τ_{gs} and their derivative values dR, dI_{gs}, $d\tau_{ds}$ and $d\tau_{gs}$ were acquired through bioristor and used in the principal components analysis (PCA) to increase the resolution analysis and emphasize the differences between genotypes. The normalized response (NR) was then calculated dividing stressed R by controls R in order to relativize stressed trend to the control once.

Physiological measurements

Stomatal conductance

Stomatal conductance (g_{sw}) was measured in situ using the AP4 porometer (Delta-T Devices, USA). Within each measurement day, a variable number of measurements (between 6 and 12) were taken per plant, with a maximum of 36 measurements per water regime. All the measurements were performed at 9:00 am.

PSII: Fv/Fm

The effect of the drought on photosystem II, Fv/Fm, was evaluated with the fluorometer FluorPen FP110 (PSI, Drásov, Czech Republic). One measurement per plant was taken for a total of 3 measurements per water regime. Readings are acquired after 15 min of darkness acclimation of the leaf. All the measurements were performed at 9:00 am.

Morphological analysis

Plant height was recorded before stress imposition (0 DAS) as well as 6 and 15 DAS. To do so, the distance between the base of the plant and the youngest node was taken into account using a flexible meter.

Stress rate (%)

All pots belonging to control and stressed were weighed on 2, 4, 5, 6, 7, 8, 11, 12, 13, 14, 15 DAS, the relative soil water content (%) was calculated as follows:

$$Relative\ soil\ water\ content\ (\%) = \frac{soil\ in\ stress\ condition\ (g) - dry\ soil\ (g)}{soil\ at\ full\ capacity\ (g) - dry\ soil\ (g)} \times 100$$

Data regarding single variety water loss during the trial are reported as a table.

Environmental monitoring

Environmental data were collected during the entire duration of the experiment using a datalogger having temperature and humidity sensors embedded, allowing the calculation of the VPD; values were reported as curves to show their trend over time (see figure 24).

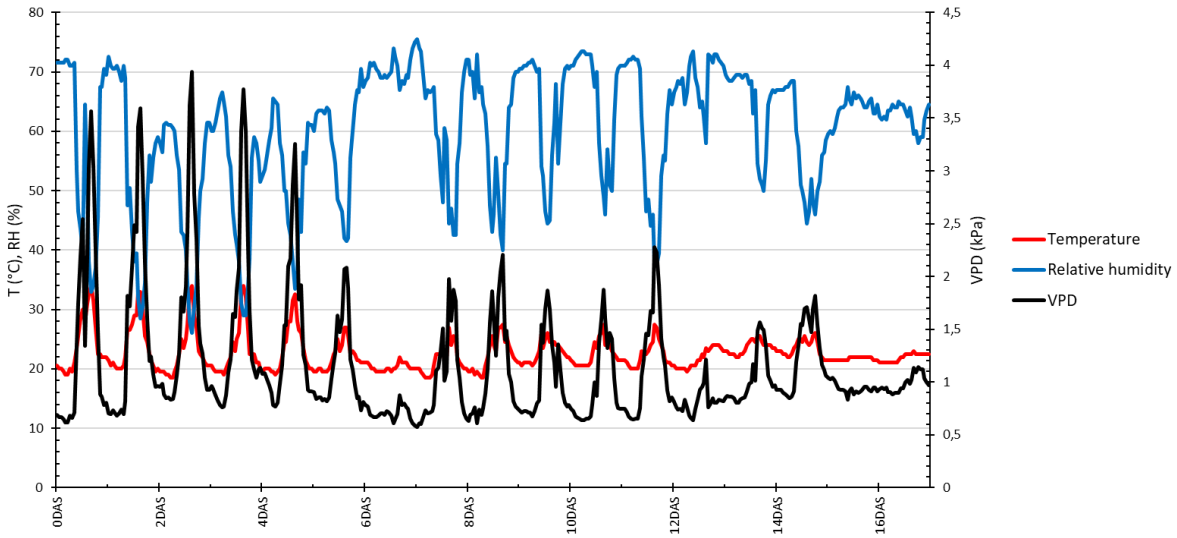

Fig. 24 - Environmental parameters: the graph shows the trend of temperature (°C), relative humidity (%) and vapor pressure deficit (kPa) during the entire experiment duration. DAS stands for days after stress

The plot highlights the presence of strong daily oscillations during all the 16 days, except for the 6 DAS and for the 16 DAS. The average vapor pressure deficit (VPD) has a sensible reduction within the 6 DAS and is stable for the rest of the time; this trend is mainly driven by the falling of the temperature, whose maximum diurnal peaks move from 34 to 27°C, whereas relative humidity oscillations keep comparable fluctuations during all the time.

Statistical analysis

All bioristor data, subjected to analysis employing MATLAB (https://uk.mathworks.com/) and Microsoft Excel 2016, were smoothed over days to mitigate variations associated with the circadian cycle. Therefore, an Anova test (p-value < 0.05) was computed utilizing a MATLAB script to evaluate the significance of the differences observed between genotypes and treatment. R studio script (https://cran.rstudio.com/), based on the factoextra package (https://cran.stat.unipd.it/bin/windows/contrib/3.5/) enabled Principal Component Analysis and k-means clustering used for thesis by leveraging sensor parameters. Fv/Fm results were analyzed by applying the

ANOVA test with p-value < 0.05, followed by Tukey's test using R software 4.2.3 applying the 'aov' function. The Student t-Test was applied to analyze the difference in plant height and stomatal conductance.

3.2 Results

Morphological traits analysis

Plants' height observation revealed a variety-dependent effect of the stress (fig. 25).

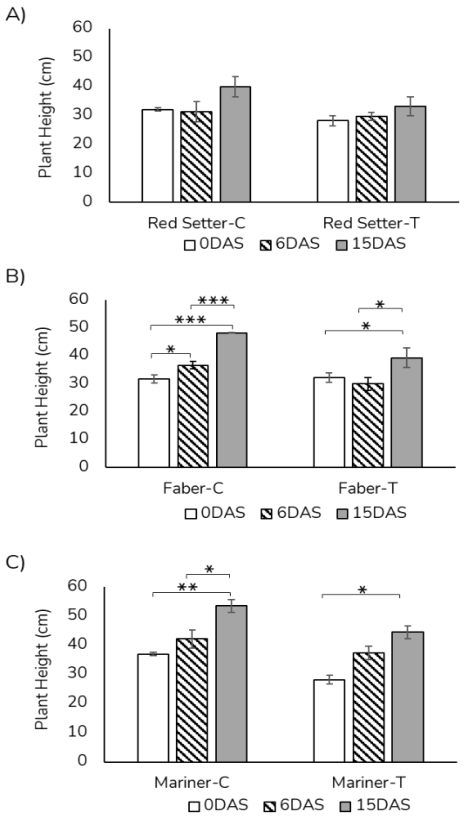

Fig. 25 - Plant height plot for the three varieties analyzed. 0 DAS, before the stress imposition, 6 DAS soon before the end of the drought stress, 15 DAS end of the recovery. A) cv. Red Setter, B) cv. Faber, C) cv. Mariner. Student's test was applied (*p<0.05, **p<0.01, ***p<0.001).

An overall decrease in plant height was observed in drought stress plants in comparison with the controls once, with the exception of Red Setter (Fig. 25 A), which did not show significant decreases even at 15

DAS. The treatment significantly reduced Faber's growth of about 31.01% (Fig. 25 B) whereas Mariner growth decreases in height was about 19.24% (Fig. 25 C).

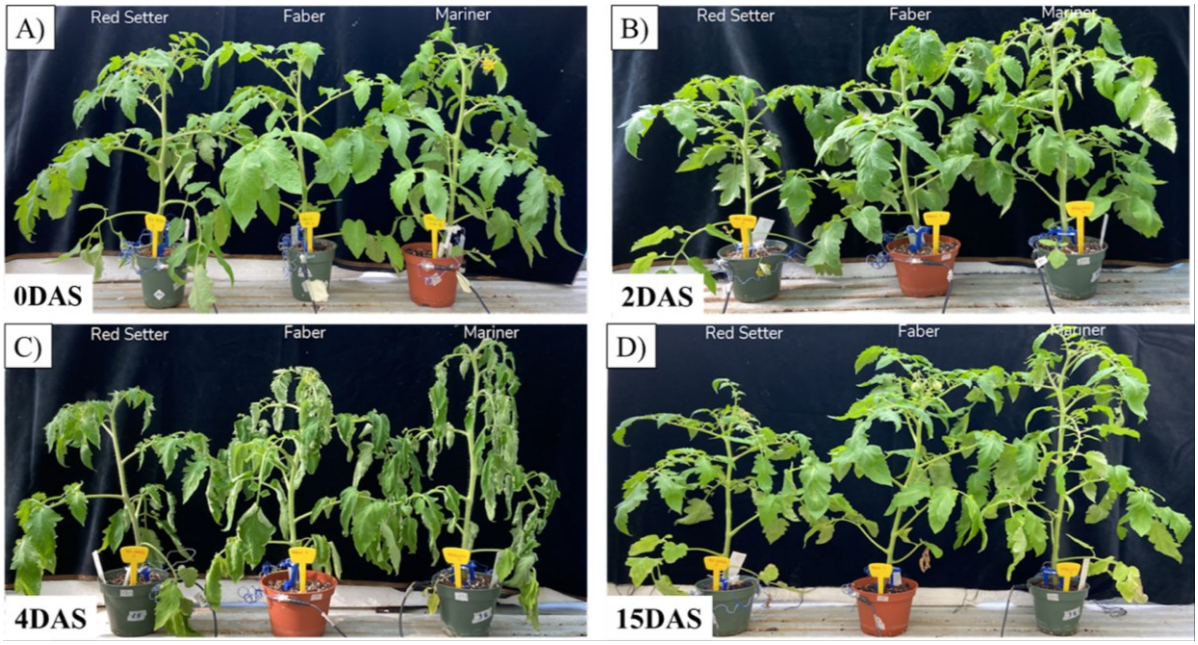

Fig. 26 - Mariner, Faber and Red Setter plants during the drought stress experiment. A) control plants at 0 DAS, B) two days after the onset of the stress (2 DAS), C) four days after the onset of stress (4 DAS), D) plants during the last day of recovery (15 DAS).

Stressed plants visually showed reduced leaves turgor at 2 DAS (Fig. 26 B) and 4 DAS (Fig. 26 C), appearing more evident in Faber and Mariner; the phenotype was fully restored after rewatering (15 DAS, Fig. 26 D).

Bioristor characterization: Normalized Sensor Response and PCA analysis

The analysis of normalized sensor response (NR) is shown in the following plot.

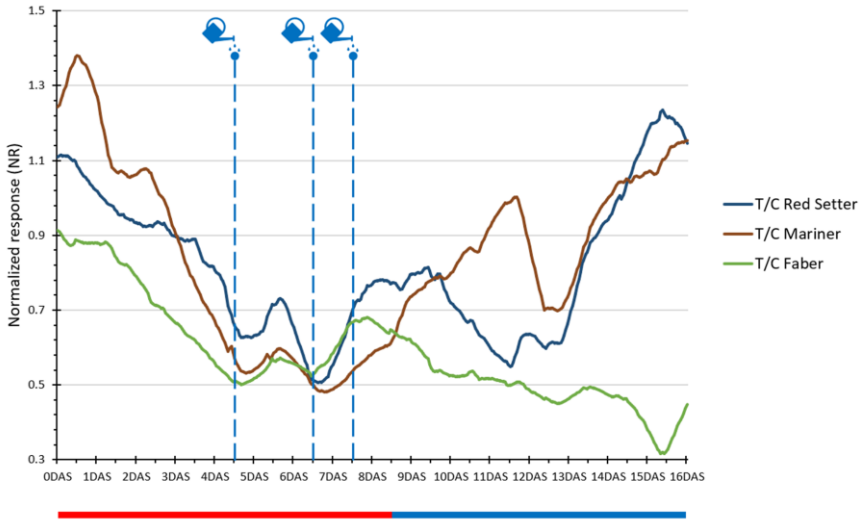

Fig. 27 - Plot of the Normalized Sensor Response (NR). Each variety is represented by a coloured curve; red bar, marks the time during which the plants have been exposed to drought, blue bar, recovery time. Light blue lines and watering cans indicate the rescue irrigation.

The analysis of normalized sensor response pointed out a strong and rapid reduction of the values within the first five days of the stress, with an acclimation peak at 2 DAS for Mariner. A rapid decrease of the NR signal was recorded in Mariner whereas Red Setter decreases much slowly (Fig. 27). In all lines, following emergency irrigations performed at 4, 6, and 7 DAS, an increase in NR was recorded. In the recovery phase Mariner showed an increase in the sensor response following rehydration (8.5 DAS) returning to pre-stress conditions, while Faber did not recover, despite the water input. Red Setter showed a variation attributable to the occurrence of a drought stress (9.5 - 11.5 DAS) and a recovery of the NR index at 11.5 DAS, three days after Mariner (Fig. 27).

Relative soil water content

The relative soil water content was monitored to ensure the establishment of the drought condition; values are visible in table 2. The water present in the pot rapidly decreases from 100% (the maximum volume of water the soil is capable of keeping) to around 58% in the first 2 DAS; the level is maintained quite stable over the whole stress because of the emergency irrigations. A consistent rise is visible at the beginning of the recovery; note, values above 100 are due to plant growth.

Tab. 2 - Relative soil water content variation over time: Treated only has been reported since Control has been maintained at fully hydration level (irrigations are always realized after sampling)

	2DAS	4DAS	5DAS	6DAS	7DAS	8DAS	11DAS	12DAS	13DAS	14DAS	15DAS
Faber - T	58,8	49,7	53,3	49,7	50,4	50,1	82,7	106,7	105,7	107,7	95,0
Mariner - T	56,8	47,7	51,6	48,9	49,7	48,9	80,6	102,4	102,7	104,4	93,4
Red Setter - T	58,9	47,4	52,5	49,8	50,5	48,0	80,5	100,6	100,8	102,0	93,9

Physiological measurements

Stomatal conductance, as a proxy of physiological stress in the plant, was measured through the entire length of the test.

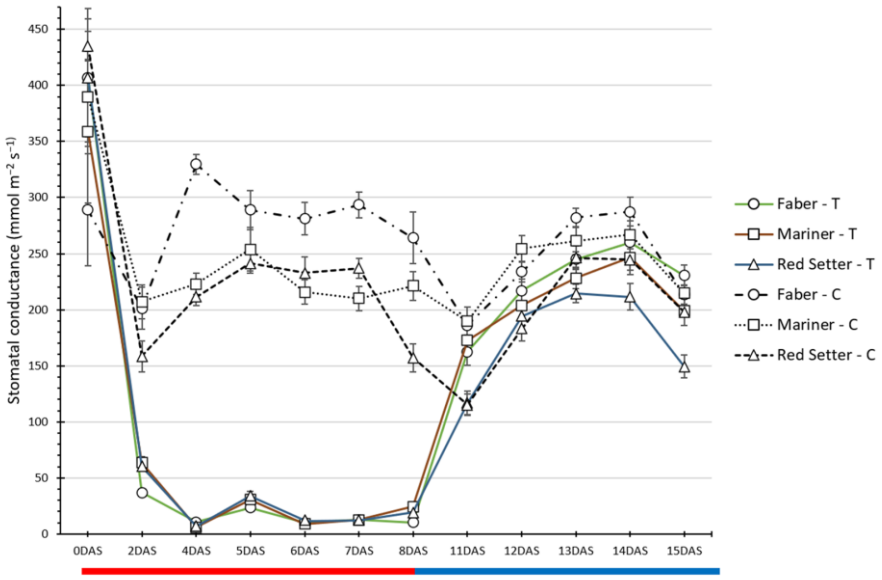

Fig. 28 - Stomatal conductance. Solid lines, stressed plants (- T), Dashed lines, controls (- C). Red bar indicates the drought stress, blue bar, the recovery (rewatering).

All the three varieties showed a considerable stomatal closure 2 DAS, after the stress occurrence. A 81.66% reduction in the stomatal conductance was observed in Faber, 69.31% in Mariner and 61.85% in Red Setter (Fig. 28) compared to the starting values.

A slight increase in the stomatal conductance, was observed at 5 DAS, due to the emergency irrigation with 50 mL. At 11 DAS, after about 2 days of recovery, all varieties restored the stomatal conductance.

Being the photosynthesis emitted by chlorophyll an important parameter for photosynthesis monitoring during abiotic stresses, and being this parameter affected by drought (Al-Yasi et al. 2020), the Fv/Fm ratio was measured to monitor the effects of the stress at the photosynthetic system level (Tab. 3).

Tab. 3 - Quantum efficiency of PSII (Fv/Fm), ANOVA test was applied: T stressed, C control.

	Faber - T	Faber - C	Mariner - T	Mariner - C	Red Setter - T	Red Setter - C
0DAS	0,66	0,64	0,62	0,61	0,65	0,64
2DAS	0,69	0,68	0,69	0,68	0,69	0,68
4DAS	0,71 **a**	0,65 **b**	0,69 **a**	0,63 **b**	0,70 **a**	0,65 **b**
6DAS	0,74	0,70	0,72	0,69	0,74	0,70
8DAS	0,73	0,71	0,73	0,70	0,71	0,70
13DAS	0,72	0,72	0,71	0,71	0,72	0,71
15DAS	0,69 **ab**	0,68 **a**	0,66 **ab**	0,67 **b**	0,68 **ab**	0,67 **ab**

A significant reduction in PSII efficiency was observed in the stressed of all lines 4 DAS (Tab. 3). The PSII efficiency of stressed plants increased, following the rescue irrigation performed between 6 and 8 DAS.

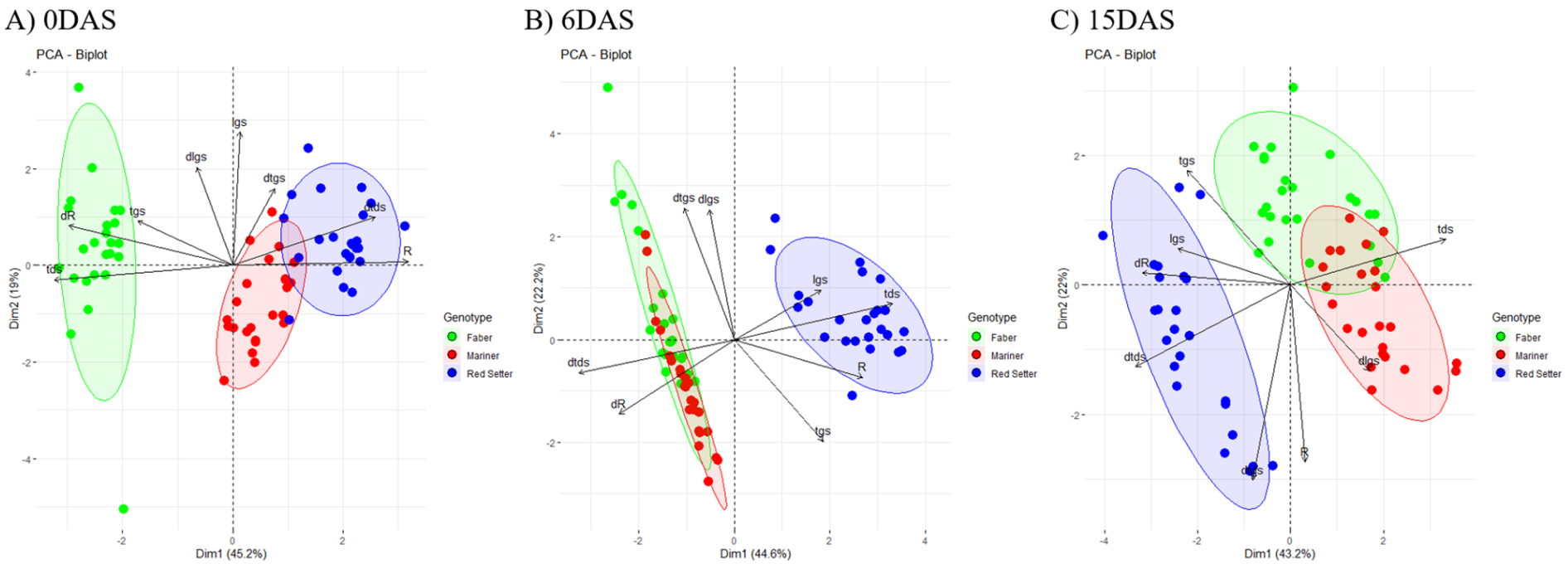

Fig. 29 - PCA plot of the bioristor parameters to identify the dynamics response. A) before the imposition of the stress, B) soon before the end of the drought stress (6 DAS), C) at the end of the recovery (15 DAS). Faber is represented by green dots, Mariner by red dots, Red Setter by blue dots.

PCA was computed with all bioristor indices and the results are plotted in Fig. 29.

At 0 DAS (Fig. 29 A), PC1 and PC2 explain 64.2% of the total variability observed in the varieties before the stress imposition, Red Setter and Mariner grouped together. I_{gs} and R are strongly anti-correlated and they exert a positive and negative influence on PC1 respectively, which results in the segregation of the groups.

Soon before the drought was stopped (Fig. 29 B), that is 6 DAS, the three varieties separated on PC1 forming two groups. τ_{gs} and I_{gs} are strongly correlated with each other but are negatively correlated with dR and $d\tau_{ds}$, the former positively contributes to PC1. At 6 DAS, PC1 and PC2 represent 66.8% of the variability.

At the end of recovery (Fig. 29 C), after rehydration (15 DAS), the first two components represent 65.2% of the overall variability. Mariner and Faber grouped, although the overlapping is partial. Faber and Mariner showed higher I_{gs}, while Red Setter higher τ_{gs}.

Vectors' orientation and length highlights the contributions of the variables to each principal component over time, particularly on PC1, thus leading to the differentiation of distinct groups. In fact, at 0 DAS, PC1 increase is mainly determined by R, τ_{gs}; in 6 DAS by τ_{gs} and I_{gs}, and less by R and the decrease of the remaining features (dR, $d\tau_{ds}$); instead, 15 DAS by I_{gs} and the decrement of all the others but R and the derivative of τ_{gs}.

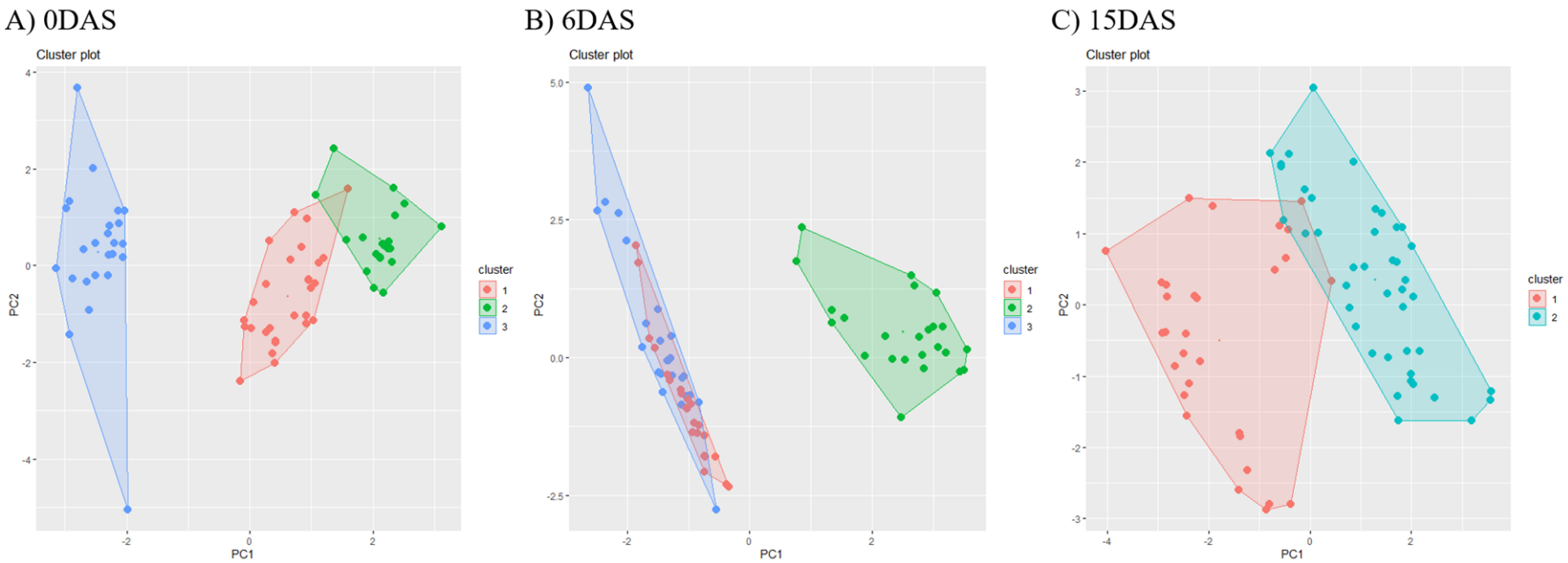

Fig. 30 - Clustering analysis of the PCA's using k-mean algorithm: A) before the imposition of the stress (0 DAS), B) close to the end of the drought stress (6 DAS), C) at the end of the recovery (15 DAS).

The cluster analysis supports the dynamic of the varieties under stress. Three groups are separated at 0 DAS (Fig. 30 A); 6 DAS the three varieties are still separated into 3 groups, despite the almost complete overlapping in the bidimensional plane (Fig. 30 B). 15 DAS Faber and Mariner joined a single cluster while Red Setter is still separated (Fig. 30 C).

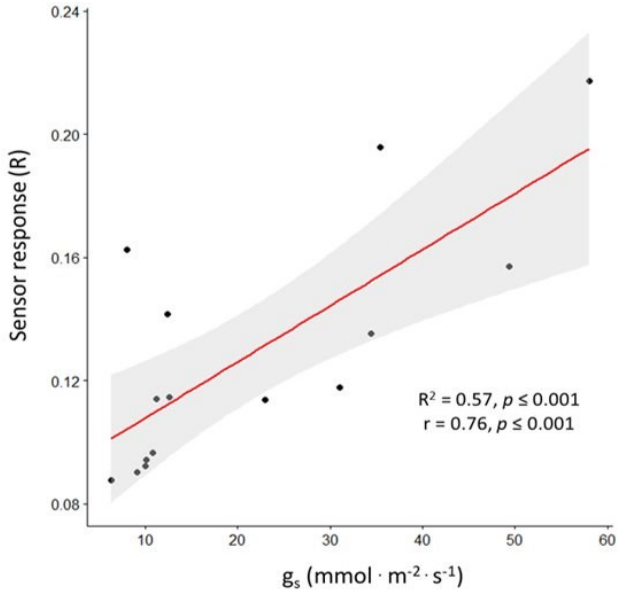

Fig. 31 - Correlation plot of transpiration (g_s) and sensor response (R).

As previously observed a correlation between the parameter and stomatal conductance was observed (figure 31). The link between them proves the strong dependence of the bioristor's parameters with the plant's physiological status, suggesting the possibility to use it as a proxy of the transpiration trend. As shown in the figure, pearson's correlation index has a value of 0.76, with a significance p-value < 0.001.

3.3 Discussion

During the experiment, three commercial varieties, Mariner, Faber and Red Setter were characterized under drought stress; in parallel, conventional phenotyping analysis was conducted to verify the plant physiological activity in comparison with the bioristor data ant to check for stress evolution. As witnessed by the negative slope seen in the transpiration level, all varieties confirmed the occurrence of a strong response to the stress imposed by closing the stomata already within the first two days of stress, as previously observed in several varieties (Liu et al. 2022), confirming that, the relative soil water content reduction seen was sufficient to trigger drought stress. Moreover, as shown by the environmental sensors, the sudden temperature variation may have emphasize the fast and severe drought and thus explains why

it was needed to add an emergency action. The entrance in the recovery phase was characterized by a fast increase of the transpiration levels.

The process used to characterize the drought response of different varieties was based on interpreting the trend of the sensor R curves (see Fig. 32) and studying the set of sensor parameters in a multivariate approach. To do so, the PCA revealed itself to be the most feasible and effective method, together with the implementation of a cluster analysis algorithm, indispensable for an objective recognition of the groups. In fact, compared to other methods, like factor analysis, discriminant analysis, t-distributed stochastic neighbor embedding or multidimensional scaling, PCA facilitates data visualization, requires less computational resources and returns more interpretable and robust results, particularly in noisy datasets.

The comparison with the conventional phenotyping methods demonstrated the advantage of using the bioristor in such studies as, despite stomatal conductance analysis also revealed the occurrence of a variety-specific recovery response, which was faster in Mariner and Faber, instead a little slower in Red Setter, and gave the picture of specific plant behavior on the day of measurement, the use of bioristor can provide more detailed and precise information on the plant health status, being also strongly correlated with the stomatal conductance, the water movements in the plant and the hydration level of the plant tissues (Vurro et al. 2019; Gentile et al. 2022).

Indeed, normalized sensor response traced the stress response dynamics for each genotype, which is observable as a rapid and remarkable reduction of R over time, visible during the first days of stress, and made possible to observe a shifted entrance to the drought for Faber with respect to the other genotypes, evidenced as a temporal shift in the onset of the fall, and a reduced slope in NR for Faber and Red Setter up to the emergency irrigation. Hence, on the basis of the slope grade and of the sensor response in early phases of the stress our data confirm the medium tolerance of Red Setter to drought (Landi et al. 2023). On the contrary, Mariner showed the most rapid slope during early phases of drought. However, Faber did not recover from the stress, as exhibited by the unstopped NR decrease during the recovery, suggesting that the stress may have left chronic effects on it, as previously reported for tomato plants (Hasanagić et al. 2020). Instead, a rapid recovery was observed in Red Setter, and less rapid in Mariner, for which an increasing trend in NR is shown during the entire recovery. Among them, Mariner showed a longer and unstopped recovery from the drought; both the varieties reached at 15 DAS values of NR comparable to those recorded before the stress imposition. Faber bottom NR at 15 DAS, while Red Setter showed an alternation of drought and recovery phases and a final recovery at 13 DAS.

These results are in accordance with the hypothesis formulated by Moshelion and coworkers in 2020 stating that a recovery phase occurs if the stress and/or the adaptation mechanisms enable the plant to

increase its vegetative activity. Moreover, they classified the plant's response to abiotic stresses by distinguishing tolerance, as a measure of the response mechanism's effectiveness and resilience, a measure of the rate of its return to optimal vegetative performance, which will allow it to fulfill its reproductive potential. Finally, resistant is the kind of plant that is not affected by stress at all (Moshelion 2020, Fig. 32).

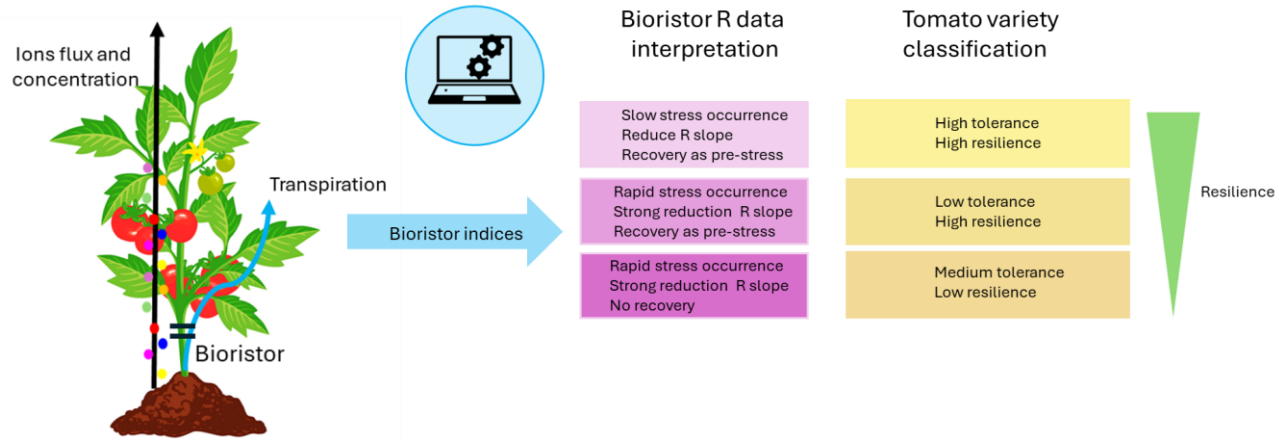

Fig. 32 - Tomato variety classification approach based on bioristor measurements.

On this basis, Red Setter has exhibited the highest resilience to the stress and the highest tolerance, Mariner the lowest tolerance but high resilience, while Faber medium tolerance and the lowest resilience.

Moreover, the similarity detected by clustering analysis between Faber and Mariner during the recovery, mainly determined by their I_{gs} and τ_{gs} values, may provide information about the different recovery strategies actualized as well as the diverse solute possibly accumulated, given their correlation with sap cation concentration (Vurro et al. 2023b); however this hypothesis has to be further investigated.

Additionally, the correlation shown between sensor response and stomatal conductance reinforces the earlier evidence of the link between bioristor's parameters and plants physiological status, together with the earlier detection of ongoing stress status, supporting its importance in functional plant phenotyping.

3.4 Conclusion

1. The experiment showed the feasibility of using the bioristor to characterize the genotype-dependent response to drought, enabling the detection of different tolerance capacity of tomato varieties and their resilience level.
2. By using the whole set of parameters returned by the sensor, the varieties characterization is made possible through a multivariate approach involving PCA and cluster analysis.
3. Given the capability of performing continuous monitoring, the implementation of the bioristor allowed us to observe the dynamic of the plant response to the stress.
4. The observation of R underlined the importance of studying not only the plant's response to the stress but also to the recovery to obtain a more complete characterization of the plant performance.
5. The current experiment, together with the previously reported results, demonstrated the correlation of the bioristor with stomatal conductance and the plant water status.

4. Project AICS international cooperation

A further test was performed for an international cooperative 'Maison Parma' project focused on Burundi Agriculture.

The objective of the project is to organize the production, processing and marketing of some products, including rice, cassava and other fruits and vegetables, according to a supply chain approach, to enable small producers to improve their activities, so as to contribute to food security and poverty mitigation.

The project will address the problems daily experienced by the population of Burundi, such as lack of means, insufficient exploitation of production, post-harvest losses and limited knowledge of processing and storage techniques, leading to a sustainable and shared agriculture and technology transfer.

'Maison Parma' represents a concrete experience of cooperation between territories (Parma and Burundi), international organizations, public and private bodies that make systems to fight hunger and poverty by promoting the skills and capabilities of our territory in the field of agri-food. Among them, the main characters were the City of Parma, the City of Burundi, Parmalimenta, Stuard and IMEM.

Here, the bioristor aimed at selecting improved varieties more adaptable to climate change and to further push the possible use of the sensor to automatic irrigation management; hence a first experiment was performed in greenhouse in pots, while the second one was performed in open field in Burundi.

4.1 Greenhouse variety bioristor monitoring

Similar to the previously described experiment, a greenhouse trial was performed to identify variations in genotype tolerance to drought, providing an additional proof of the bioristor application in plant breeding.

4.1.1 Materials and Methods

Plant material

For the experiment were used the Tomato (Solanum lycopersicum) varieties 38244, 33012 and 25561 kindly provided by 'ISI sementi' and previously selected by the same company according to their better adaptability to the burundian environment. 30 to 50 seeds of these varieties were sowed in seedbeds, and grown for 3 weeks after germination. Seedlings were transplanted and sensors inserted at the fourth leaves stage. A total of 18 plants were monitored using the bioristor, 9 control plants and 9 stressed plants; each variety was replicated in 6 plants.

Environmental data

Air temperature and relative humidity (T°C, RH%) have been recorded for the entire length of the experiments using a data logger, allowing for the calculation of the VPD (see figure below).

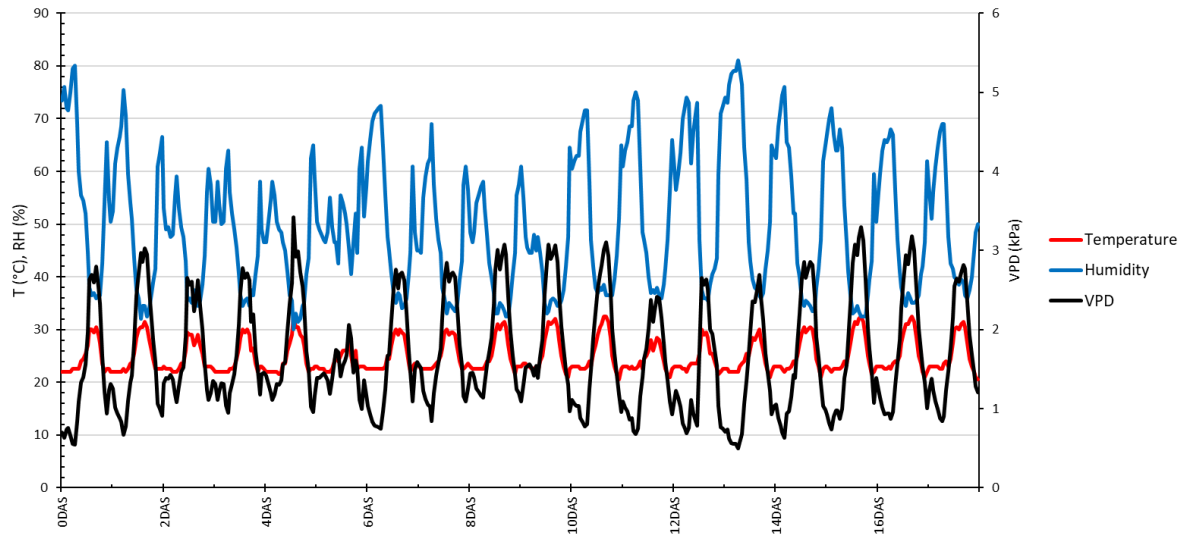

Fig. 33 - Environmental parameters: the graph shows the trend of temperature (°C), relative humidity (%) and vapor pressure deficit (kPa) during the entire experiment duration.

As it turned out, the day-night temperature fluctuations remained constant throughout the experiment; relative humidity varied more, but only slightly affected VPD, which fell sharply only on the fifth day.

Drought treatment

Drought stress was imposed for 10 days by water withholding, leading to a gradual reduction of the relative soil water content; plants were later fully rehydrated during the recovery phase. At 6 DAS an emergency irrigation was operated to avoid irreversible damages as a consequence of the severe drought. Stress level was supervised by means of porometer measuring and pot weighting; the experimental design has been summarized in Fig. 34.

Relative soil water content was assessed by weighting the pots and using the following formula.

$$Relative\ soil\ water\ content\ (\%) = \frac{soil\ in\ stress\ condition\ (g) - dry\ soil\ (g)}{soil\ at\ full\ capacity\ (g) - dry\ soil\ (g)} \times 100$$

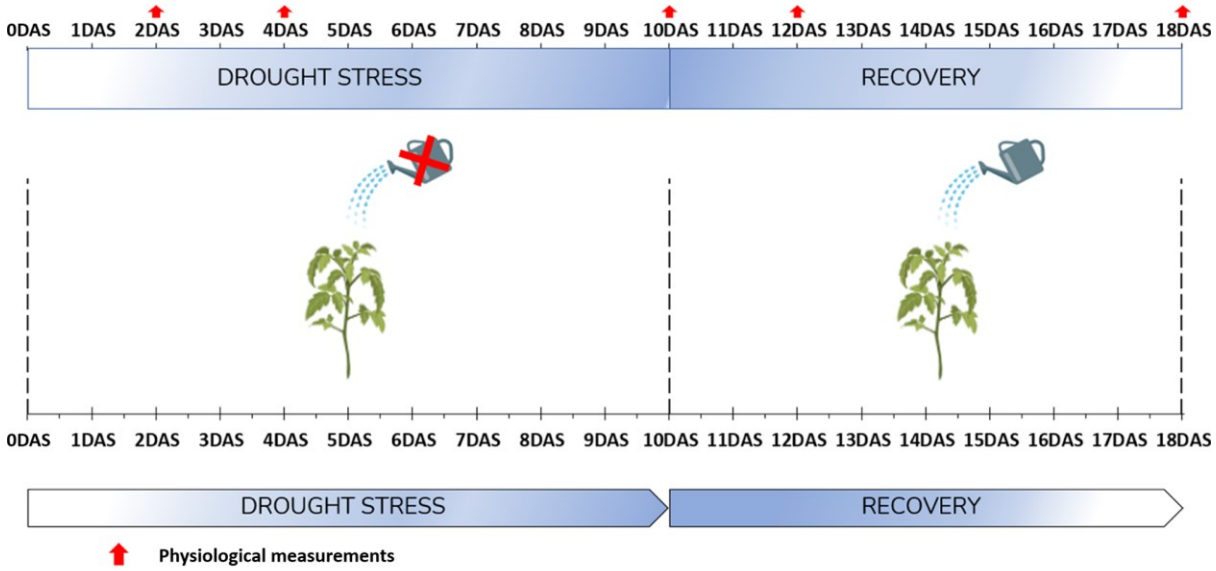

Fig. 34 - Experimental design for Burundi experimental trial. Drought stress 0-10 DAS, Recovery 10-18 DAS. Red arrows indicate the physiological measurements days.

Physiological measurements

Stomatal conductance, together with relative soil water content analysis, was chosen to trace the evolution of the stress and was measured by using the AP4 porometer (Delta-T Devices, USA). Five measurements

were performed at 2, 4 and 10 DAS when stress conditions reached their maximum level, and 12 and 18 DAS after the beginning of recovery. All the measurements were conducted at 9:00 am to ensure an optimal comparability and to prevent physiological daily plant fluctuation from influencing the data.

Bioristor implementation in plant

Bioristor were inserted at 4-leaves stage in the internode located just above the cotyledons (around 5 cm above the collar); each plant was equipped with one bioristor. Data collection was managed with the MATLAB script (https://uk.mathworks.com/) described above, then the PCA was computed from the main sensor parameters R, I_{gs}, τ_{ds}, τ_{gs} and their derivative values.

Statistical analysis

Data reliability was evaluated using the k-mean clustering algorithm with 1000 iteration cycles. During the analysis, among the clusters having different numbers of input clusters, the best clustering was selected as the one that better divides the data into theses; a smaller number of clusters was preferred if they provide a better separation into different groups of varieties.

4.1.2 Results

Relative soil water content

The relative soil water content was monitored to ensure the establishment and evolution of the drought condition; as visible in Tab. 4, values rapidly decreases from field capacity (FC, 100%) to 60% of FC in the first 2 DAS; the decrease is reduced by the emergency irrigations (6 DAS). A consistent rise is visible 2 days after the beginning of the recovery (12 DAS); note, values above 100 are due to the increased weight resulting from plant growth.

Tab. 4 – Relative soil water content percentage: 2, 4 and 10 DAS are referred to the stress period, 12 and 18 DAS are during the recovery

	2DAS	4DAS	10DAS	12DAS	18DAS
33012-T	55.7	53.0	46.1	88.6	96.0
25561-T	63.4	61.4	52.6	94.7	101.6
38244-T	63.2	60.1	49.9	93.8	102.7

Bioristor parameters

The analysis of the sensor response showed a negative trend of R for all lines during the drought stress already at 1 DAS and a stabilization at 6 DAS, as a possible consequence of the re-watering (Fig. 35). An unexpected behavior of R, with a negative slope, was observed in control plants. At recovery (10 DAS) an increase in the R signal was observed for all lines, reaching the maximum at 14 DAS and a subsequent decrease, with the exception of line 25561. A virtually overlapping trend of 38244 and 33012 was observed during recovery with 38244, that showed a rapid and deeper decrease during drought (Fig. 35),

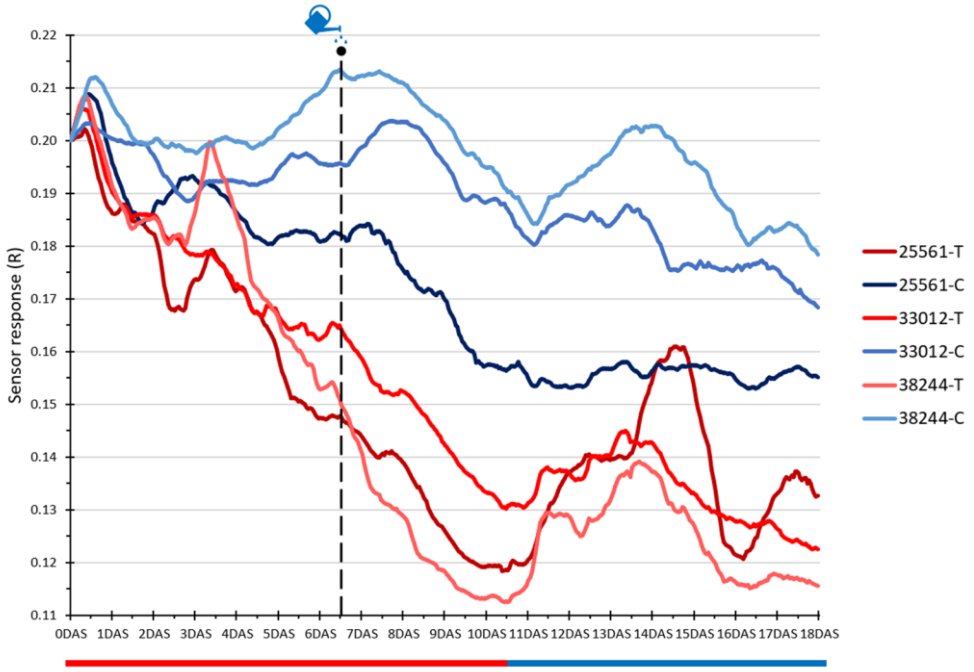

Fig. 35 - Plot of sensor response. Mean values of the sensor response were reported. Blue, control, Red, stressed. Black dashed line indicates emergency irrigation performed in the stressed plants at 6 DAS. Red bar indicates a period of drought stress, blue bar indicates the recovery phase.

A strong influence on the sensor response of environmental parameters was already reported by Vurro et al., 2019, as a likely consequence of the environment on the transpiration.

In fact, the analysis of the 24 hours smoothed VPD trend during the experiment, explains the abnormal R trend in the controls, since it is visible the correspondence of the negative VPD peaks with the positive sensor response peaks, as previously reported in Vurro et al., 2019 (Fig. 36).

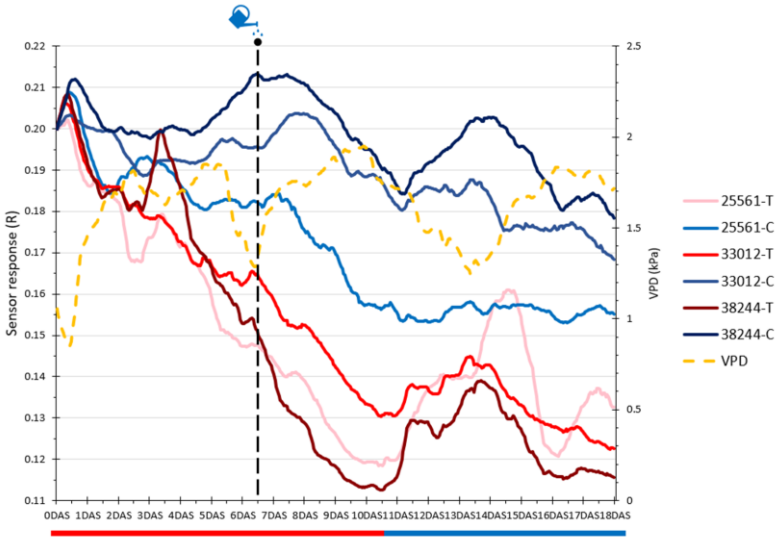

Fig. 36 - VPD influence on the sensor response. Yellow dashed line, VPD. Black dashed line indicates the emergency irrigation performed in the stressed plants at 6 DAS. Red bar indicates a period of drought stress, blue bar indicates the recovery phase.

To highlight the differences recorded with the bioristor among the lines, all the sensor parameters were considered and used to perform PCA analysis during 3 target days.

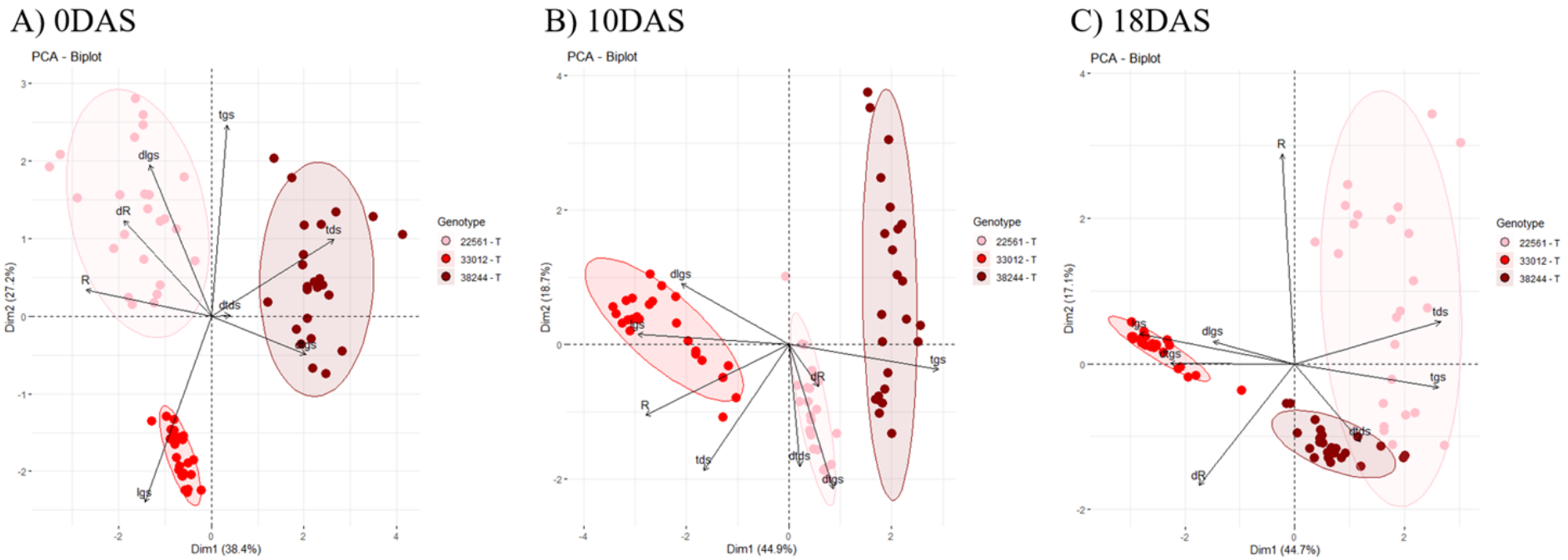

Fig. 37 - PCA results of the normalized values of the stressed genotypes. A) 0 DAS control conditions, B) 10 DAS maximum level of stress, C) 18 DAS, end of the recovery.

The use of the bioristor enables to observe a marked separation among the varieties over time, leading to the distinction of three groups. At the beginning of the experiment (0 DAS, Fig. 37 A) they almost equally fill the bidimensional space, with line 33012 highly influenced by I_{gs}, whereas the 38244, more influenced by τ_{ds} and τ_{gs} and 22561 by R; during that day, the first two principal components account for 65.6% of the total variability. At 10 DAS, lines are equally distributed along PC1 (Fig. 37 B) and, varieties 38244 and 33012, which are oppositely lying, are mainly separated by the values of τ_{gs}, I_{gs} and its derivative. The represented variability in the second moment analyzed is 63.6% of the total. At 18 DAS, the end of the recovery (Fig. 37 C), lines 38244 and 22561 are closer along PC1. At 0 DAS, PC1 mainly represents R, τ_{ds} and the derivative of τ_{gs}, at 10 DAS from I_{gs}, τ_{gs}, R and the derivative of I_{gs}, and at the end of the recovery I_{gs}, τ_{ds}, τ_{gs}, the derivative of τ_{gs} and the derivative of I_{gs}.

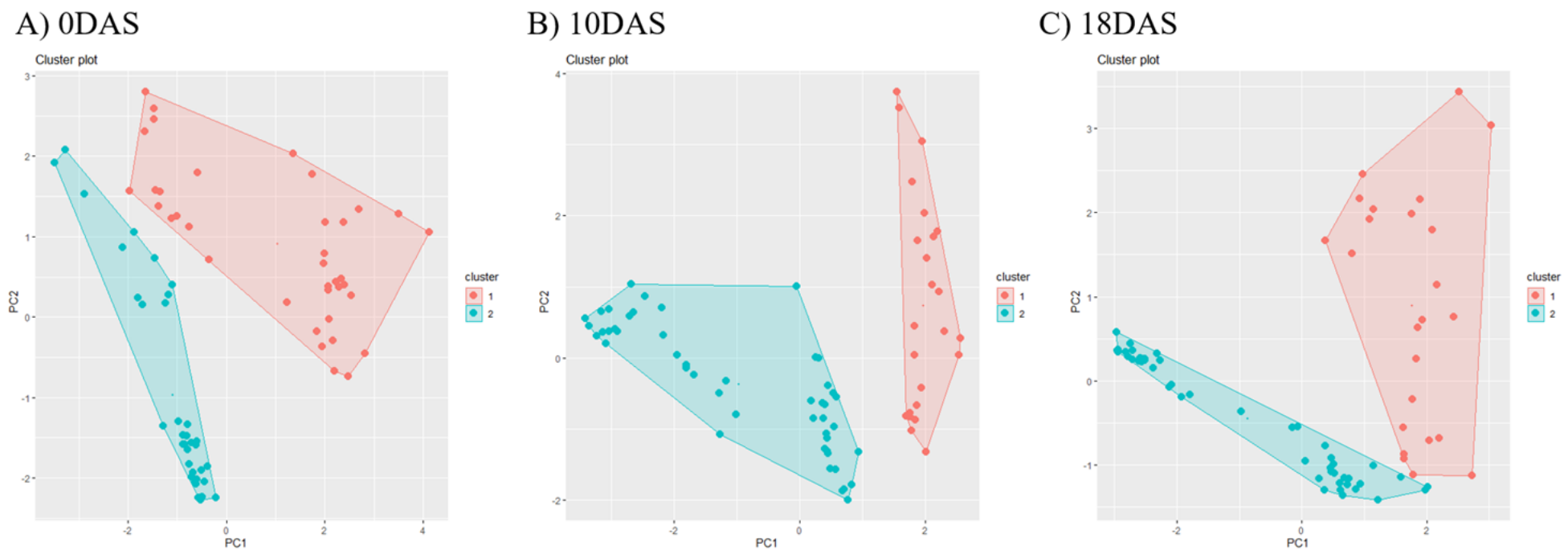

Fig. 38 - Clustering analysis of bioristor's parameters during: A) 0 DAS, B) 10 DAS, C) 18 DAS. Only stressed plants were considered for the analysis.

The k-means clustering algorithm, used to analyze the bioristor indices, allowed to trace the dynamics of the drought response and cluster the varieties according to that (Fig. 38).

At 0 DAS, before the stress, and at 18 DAS, post recovery, 22561 and 38244 clustered together while only 33012 clustered separately (Fig. 38 A).

During the stress at 10 DAS, 22561 grouped with 33012 while 38244 was separated, identifying a specific trend in the response and possibly, a different level of tolerance to the drought stress (Fig. 38 B). The pattern changed at the end of the recovery (Fig. 38 C), showing a higher similarity of the response to rewatering between lines 33012 and 38244.

Fig. 39 - Morphological analysis performed at 10 DAS; A-C) stressed plants, D-F) controls.

The analysis of the plant morphology confirmed the clustering observation highlighting a higher sensitivity of the 38244 to the stress (Fig. 39 C). If compared to that, the others (Fig. 39 A, B) look to better tolerate the stress as the former shows the wilty phenotype, typical symptom of turgidity loss due to the drought.

To confirm the ability of the bioristor in the detection of ionic changes occurring in plant sap, the correlation between R and stomatal conductance were studied, proving that they are highly correlated (r = 0.80) in this test too (see plot below).

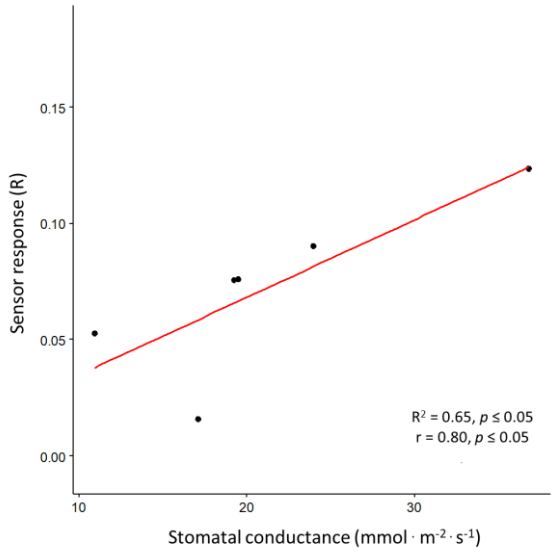

Fig. 40 - Correlation plot between R (sensor response) and gs (stomatal conductance). Analysis performed at 4 DAS and 10 DAS; the trend line as well as pearson's index have been reported.

The correlation between sensor response and stomatal conductance was evaluated also for this experiment, and provided a correlation index R = 0.8 with a p-value 0.05, reaching a comparable level to that of the previous correlation analysis.

The validity of the analysis has been supported by an open field trial. Here the tomato varieties, already tested with bioristor, have been cultivated in Burundi in open field showing a difference in yield consistent with the reported bioristor data analysis. ISI 33012 produced 11.9 t/ha, ISI 2556 produced 19.0 t/ha and ISI 38244 produced 9.7 t/ha (Stuard personal communication).

4.2 Field trial in the Maison Parma project

Due to socio-economic issues, the variety Leonardo has been tested with bioristor in open field in Burundi. Here, plants have been monitored with the bioristor and two irrigation conditions were adopted, one based on bioristor monitoring, and the other conventionally irrigated, as the aim of this experiment has been to test the possibility of using the bioristor in automating irrigation systems

4.2.1 Material and Methods

Plant material

For the experiment sixteen plants of the tomato variety Leonardo were used. The plants were sown seedbeds and transplanted in open field. Bioristor was inserted in sixteen plants.

Here the scheme of the experiment is reported.

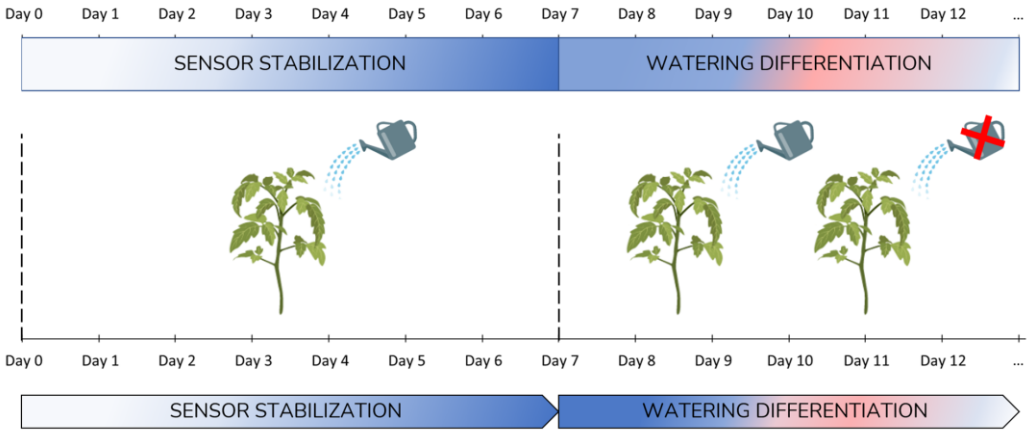

Fig. 41 - Experimental design: day 0-7, Sensor stabilization, day 7-12, watering differentiation based on the bioristor data.

Two water regimes are included in the trial: one traditionally irrigated, and the second bioristor guided. Plants were grown in optimal water conditions during the first 7 days to allow sensor stabilization, then different irrigation was applied.

Fig. 42 - Training of local people in Burundi for the use of bioristor; the photo is taken soon after a practical lesson. On the table is visible part of the material used for the dissemination, whereas the plants used for sensor insertion training are on the ground.

A focus of the project has been the training, so training sessions about the sensor preparation and use were held with the aim of sharing knowledge and technology on the subject (Figure 42). To this end, theoretical and practical lectures were done on the operating principle of the control unit and sensor, data acquisition, sensor insertion and plant monitoring.

4.2.2 Results

Sensor response along the entire duration of the experiment will be recorded, here it is the monitoring of the first days. This is also called the “stabilization period” and is needed for the sensor to establish a secure contact with the plant.

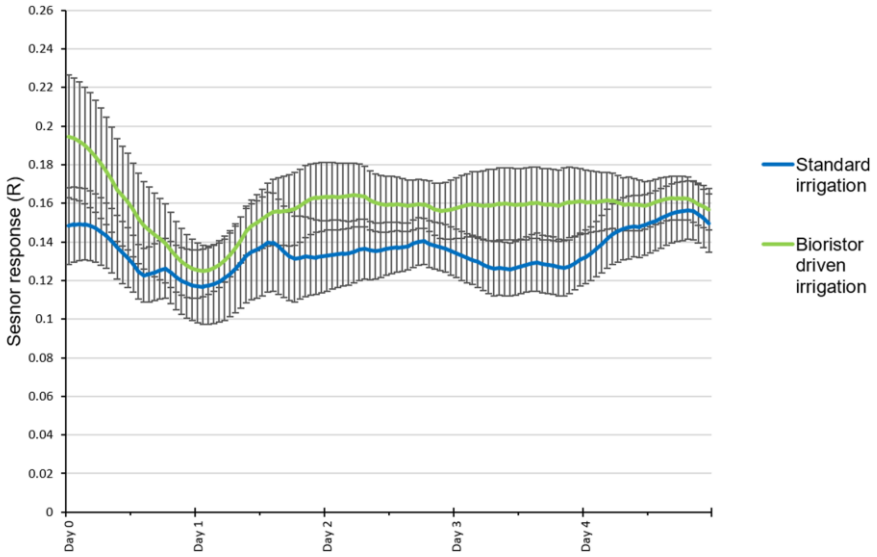

Fig. 43 - Field bioristor test, first days of monitoring. Blue line, standard irrigated thesis; Green line, bioristor driven irrigated field. Standard error is reported.

The two R curves exhibit slight oscillations, indicating no significant differences between the water regimes, as expected being the watering differentiation not applied yet. Furthermore, their overall trend remains constant, aligning with the typical response of sensors during a stabilization period (Fig. 43).

The experiment encountered difficulties and was not terminated due to the complete damage of the sensors installed and the difficulty to manage the replacement remotely. However, thanks to the first local experience and based on the video material produced for the Maison Parma project, a second round of cultivation as well as the application of bioristor will be conducted. Moreover, the variety Leonardo will be soon tested in controlled conditions to verify its tolerance to drought. The project thus stimulated collaboration between the two countries by paving the way for wider use of the sensor, demonstrating the potential of phenotyping and electronics, and promoting its study.

4.3 Discussion

The results of this second drought stress trial provided an additional evidence of the bioristor's ability in distinguishing different responses to drought stress, which has been detected in the R trend first, shown as an unequal falling trend, and confirmed by clustering all the bioristor indices then, where the study enabled the identification of two groups; the interpretation of R as a plant physiological status index has

been later justified by further testing the correlation between the index and stomatal conductance. This, in turn, suggested that the method developed for the analysis of bioristor's data involving the observation of R trend, the PCA and the cluster analysis is successful.

A strong influence of VPD values on the sensor response were recorded as well, and it was seen to affect the trend of the controls plants in particular, as transpiration in them was regulated more according to VPD than to the drought stress, a regulation previously seen in Grossiord et al. 2020.

Based on the field trial data recorded by Stuard in Burundi in 2022, some consistency with yield data have been found and this can be assumed as a further validation of the bioristor efficacy in characterizing varieties. In fact, as reported in results, 33012 produced 11.9 t/ha, 2556 produced 19.0 t/ha and 38244 produced 9.7 t/ha.

Therefore, the clusters revealed by bioristor, with varieties 33012 and 22561 within the same cluster, are in agreement with the yield data and demonstrate the effectiveness of the sensor in identifying different levels of drought tolerance.

These results, together with the small number of plants required to obtain such data, underscore the profound improvement represented by the bioristor in plant phenotyping, declaring its potential to address the bottleneck problem of phenotyping, both under control and field conditions.

The application of the sensors in Burundi demonstrates the high readiness level achieved by this technology, which can be easily transported and installed in most terrestrial scenarios; the main limitation of this setup is the need for an Internet connection, which was sometimes interrupted during the experiment. However, the control unit is equipped with an internal storage that allows to collect and analyse bioristor data locally, therefore the issue only slowed down data streaming. Moreover, this proof supports the feasibility of using the bioristor not only for breeding purposes, but also to automate irrigation systems in a sensor-driven approach (Vurro et al. 2023a).

The case study represented by the AICS international cooperation project offered the chance to apply a smart innovative technology in a difficult climatic contest.

Burundi is a low-income economy where 80% of the population is employed in agriculture. It is one of the most densely populated countries in Sub-Saharan Africa with 11.6 million people of which 50.4% (2019) are women. The agriculture sector, dominated by subsistence farming, accounts for nearly half of the country's GDP (2019).

The country is vulnerable to the impacts of climate change from changing climate patterns, such as increased rainfall and heat, as well as catastrophic situations, which impact the country's development efforts and its key economic sector.

Thus, here the improvement in water use efficiency and in the possibility to achieve higher yields in a high cost-effective agricultural activity, is of help in achieving the sustainable development goal 2, toward zero hunger, and in addressing the climate smart paradigm, sustainable agriculture and shared knowledge available for all.

This experiment, is a case study on the application of bioristor to increase the sustainability in agriculture where water is a real issue in food safety. This application supports the importance of bioristor as an *in vivo* tool for in field monitoring and functional phenotyping.

The possibility to increase the local population's knowledge through training was another goal successfully performed.

4.4 Conclusions

1. The bioristor allowed discrimination among three tomato varieties selected as adapted to grow and produce in extreme environments such as the Burundi region.
2. The results obtained under controlled conditions were supported by the final yield data recorded in the open field, raising the variety 33012 as the most tolerant, based on the bioristor data.
3. The correlation of sensor response with stomatal conductance was verified over again.
4. Overall, bioristor has proven to be a valuable tool for selecting varieties due to the possibility to monitor in real time and continuously the dynamic of each variety to drought and prompt its use in conditions where water availability is already a real problem for food security.

5. Tomato Introgression Lines

To further test the possibility to characterize different varieties based on bioristor data, in the following trial we have tested a more complex genetic background by monitoring the response of five introgression lines of tomato to the drought stress.

5.1 Material and Methods

Plant material

The Introgression lines (ILs) experiment was performed during the visiting period at the Universitat Jaume I, Castellón de la Plana, Spain. A set of 4 Introgression Lines (ILs) were randomly selected within the population developed by Eshed and Zamir (Eshed and Zamir 1995), currently composed of 76 lineages (ILs) (Gur and Zamir 2004). This population was formed by initially crossing the processing tomato cultivar M82 with the *S. pennellii* wild accession LA716. The next generation was then subjected to recurrents cycles of backcrossing and marker-assisted selection (MAS), with M82 as the recipient parent, so that each IL is genetically identical to M82, except for a single homozygous chromosome segment donated by the wild relative (*S. pennellii*). The line 3475, corresponding to the parental M82, was included as reference of low tolerance to the drought and heat stress.

A list of the used ILs is reported in Tab. 5 (IL number and the correspondence chromosomal fragment herited by the ancestor).

Tab. 5 - Introgression lines (ILs) used in the trial.

IL number	IL genotype
3475	Variety M82
4099	IL12-2
4091	IL10-3
4093	IL11-2
4087	IL10-1

For the experiment, 15 seeds for each tomato genotype were germinated in the seedbed and transplanted in 0.7 L pots filled with 260-270 g of coconut fiber. Plants were grown in a greenhouse under natural light

photoperiod 14/10 (day/night) for 13 days at 35/20 °C (day/night). For each IL, 2 plants were used as control and 3 as stressed.

Environmental data

Environmental data, such as air temperature and relative humidity (T °C, RH %), have been recorded for the entire length of the experiments in both locations using a datalogger; VPD has been later calculated from these (see figure below).

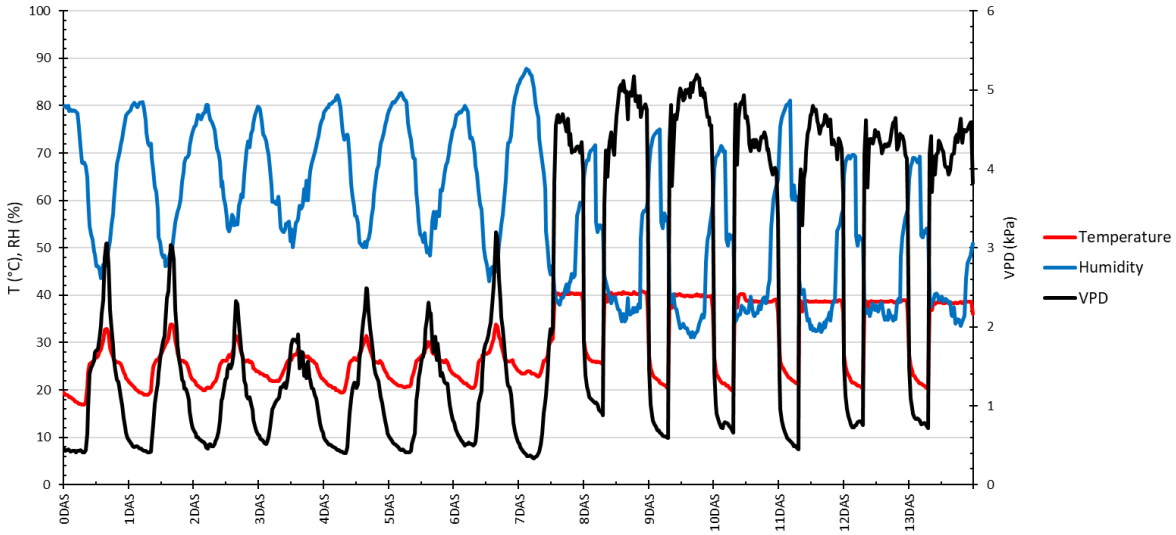

Fig. 44 - Environmental parameters: the graph shows the trend of temperature (°C), relative humidity (%) and vapor pressure deficit (kPa) during the entire experiment duration.

The graph reports strong daily fluctuations during all 13 days. The averaged VPD increased significantly after 7 DAS as plants and datalogger were moved inside the heated growth chamber and the double stress started. The temperature rose to 39°C and fluctuations in humidity and VPD also increased.

Drought and heat stress

In the trial, plants were grown up to the expansion of the 4th leaves and, at this stage, equipped with the bioristor. After the 6 days of sensor stabilization period (0 DAS), drought stress was imposed by water withdrawal to the stressed plants, whereas control plants were kept fully hydrated. At 7 DAS, a combined

stress (heat + drought) was imposed placing all plants in a growth chamber and applying a constant temperature of 39 °C. During the combined stress, the control plants were irrigated every day to avoid drought occurrence although exposed to heat (Fig. 45).

The experimental plan was conceived as follows.

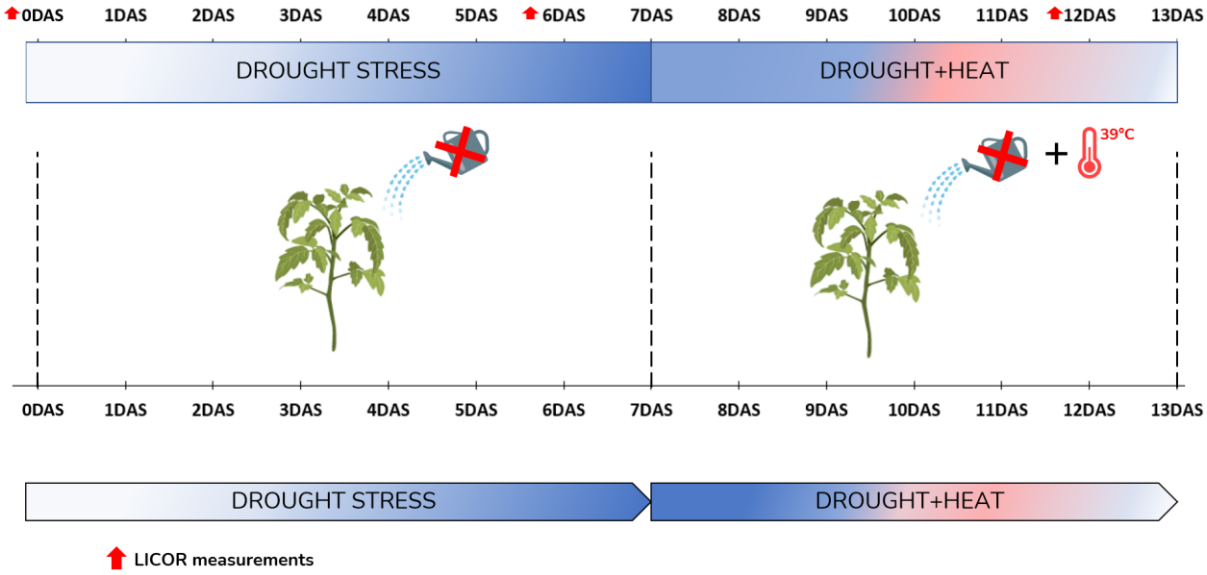

Fig. 45 - Experimental plan of the tomato ILs trial. DAS, Days after stress; red arrows indicate the physiological measurements performed with LI-COR. During double stress, controls were moved inside the heated growth chamber but kept fully hydrated to have an environmental reference.

Physiological measurements

Gas exchange

Stomatal conductance was measured using the LI-COR 6800 (LI-6800, Lincoln, NE) portable photosynthesis system, accounting for one of the mains indicators of the plant physiology (Curtis 1926; Yoo et al. 2009; Wohlfahrt and Gu 2015; Zandalinas et al. 2016). Three measurements were carried out at 0 DAS, 6 DAS, 12 DAS; all performed at 9.00 am.

Bioristor implementation in plant

Biorsitor was implemented in a total of 25 tomato plants at the 4-leaves stage. The internode between the cotyledons and the first node was chosen as insertion point. Plants were kept fully irrigated for 6 days,

leading the sensors to acclimatize and establish a secure contact with plant vessels. A MATLAB script (https://uk.mathworks.com/) were used for data downloading from the server and for data analysis. Bioristor sensor indices R, I_{gs}, τ_{ds}, τ_{gs} and their derivative values dR, dI_{gs}, $d\tau_{ds}$ and $d\tau_{gs}$ were acquired through bioristor and used in the PCA analysis. The plants used for the experiment can be seen in the figure below.

Fig. 46 - ILs lines during the drought stress (8 DAS).

Statistical analysis

The average of bioristor data was calculated to reduce noise effects. The ANOVA test was performed through MATLAB to evaluate the significance of the differences observed between genotypes and treatments. The Principal Component analysis and clustering was performed using an R script (https://cran.rstudio.com/).

Drought treatment

Conditions suitable for the drought stress' occurrence were obtained by water withdrawal, this mode led the drought to be reached gradually and similarly to what plants experience in natural environments. Stress evolution was monitored by weighting pots and estimating relative soil water content (RSWC) as:

$$Relative\ soil\ water\ content\ (\%) = \frac{soil\ in\ stress\ condition\ (g) - dry\ soil\ (g)}{soil\ at\ full\ capacity\ (g) - dry\ soil\ (g)} \times 100$$

5.2 Results

The R index plot is reported for the thirteen days of continuous monitoring (Fig. 47 A).

The R index in IL4093 and IL4087 increased compared with controls among 4 DAS and 7 DAS while R of IL3475 drops severely (-33%) and rapidly in the same interval showing also a series of acclimation peaks in the drought stress plants at 10 and 11 DAS.

In the I_{gs} plot (Fig. 47 B), IL3475 and IL4093 show a comparable trend with a signal gradually dropping from 1-2 DAS until the end of the experiment. A sharp increase of the I_{gs} was observed in IL4087 and IL4099, 24 hours after the heat stress began following the rehydration. On the contrary, ILs 4091, 4093 and 3475 trend is unchanged showing no rehydration effects.

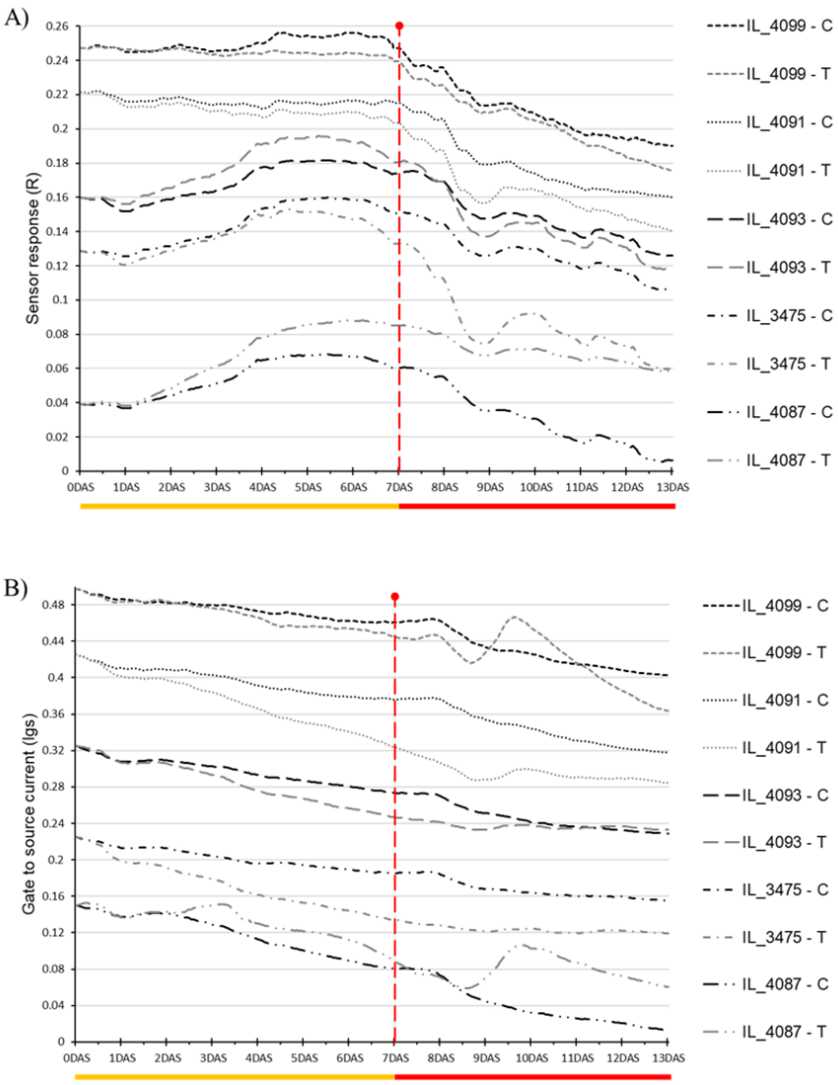

Fig. 47 - Plot of the bioristor indices: (A) Sensor response, R, (B) Gate to source current (I_{gs}) for the 5 ILs analyzed. C, control, T, stressed. Orange bar indicates the imposition of drought stress, red bar indicates the days of heat+ drought stress. Dashed red line indicates the shift from single to double stress.

To further understand the link between plant response and the bioristor signal (Gentile et al. 2022), all the indices of the sensor were examined in a principal component analysis (PCA), aiming at fully tracing the dynamics of the response of the different genotypes. This increased the investigation power of bioristor analysis and consequently conferred a higher chance to discriminate between genotypes.

The PCA plots are reported in Fig. 48 A, B, C.

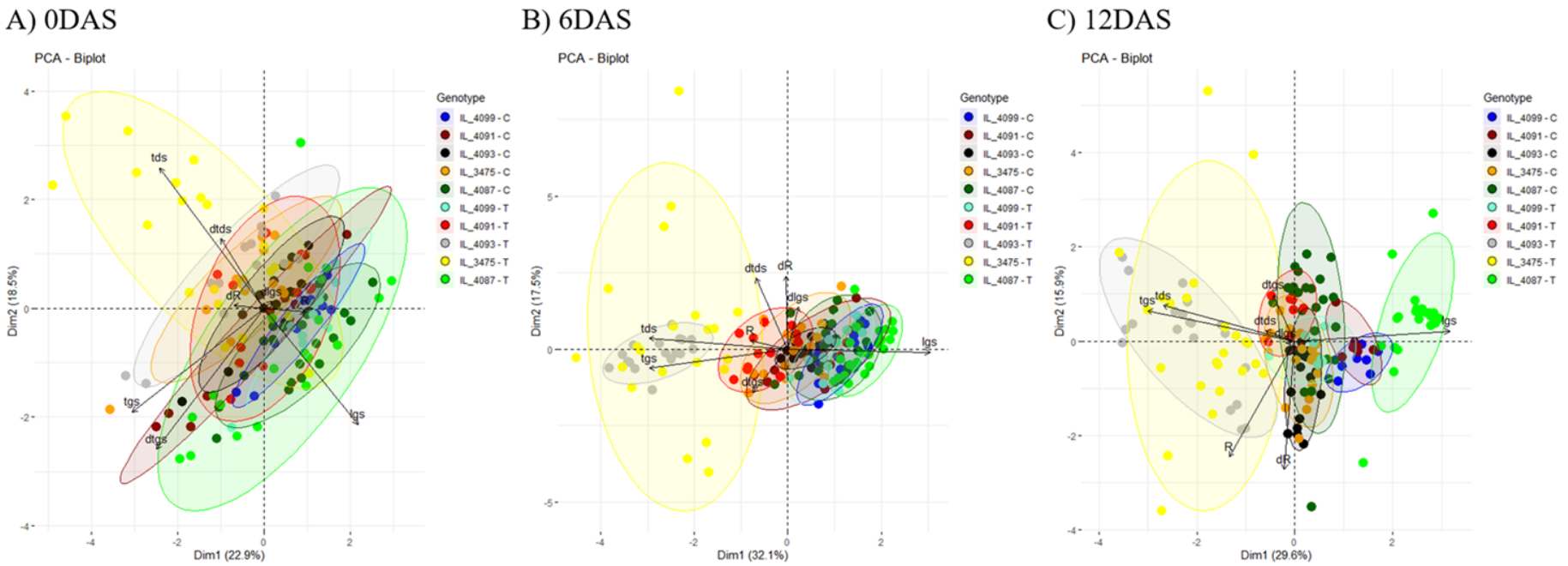

Fig. 48 - PCA plot of bioristor traits. A) 0 DAS, no stress imposed, B) 6 DAS maximum drought, C) 12 DAS, end of the combined stress. Stressed and Control plants for all the 5 genotypes are shown.

Considering both controls and stressed plants, during 0 DAS (figure 48 A) no significant difference was observed among the ILs. At 6 DAS (figure 48 B) till the end of the drought stress, IL4093 stressed plants (IL4093-T) and IL3475 stressed (IL3745-T), clustered separately. At the end of the combined stress (12 DAS) an increased difference within the thesis was observed (figure 48 C). IL3475, IL4093 clustered separately on the PC2 while IL4087 clustered separately on PC1, indicating a different response of the ILs under heat stress. However, being the separation not sufficiently clear because the large number of theses plotted causes a considerable overlap leading to a near overloading of the space, a second PCA was calculated.

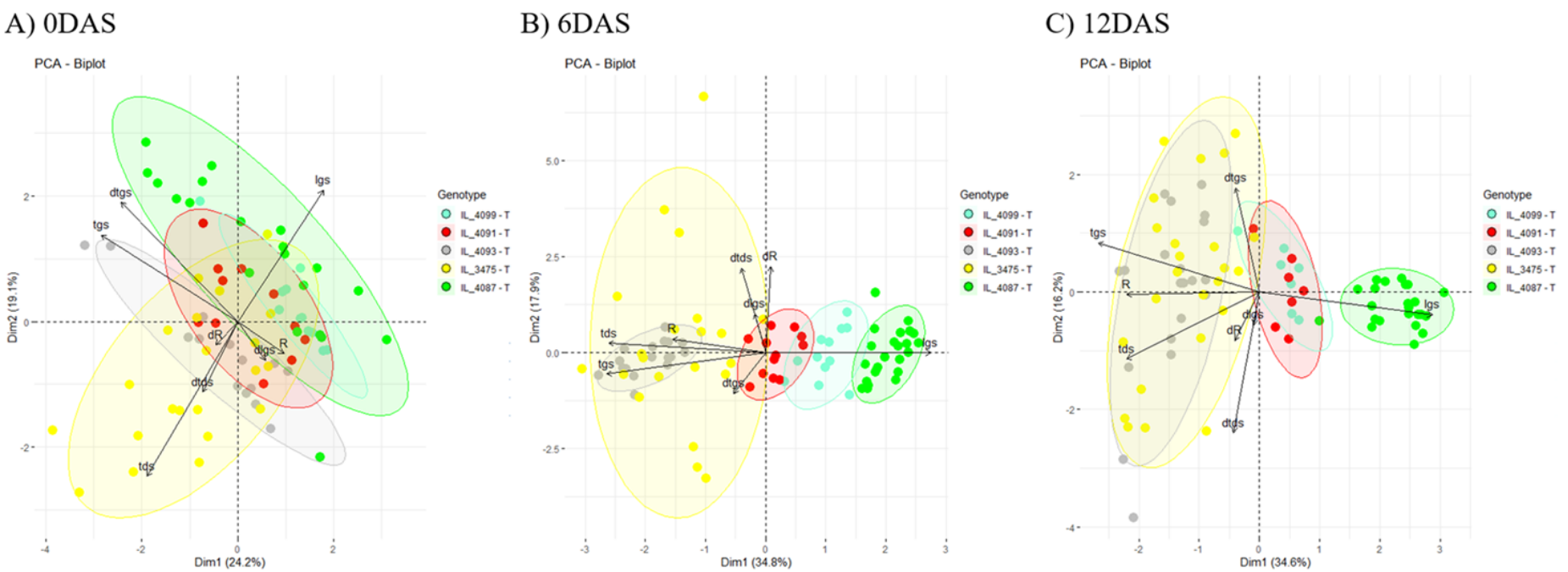

Fig. 49 - PCA plot of bioristor indices in time. A) 0 DAS, no stress imposed, B) 6 DAS maximum drought level reached, C) 12 DAS, end of the combined stress. Only stressed plants were reported.

The PCA plots (Fig. 49) report the dynamic of the ILs response of stressed plants under drought and combined stress; the analysis was focused on the sole stressed plants to better understand their differences.

Before the stress imposition data were overlapped and no differences were detected among the genotypes (Fig. 49 A). Drought separated the ILs (Fig. 49 B) along the PC1, that mainly determined by the I_{gs}, τ_{gs}, τ_{ds}, and R. At 6 DAS, IL4093 and IL3475 grouped together and apart from the others (Fig. 49 B). Compared to the other lines, the 3475 is the one with the maximum dispersion along the second PC.

After the combined stress, a similar pattern is visible despite the variation in loadings. IL4087 is separated by the others as previously observed along the PC1, IL4099 and IL4091 overlapped in the center of the plot and ILs 4093 and 3475 grouped together along the PC2. During the drought and the combined stress, PC1 and PC2 account for 52.7% and 50.8% of the total variability respectively (Fig. 49 B and C).

These observations are confirmed also by the clustering analysis performed at 6 and 12 DAS (Fig. 50 A and B).

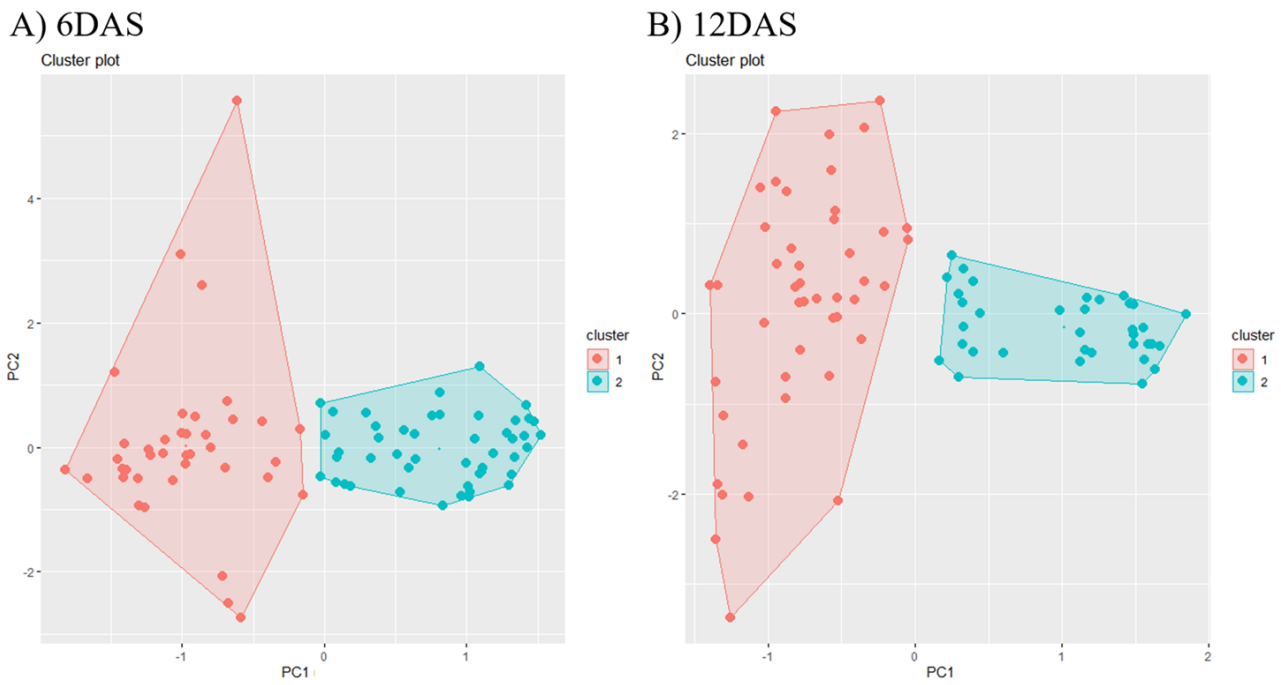

Fig. 50 - Cluster analysis using k-mean algorithm: A) 6 DAS, B) 12 DAS.

At about the end of the drought stress (6 DAS, Fig. 50 A), IL3475 and IL4093 grouped together, while ILs 4087, 4099 and 4091 formed a single group. The same composition remains stable also following the combined stress (Fig. 50 B).

The model failed to separate less than 3.5% of the data.

Observing the relative soil water content, revealed a fast and deep reduction of the water in the pot during the drought stress; as expected at 10 DAS an increase of the values is observed, as a result of the emergency irrigation at 8 DAS after the plants weighting.

Tab. 6 – Relative soil water content of the stressed, meaned within genotype.

	2DAS	3DAS	6DAS	8DAS	10DAS	14DAS
4099 - T	71.3	47.9	36.1	25.6	46.8	22.1
4091 - T	68.7	43.0	32.1	25.9	41.1	25.7
4093 - T	63.5	40.5	29.4	24.9	46.7	28.6
3475 - T	59.4	41.2	31.4	24.6	45.3	25.0
4087 - T	57.8	40.6	30.3	24.8	49.0	24.8

Physiological measurements

Conventional physiological measurements were performed in order to better link the bioristor data to the plant physiological conditions.

Physiological traits observation revealed a severe reduction in stomatal conductance 6 DAS for all the lines. This reduction was increased during the combined stress (12 DAS) leading to a complete stop of the transpiration process for IL4099 and IL4091.

To note that controls decrease in stomatal conductance recorded 12 DAS is a consequence of the heat stress to which they have been subjected (Fig. 51).

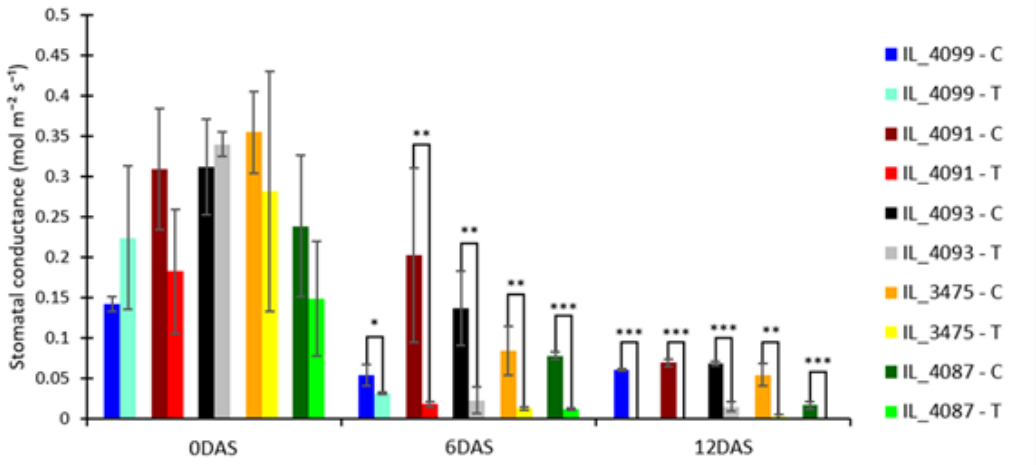

Fig. 51 - Stomatal conductance analysis performed at 0 DAS, 6 DAS and 12 DAS. Student's test was applied (*p<0.05, **p<0.01, ***p<0.001).

5.3 Discussion

The 13 days of continuous monitoring with the bioristor of ILs lines under different stresses allowed to trace, directly in the plant, the stress response dynamic over time, also demonstrating that the sensor can recognize phenotypic differences determined by reduced chromosome portions, such as the ones owned by the ILs.

With respect to what previously considered a typical curve in monitoring a stressed plant, a different trend was observed; this unexpected behavior, consisting of an increase of the R signal during the stress, can be explained as an overall increase of sap enrichment with osmolytes (Giordano et al. 2021) or a pH reduction (Davies et al. 2005; Pagliarani et al. 2019), before plant tissues dehydration. In fact, an increased sensor response may be the direct effect of two factors' combination: the reduction of plant dehydration, which is the driving force leading the sensor response to fall, and the sap ion concentration increase (Trifilò et al. 2011), which may drive a stressed plant R to rise.

The I_{gs}, providing an indication of the sap ion concentration, supports this hypothesis since, as recorded for IL4087, soon after drought imposition a rising is visible. IL4093 showed an opposite I_{gs} trend, although less pronounced; moreover, compared to other stressed, it presents the maximum stomatal conductance level during drought, even though this is lower if compared to its own control. The fact can be due to a different response strategy to the stress leading to a temporary increased flux speed in xylem vessels, which accelerates ion flux moving the current I_0 to less negative values; however further examinations are required to explain this uncommon behavior.

The analysis of sensor response over time also highlighted a rapid and deep reduction in IL3475 soon after combined stress imposition, confirming the higher sensitivity to a similar stress of this line compared to the others as already reported (Pessoa et al. 2022).

The rescue irrigation highlights two interesting behaviors: in IL4099 and IL4087 the rapid increase observed in the I_{gs} trend indicates the beginning of the recovery, as a result of the temporary increase of the transpiration, which led the ions mobilized by the water to be absorbed. This could be assumed as a sign of their higher resilience, as previously observed (Gosa et al. 2022).

Bioristor's data are supported by the data reported by Gosa et al., 2022 (Gosa et al. 2022), pointing out that IL10-1 (corresponding to IL4087) showed good vegetative growth but had low yields under both wet and dry conditions (Gosa et al., 2022).

In particular, IL4087 showed an increase in R and I_{gs} in response to the drought and maintained higher values than the control during all the experiment; the fact should be further investigated in order to comprehend the reasons for this unique behavior.

The higher bioristor sensitivity, demonstrated in ILs performance discrimination, would be interestingly applied for pre-breeding selection as a good index for response to single and combined stress. Moreover, I_{gs} and τ_{gs} are bioristor traits that surely need to be kept in consideration for variety selection.

Cluster analysis split the ILs into two groups, founding similarities between IL3475 and IL4093 as well as between IL4087, IL4099 and IL4091 during both drought and combined stress, given their high values in I_{gs} and low τ_{ds}, τ_{gs} and R. The result of this characterization in terms of response to abiotic stress needs to be clarified.

The results obtained by using the same bioristor indices to separate different genotypes in different stress conditions suggest that the sensor could have provided new evidences of the existence of similarities in plants' response to these stresses, such as osmotic imbalance and reactive oxygen species (ROS) production, that can take place in both conditions altering the ionomic homeostasis as previously suggested for other plant species (Jia et al., 2020, Hosseini et al. 2021; Giordano et al. 2021).

The ionomic profile of plants grown in a common environment may reflect adaptations to their native local environment (Huang and Salt 2016). The accumulation of a given element is a complex process controlled by a network of gene products critical for uptake, binding, transportation, and sequestration. Many of these genes and physiological processes affect more than one element (Baxter 2009). Thus, the possibility to monitor in real time the positive ion accumulation and movement during the plant growth, development and under abiotic stress is crucial to perform a timing and efficient variety selection.

5.4 Conclusions

1. The experiment demonstrates the high sensitivity of bioristor in classifying complex genetic material as the tomato introgression lines on the basis of their diverse response to the stress and tolerance to single as combined stress.
2. The analysis of the bioristor data allowed to trace the dynamic of the response to abiotic stress, magnifying the possibility to understand the intensity and the evolution of the stress as well as the strategy adopted by the plant to survive.
3. These results can be exploited to further characterize tomato ILs, providing the evidence of a drought and heat tolerance.
4. Finally, the set of variables identified a useful tool to discriminate and characterize plants' response to the single drought as well as to combined stress, for the first time in vivo and in continuous.

6. Integration of Bioristor in the Scanalizer Platform

Development of bioristor control unit compatible with the high throughput platform in ALSIA Metapontum Agrobios

Last section of this thesis is the concrete application of the bioristor system for plant phenotyping, thus its integration in a high throughput phenotyping platform. To date, no comparable sensor to the bioristor has been integrated and used in a phenotyping platform. Hence, this study represents a step forward in the state of the art of phenotyping since the availability of continuous sensor data, so strictly correlated with plant's physiology, will strongly increase the phenotyping impact in breeding and plant physiology.

This task has been done in collaboration with ALSIA Metapontum Agrobios research institute (Metaponto, Matera). ALSIA is a coordinator, together with CNR, of Phen-Italy. Phen-Italy is the Italian Plant Phenotyping consortium, gathering the national scientific community that is developing and using high throughput phenotyping research infrastructures, with the principal node in Basilicata. Phen-Italy represents the Italian node of the European Strategy Forum on Research Infrastructures (ESFRI) project named EMPHASIS, part of ESFRI 2016 Roadmap, the Italian node of the EMPHASIS.

To this aim, a bioristor control unit fully integrated in the Scanalizer platform was conceived.

6.1 Materials and methods

Study of the use case

ALSIA hosts the first Italian High-Throughput phenotyping platform (HTPP) enabling the monitoring of 456 plants. The system is constituted of a highly automated greenhouse in which plants are grown on pots upon carts; each cart is moved by a conveyor that drives the plants inside an imaging chamber, where RGB, fluorescence and near infrared (NIR) sensors. measure plants' reflectance, extracting image-based indices.

The conveyor is surrounded by 9 stations used for environmental monitoring and guaranteeing the best suitable conditions for plant growth; these stations are equipped with sensors for measuring PAR, temperature, humidity and carbon dioxide (Fig. 52).

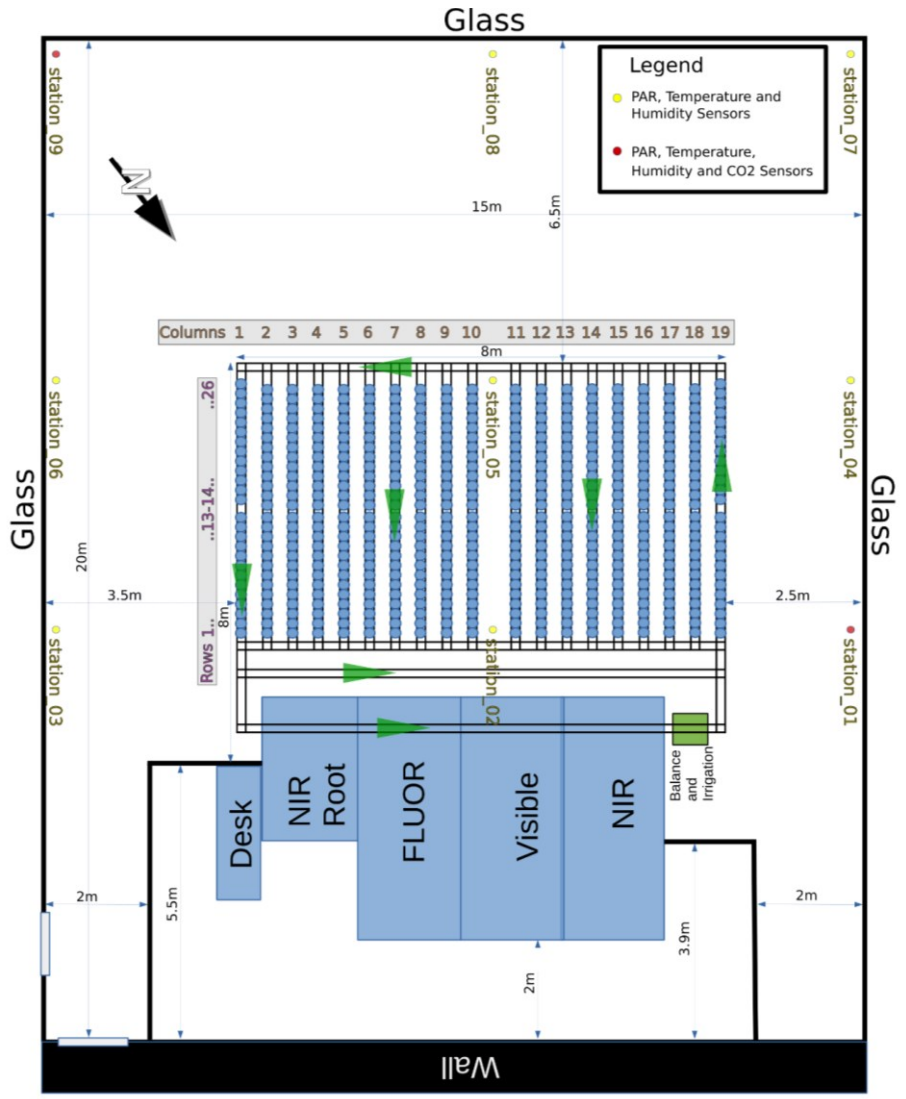

Fig. 52 - Scheme of the HTPP platform (courtesy of ALSIA). The facility is organized into 2 spaces; the bigger one represents plants' stationary space and is intended to provide a homogeneous environment where the plants are left to grow. This area hosts the conveyor, which communicates with the imaging chamber room, divided into 4 sectors, one per sensor installed (NIR for under the soil analysis, fluorescence, visible and NIR for above the soil analysis). The second space is the control room, where the operators stand and manage the platform.

Fig. 53 - High-throughput phenotyping platform, front view. The conveyor with the carts laying upon it is clearly visible in the foreground. The image chambers are the 4 cubic structures in the figure center, the control room is behind them.

The goal of this study involved integrating the bioristor into the platform (Fig. 53), designing a control unit fully integrated into the carriage and controlling multiple plant monitoring sensors to provide a plant-specific view.

Each control unit were designed with the following equipment:

- 2 bioristor readout channels
- Soil humidity sensor
- Soil conductivity sensor
- Temperature and relative humidity sensor
- Integrated WiFi module
- MicroSD card slot
- LiPo battery 1100mAh (10h autonomy)
- On-platform charging system
- OLED display
- Buzzer

The idea was to install in the HTPP facility a novel tool that enables the continuous physiology plant monitoring through bioristor adding to them some other essential information such as soil humidity and air characteristics. WiFi connection was chosen as the most suitable protocol for data exchanging with the server, whereas the embedded micro-SD card slot and a battery were installed to prevent data loss.

Indispensable requisite to allow the full operation in the Scanalizer platform is the possibility to automatically recharge the battery of the control unit in the conveyor; thus, a recharging station and external contacts were developed.

The control unit design was concluded providing a simple user interface, consisting of an OLED display, showing all the information instantly collected by the control unit, and a buzzer, as an acoustic transducer. A metallic male pin-header allows to browse the data, turn on and off the bioristor gate voltage and calibrate the bioristor readout channels.

Control unit design

The main bottleneck in the control unit designing has been the cart free volume together with the need for reaching the cart edges, to ease the cart-to-cart link (Fig. 53 B); this constraint has been examined and solved during the design phase by means of including plant pot saucer to the case. The intuition leads to gaining enough space to fit inside the circuit and the battery (see figure 54).

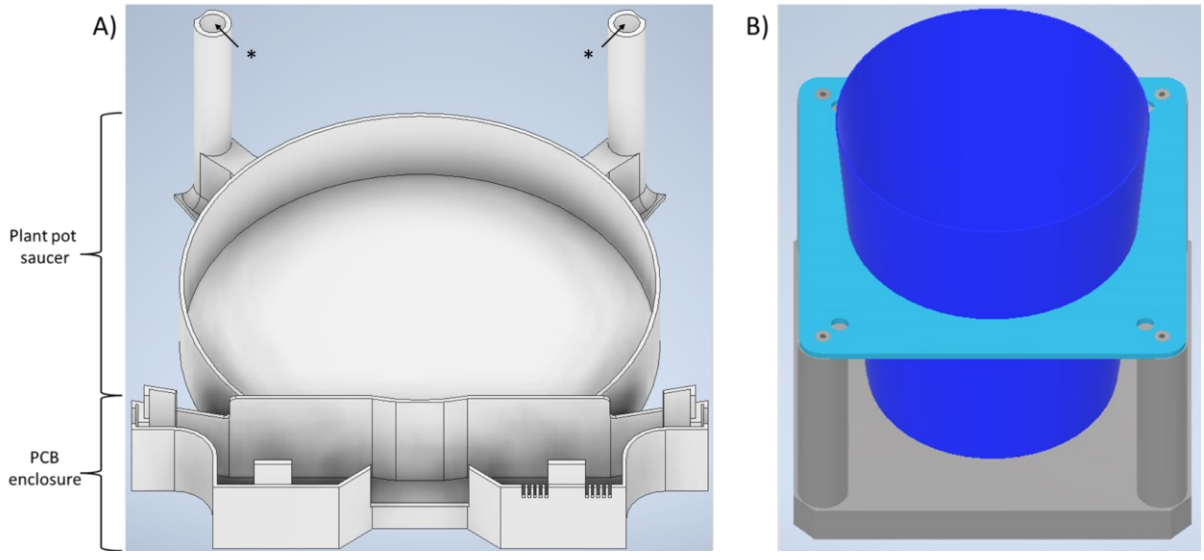

Fig. 54 - Scheme of the control unit case. A) Base of the control unit case, B) the cart. The asterisks visible in figure A mark the insertion points of the cage used for higher plant support.

The two halves of the box, thanks to an interlocking system, can close, preventing the electronics from getting wet or damaged (Fig. 54 A). The prototype of the box was designed using the program Inventor (Autodesk, San Rafael, California), then sliced and printed using the CR-10 S5 3D printer (Creality, Shenzhen, China).

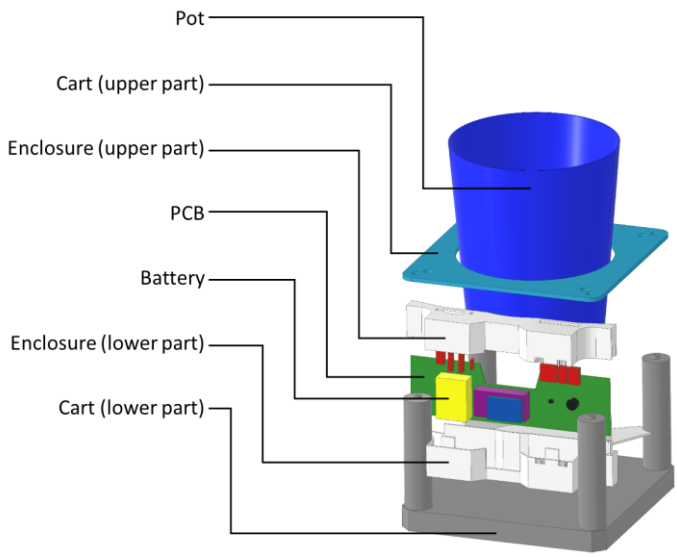

Fig. 55 - Scheme of the control unit's main components. Four parts of the control units are visible: the case (upper and lower), the printed circuit board (PCB) and the battery. PCB and battery are enclosed in the case and held inside the cart.

The control unit positioning procedure implies the dismounting of the cart's top and the lowering of the case within the cart's four columns; the position is maintained thanks to the pot weight. The PCB is designed to get perfectly stacked between the two parts of the enclosure contributing to maintain them joint with each other (Fig. 55).

Circuit project was conceived using Eagle (Autodesk, San Rafael, California), see figure below.

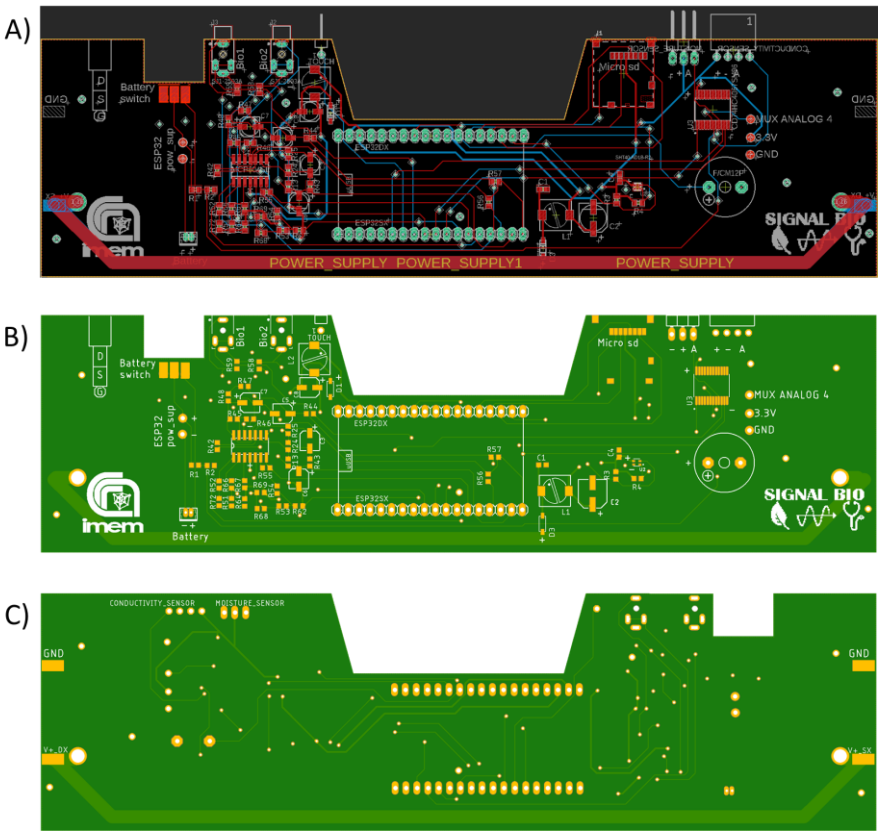

Fig. 56 - Printed circuit board project. A) preprinting schematics, B) printed circuit, front view, C) printed circuit, rear view.

The shape of the board is designed to have a power distribution line running through each control unit, enabling the use of PCB conductors as cords. The pads located on the right and left edges represent the ends of these conductors (see the yellow rectangles on Fig. 56 C); each pad hosts a manually soldered spring contact that establishes continuity between the PCBs of two adjacent carts.

Therefore, the PCB architecture allows a single charging station to be placed at the front of the rail, as the power supply of the first control unit of the line is propagated to all carts up to the last one (see photo 57).

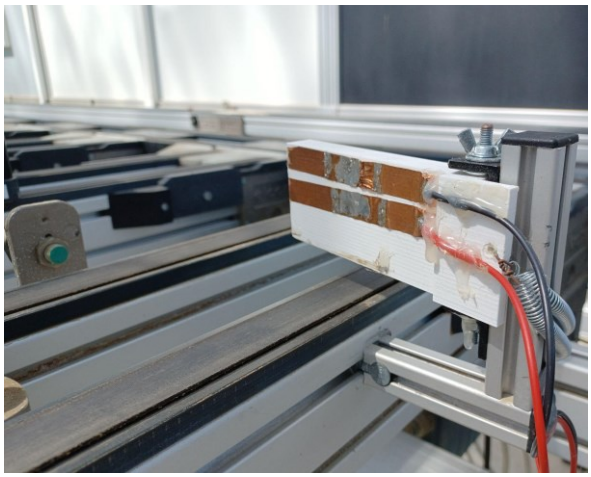

Fig. 57 - Charging station. Powering cables soldered to the copper strips used for establishing contact with the control units. On the right, the springs required to maintain the white flag-like structure in position after the carts pass.

Since the control units require continuous voltage to work, a switched-mode power supply was employed to rectify and decrease grid voltage; the voltage used was 7.6V and, given the 2.8A, the peak power consumption was approximately 21W (in case all the batteries are discharged).

Image based traits acquired

The projected shoot area and the plant height were recorded through the RGB image sensors. The Projected shoot area is the sum of the projected area of the plant from three orthogonal views (two from the side and one from the top), converted from pixel area units to cm^2; the value provides an estimation of the area occupied by the plant. Plant's height is measured as the distance between the highest part of the plant and a reference point, usually the collar.

6.2 Plant test

To verify the efficacy of the bioristor reading system developed and the possibility of the system to correctly operate in real conditions, a test on leaving plants has been conducted.

Fig. 58 - Trial of the bioristor control unit in the Scanalizer platform on tomato plants.

Twentysix plants of the variety ‘cuore di bue’ have been growing in the phenotyping platform under normal growth conditions whereas 13 bioristors have been installed and plants were monitored both with bioristor as with the Lemnateh Scanalizer imagining system (Fig. 58 and Fig. 59).

Fig. 59 - Bioristor control unit installed in the Scanalizer conveyor line.

All bioristors were connected via coaxial cables to the control unit so that data would be recorded and sent to the server.

Data acquired was analyzed with MATLAB scripts (https://uk.mathworks.com/) and mined in Excel (Microsoft Excel 2016). Elaboration process started with data cleaning by eliminating outliers and spikes; the reliability of each sensor was checked and a 24 hours wide moving average was calculated to smooth the day-night typical oscillation. Finally, data collected for each thesis were averaged to derive the respective trends for individual theses.

6.3 Results

Analysis results are summarized in the following plot.

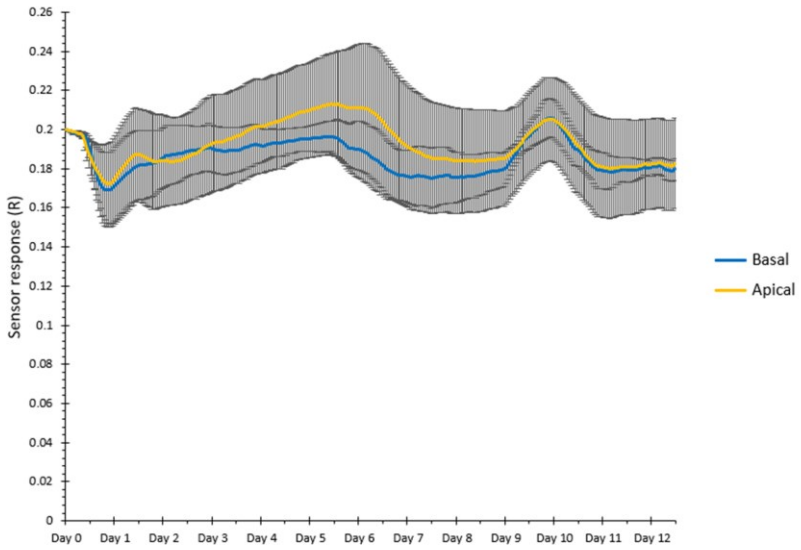

Fig. 60 - Plot of the Sensor Response during 12 days monitoring. Apical and Basal refer to the position of the sensor in the plant stem. Bars represent standard error.

The plot above shows an unstopped monitoring lasted for the entire duration of the experiment.

Bioristor enable the correct functionality of the sensors in the 12 days of monitoring.

The sensor response showed increases and decreases typical of small periods of stress although plants were regularly irrigated (Fig. 60).

Contemporary imaged-based indexes were acquired to verify the normal plant growth and development (Fig. 61 A, B).

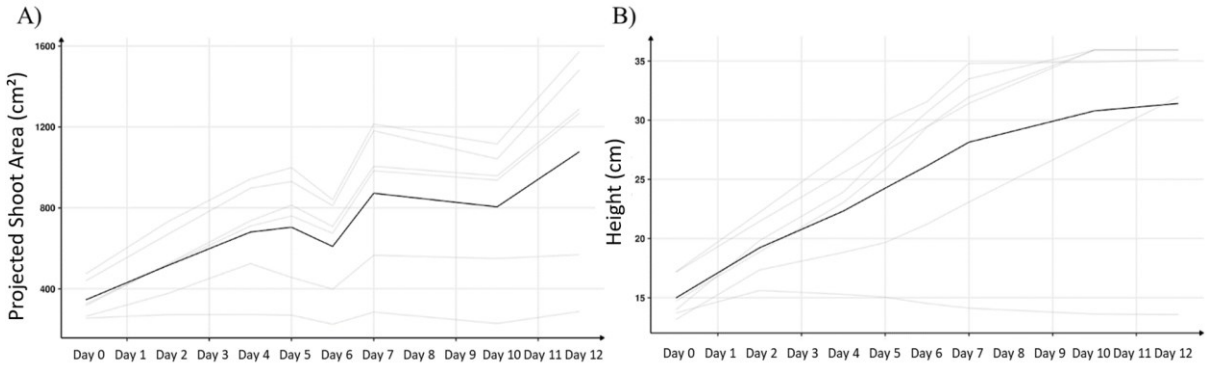

Fig. 61 - Indices of the phenotyping platform. A) Projected shoot area, B) Plant height. Gray lines represent single plants, the black lines represent the average.

In both the cases a rising trend is maintained, observing only few oscillations regarding the index in Fig. 61 A.

6.4 Discussion

This study has successfully produced bioristor readout control units (CUs) integrated into the Scanalizer phenotyping platform, resulting in an easy-to-install and easy-to-use tool able to ensure full bioristor operation for the entire set of phenotyping platform measurements. An example is the charging station, which is rapidly deployable thanks to a screw fixing system, as well as the case assembling, which only takes the two halves to be connected; this shape maximizes structure performance in the existing conveyor system. Moreover, it confers high water resistance of the CUs, reducing PCB's oxidation and keeps mechanical stability.

The control unit allowed to control 2 bioristors per pot, increasing the sampling rate and equipping the system with an additional measure, that is the continuous reading of the changes occurring in the plant sap during growth, development and under stress. Moreover, it also brings a set of air temperature, air humidity, soil moisture and soil conductivity sensors, which make it possible to compare the bioristor's data with the surrounding environment state, enriching the acquired information.

The data management algorithm was properly developed to support the installed devices as the number of devices simultaneously connected via WiFi to the cloud can be up to 250, making the system scalable

(Abdelmoneem et al. 2020; Lifewire 2022); data is also saved in the SD card mounted on the motherboard preventing data loss. The battery ensures the powering of CUs during the measurements in the imaging room and protects the CU from unexpected platform malfunctions and blackouts. For the battery charging, as well as to constantly power the devices, a flag-shaped charging station was developed. This function was achievable thanks to a well dimensioned PCB's conductor; allowing the control unit to be charged even further away from the station. The user interface, constituted by the OLED and the buzzer, represented an intuitive and user-friendly strategy for the communication with the devices and a rapid debugging instrument.

The continuous in-vivo monitoring allowed by bioristor has significantly enhanced the traits analyzed in the phenotyping platform, allowing for a 24 hours continuous picture of the plant functional physiology.

Summarizing, the designed CUs are perfectly fitted in the HTPP without requiring any adjustment of the latter, improving phenotyping accuracy by adding new monitoring parameters and enormously increasing the sampling rate.

6.5 Conclusions

1. The possibility to integrate the bioristor into the ALSIA phenotyping platform was successfully obtained during the PhD and has been clearly demonstrated in the experiment.
2. The number of CUs installed can be easily scaled up to cover all available carts.
3. The environmental sensors added to the control unit can significantly improve the quality of the bioristor data and provide a plant-specific analysis of the surrounding environment, which in turn can be useful to study environment contribution in the determination of a specific phenotype.
4. Real-time in vivo and continuous acquired indices can concretely improve platform's effectiveness by significantly increasing the range of monitoring parameters and providing indexes more closely related to plant physiology, allowing for an exhaustive phenotyping and a way more precise plant selection.
5. Overall, the trial showed that the implementation of bioristor can significantly increase the level of automation of the platform.

7. Final conclusions

Modern agriculture demands for higher yields and higher effectiveness to increase food security in the upcoming future, thus novel strategies must be found.

Part of this needs will be addressed by increasing crop intensity, with the remainder coming from land expansion, since land equipped for irrigation would expand by some 32 million ha (11 percent), while harvested irrigated land by 17 percent (FAO 2009).

Crop breeders are expected to cope with this challenge and come up with novel high-yield varieties, but the prospects of even maintaining the current rate of yield improvement in light of climate change are unclear. Thus, the exploitation of good agronomic practices, reduced water consumption and improved varieties is becoming a focus of the research community.

Here we applied a novel sensor developed in IMEM-CNR that enables the in vivo continuous monitoring of the plant physiological functions whose name is bioristor as a novel tool for plant phenotyping, and we propose it as an answer to the agriculture needs as well as a solution to overcome the bottleneck which is slowing down the development of novel varieties.

In this work we demonstrated for the first time the ability of bioristor to characterize varieties under drought stress and to hypothesize their tolerance and resilience against it. This was revealed to be correct both in commercial varieties, where the tolerance level to drought is not known, as well as in more complex genomic materials like ILs tomato lines, that were already tested in several phenotyping trials. However, novel insights in the dynamics of the response of ILs tomato lines were retrieved by applying a bioristor, such as the possibility to conduct uninterrupted monitoring without any human intervention except for sensor insertion, or the in vivo plant's sap analysis, the automatic study of the stomatal conductance and the one of the plant's responses to abiotic stresses.

As the final step in the application of bioristor in plant phenotyping, in this work, the system has been integrated and tested in a high throughput phenotyping platform, addressing the needs for continuous methods capable of tracing the dynamic of the response to drought and demonstrating the high readiness level reached.

Moreover, in this study the bioristor proved to be a good indicator of plant transpiration and movement of ions in the transpiration stream (Fig. 62). This is also supported by previous field experiments, where R was correlated with water stress (CSWI) and water related index (RWC). While a lack of correlation was observed with chlorophyll related traits as chlorophyll content (measured with SPAD), and RGB image-based indices (greener area, GGA, Crop stress index, CSI, NDVI, Vurro et al 2023, Fig. 62).

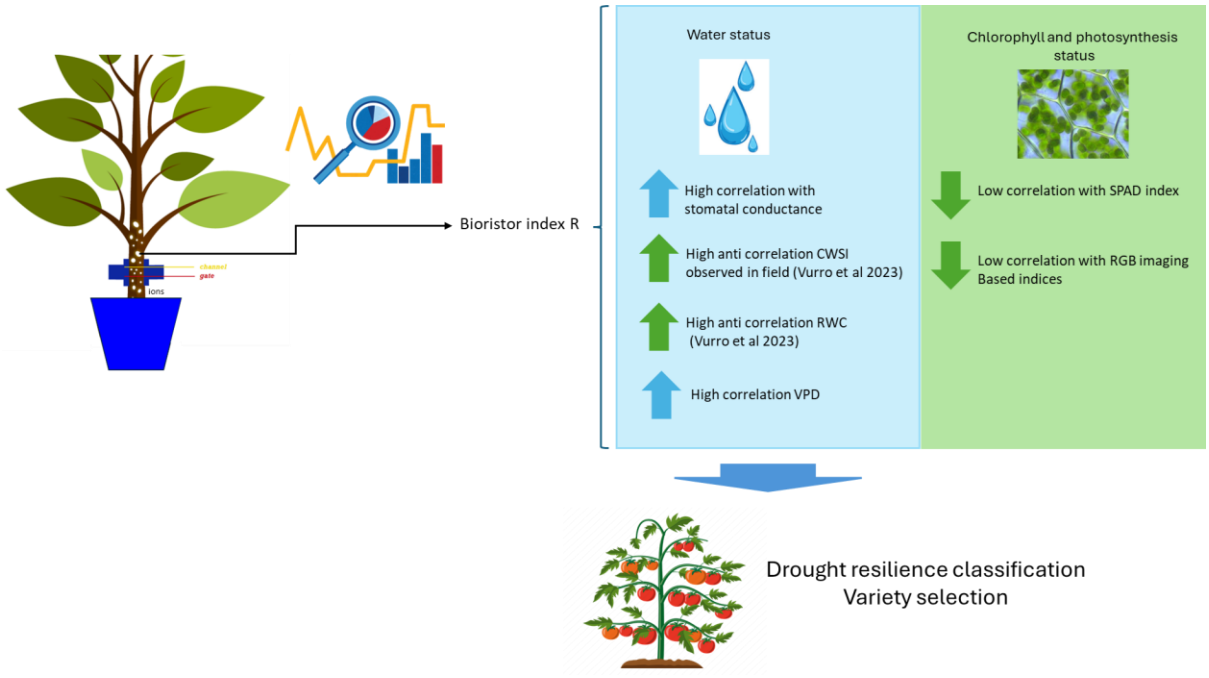

Fig. 62 - Correlation of bioristor index R with physiological related traits.

Last but not least, the bioristor was used in a climate smart agriculture approach, in the frame of an international cooperation project in view of technological transfer. In that context, variety selection was successful in highlighting the different behavior between varieties under drought stress. Interestingly, the results obtained with the bioristor were supported by field work trials operated in 2022.

Finally, this work paves the way for the introduction of in vivo phenotyping as a crucial add-on in the high throughput phenotyping scenario. Summarizing, the use of bioristor is aimed at performing more accurate selection through more precise phenotyping; the example of bioristor application and data flow, from acquisition to use, are schematized in Fig. 63.

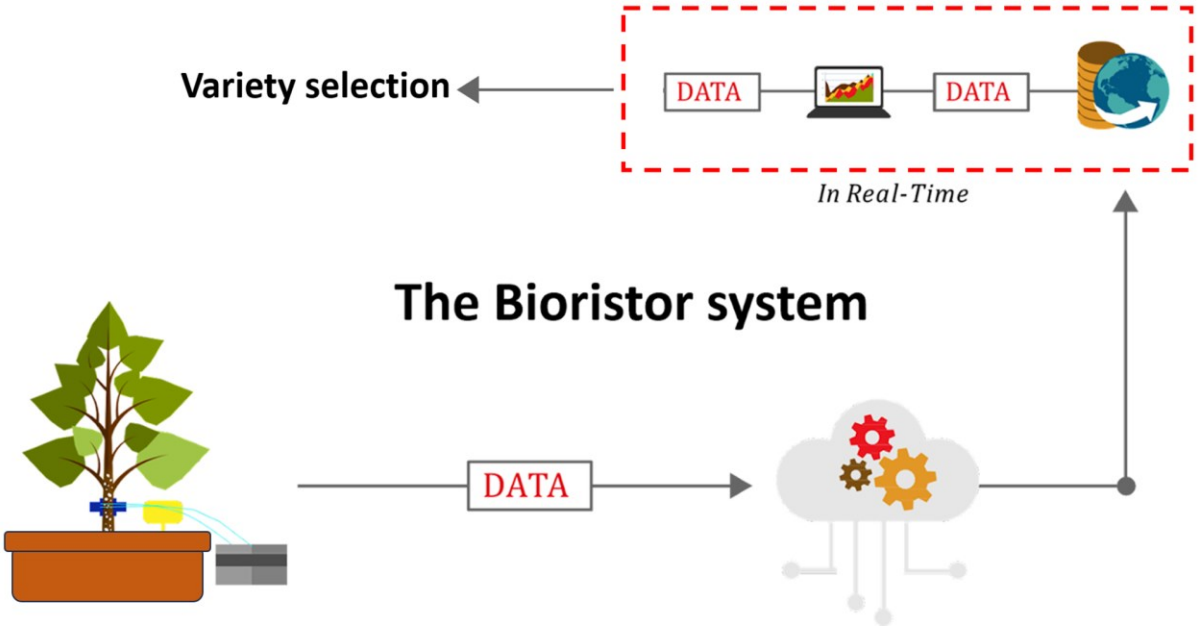

Fig. 63 - Bioristor application and data streaming: data are acquired by the readout system directly on-site. Raw data are then sent to the central server and analyzed in real time, the resulting information is used to perform phenotyping.

8. Products of the research

1. Vurro F., Manfredi R., Bettelli M., Bocci G., Cologni A., Cornali S., Reggiani R., Marchetti E., Coppedè N., Caselli S., Zappettini A., Janni M. (2023). Application of in vivo sensing technology to monitor tomato plants in field conditions and optimize crop water management. Precision Agric 24, 2479–2499 https://doi.org/10.1007/s11119-023-10049-1

2. Vurro, F., Marchetti, E., Bettelli, M., Manfrini, L., Finco, A., Sportolaro, C., et al. (2023). Application of the OECT-Based In Vivo Biosensor Bioristor in Fruit Tree Monitoring to Improve Agricultural Sustainability. Chemosensors, 11(7), 374. https://doi.org/10.3390/chemosensors11070374

3. Vurro, F., Croci, M., Impollonia, G., Marchetti, E., Gracia-Romero, A., Bettelli, M., et al. (2023). Field plant monitoring from macro to micro scale: feasibility and validation of combined field monitoring approaches to cope with drought stress in tomato.
   https://doi.org/10.3390/plants12223851

4. Marchetti, E., Palermo, N., Vurro, F., Acién, J. M., Gonzalez, Guzman, M., Cotti, G., Damiano, B., Arbona, V., Beretta, M., Bettelli, M., Marmiroli N., Janni. M., Accelerate phenotyping selection for drought tolerance in tomato through in vivo monitoring of plant sap dynamic changes with bioristor
   (draft under finalization)

9. Bibliography

Abbass K, Qasim MZ, Song H, et al (2022) A review of the global climate change impacts, adaptation, and sustainable mitigation measures. Environ Sci Pollut Res 29:42539–42559. https://doi.org/10.1007/s11356-022-19718-6

Abdelmoneem RM, Benslimane A, Shaaban E (2020) Mobility-aware task scheduling in cloud-Fog IoT-based healthcare architectures. Comput Netw 179:107348. https://doi.org/10.1016/j.comnet.2020.107348

Ahmar S, Gill RA, Jung K-H, et al (2020) Conventional and Molecular Techniques from Simple Breeding to Speed Breeding in Crop Plants: Recent Advances and Future Outlook. Int J Mol Sci 21:2590. https://doi.org/10.3390/ijms21072590

Ahn E, Botkin J, Curtin SJ, Zsögön A (2023) Ideotype breeding and genome engineering for legume crop improvement. Curr Opin Biotechnol 82:102961. https://doi.org/10.1016/j.copbio.2023.102961

Alexopoulos A, Koutras K, Ali SB, et al (2023) Complementary Use of Ground-Based Proximal Sensing and Airborne/Spaceborne Remote Sensing Techniques in Precision Agriculture: A Systematic Review. Agronomy 13:1942. https://doi.org/10.3390/agronomy13071942

Alfian G, Syafrudin M, Farooq U, et al (2020) Improving efficiency of RFID-based traceability system for perishable food by utilizing IoT sensors and machine learning model. Food Control 110:107016. https://doi.org/10.1016/j.foodcont.2019.107016

Altman A, Hasegawa PM (eds) (2012) Front-matter. In: Plant Biotechnology and Agriculture. Academic Press, San Diego, pp i–iii

Al-Yasi H, Attia H, Alamer K, et al (2020) Impact of drought on growth, photosynthesis, osmotic adjustment, and cell wall elasticity in Damask rose. Plant Physiol Biochem 150:133–139. https://doi.org/10.1016/j.plaphy.2020.02.038

Ansar SA, Jaiswal K, Pathak PC, Khan RA (2023) A Step Towards Smart Farming: Unified Role of AI and IoT. In: Shukla PK, Mittal H, Engelbrecht A (eds) Computer Vision and Robotics. Springer Nature, Singapore, pp 557–578

Aqeel-ur-Rehman, Abbasi AZ, Islam N, Shaikh ZA (2014) A review of wireless sensors and networks' applications in agriculture. Comput Stand Interfaces 36:263–270. https://doi.org/10.1016/j.csi.2011.03.004

Aquilani C, Confessore A, Bozzi R, et al (2022) Review: Precision Livestock Farming technologies in

pasture-based livestock systems. Animal 16:100429. https://doi.org/10.1016/j.animal.2021.100429

Atefi A, Ge Y, Pitla S, Schnable J (2021) Robotic Technologies for High-Throughput Plant Phenotyping: Contemporary Reviews and Future Perspectives. Front Plant Sci 12:

Atzori L, Iera A, Morabito G (2010) The Internet of Things: A survey. Comput Netw 54:2787–2805. https://doi.org/10.1016/j.comnet.2010.05.010

Atzori L, Iera A, Morabito G (2014) From "smart objects" to "social objects": The next evolutionary step of the internet of things. IEEE Commun Mag 52:97–105. https://doi.org/10.1109/MCOM.2014.6710070

Azadi H, Keramati P, Taheri F, et al (2018) Agricultural land conversion: Reviewing drought impacts and coping strategies. Int J Disaster Risk Reduct 31:184–195. https://doi.org/10.1016/j.ijdrr.2018.05.003

Bai Y, Lindhout P (2007) Domestication and Breeding of Tomatoes: What have We Gained and What Can We Gain in the Future? Ann Bot 100:1085–1094. https://doi.org/10.1093/aob/mcm150

Bansod B, Singh R, Thakur R, Singhal G (2017) A comparision between satellite based and drone based remote sensing technology to achieve sustainable development: a review. J Agric Environ Int Dev JAEID 111:383–407. https://doi.org/10.12895/jaeid.20172.690

Barbedo JGA (2023) A review on the combination of deep learning techniques with proximal hyperspectral images in agriculture. Comput Electron Agric 210:107920. https://doi.org/10.1016/j.compag.2023.107920

Bargigia I, Savagian LR, Österholm AM, et al (2021) Charge-Transfer Intermediates in the Electrochemical Doping Mechanism of Conjugated Polymers. J Am Chem Soc 143:294–308. https://doi.org/10.1021/jacs.0c10692

Baxter I (2009) Ionomics: studying the social network of mineral nutrients. Curr Opin Plant Biol 12:381–386. https://doi.org/10.1016/j.pbi.2009.05.002

Bayılmış C, Ebleme MA, Çavuşoğlu Ü, et al (2022) A survey on communication protocols and performance evaluations for Internet of Things. Digit Commun Netw 8:1094–1104. https://doi.org/10.1016/j.dcan.2022.03.013

Beloev I, Kinaneva D, Georgiev G, et al (2021) Artificial Intelligence-Driven Autonomous Robot for Precision Agriculture. Acta Technol Agric 24:48–54

Berggren M, Crispin X, Fabiano S, et al (2019) Ion Electron–Coupled Functionality in Materials and

Devices Based on Conjugated Polymers. Adv Mater 31:1805813. https://doi.org/10.1002/adma.201805813

Berggren M, Richter-Dahlfors A (2007) Organic Bioelectronics. Adv Mater 19:3201–3213. https://doi.org/10.1002/adma.200700419

Bernacka-Wojcik I, Huerta M, Tybrandt K, et al (2019) Implantable Bioelectronics: Implantable Organic Electronic Ion Pump Enables ABA Hormone Delivery for Control of Stomata in an Intact Tobacco Plant (Small 43/2019). Small 15:1970233. https://doi.org/10.1002/smll.201970233

Bernards DA, Malliaras GG (2007a) Steady-State and Transient Behavior of Organic Electrochemical Transistors. Adv Funct Mater 17:3538–3544. https://doi.org/10.1002/adfm.200601239

Bernards DA, Malliaras GG (2007b) Steady-State and Transient Behavior of Organic Electrochemical Transistors. Adv Funct Mater 17:3538–3544. https://doi.org/10.1002/adfm.200601239

Betts J, Young RP, Hilton-Taylor C, et al (2020) A framework for evaluating the impact of the IUCN Red List of threatened species. Conserv Biol 34:632–643. https://doi.org/10.1111/cobi.13454

Bolger A, Scossa F, Bolger ME, et al (2014) The genome of the stress-tolerant wild tomato species Solanum pennellii. Nat Genet 46:1034–1038. https://doi.org/10.1038/ng.3046

Bolin B, Doos BR (1989) Greenhouse effect

Botta A, Cavallone P, Baglieri L, et al (2022) A Review of Robots, Perception, and Tasks in Precision Agriculture. Appl Mech 3:830–854. https://doi.org/10.3390/applmech3030049

Burton PR, Clayton DG, Cardon LR, et al (2007) Genome-wide association study of 14,000 cases of seven common diseases and 3,000 shared controls. Nature 447:661–678. https://doi.org/10.1038/nature05911

Cammarano D, Van Evert FK, Kempenaar C (eds) (2023) Precision Agriculture: Modelling. Springer International Publishing, Cham

Cano-Gamez E, Trynka G (2020) From GWAS to Function: Using Functional Genomics to Identify the Mechanisms Underlying Complex Diseases. Front Genet 11:

Cappetta E, Andolfo G, Di Matteo A, et al (2020) Accelerating Tomato Breeding by Exploiting Genomic Selection Approaches. Plants 9:1236. https://doi.org/10.3390/plants9091236

Cardellicchio A, Solimani F, Dimauro G, et al (2023) Detection of tomato plant phenotyping traits using YOLOv5-based single stage detectors. Comput Electron Agric 207:107757. https://doi.org/10.1016/j.compag.2023.107757

Carvalho GC, de Camargo BAF, de Araújo JTC, Chorilli M (2021a) Lycopene: From tomato to its nutraceutical use and its association with nanotechnology. Trends Food Sci Technol 118:447–458. https://doi.org/10.1016/j.tifs.2021.10.015

Carvalho LC, Gonçalves EF, Marques da Silva J, Costa JM (2021b) Potential Phenotyping Methodologies to Assess Inter- and Intravarietal Variability and to Select Grapevine Genotypes Tolerant to Abiotic Stress. Front Plant Sci 12:

Causse M, Zhao J, Diouf I, et al (2020) Genomic Designing for Climate-Smart Tomato. In: Kole C (ed) Genomic Designing of Climate-Smart Vegetable Crops. Springer International Publishing, Cham, pp 47–159

Ceccarelli S, Grando S, Maatougui M, et al (2010) Plant breeding and climate changes. J Agric Sci 148:627–637. https://doi.org/10.1017/S0021859610000651

Chaudhary J, Khatri P, Singla P, et al (2019) Advances in Omics Approaches for Abiotic Stress Tolerance in Tomato. Biology 8:90. https://doi.org/10.3390/biology8040090

Chaudhary P, Sharma A, Singh B, Nagpal AK (2018) Bioactivities of phytochemicals present in tomato. J Food Sci Technol 55:2833–2849. https://doi.org/10.1007/s13197-018-3221-z

Chawade A, Van Ham J, Blomquist H, et al (2019) High-Throughput Field-Phenotyping Tools for Plant Breeding and Precision Agriculture. Agronomy 9:258. https://doi.org/10.3390/agronomy9050258

Contardi UA, Morikawa M, Brunelli B, Thomaz DV (2021) MAX30102 Photometric Biosensor Coupled to ESP32-Webserver Capabilities for Continuous Point of Care Oxygen Saturation and Heartrate Monitoring. Eng Proc 16:9. https://doi.org/10.3390/IECB2022-11114

Conti V, Romi M, Parri S, et al (2021) Morpho-Physiological Classification of Italian Tomato Cultivars (Solanum lycopersicum L.) According to Drought Tolerance during Vegetative and Reproductive Growth. Plants 10:1826. https://doi.org/10.3390/plants10091826

Coppedè N, Janni M, Bettelli M, et al (2017) An in vivo biosensing, biomimetic electrochemical transistor with applications in plant science and precision farming. Sci Rep 7:16195. https://doi.org/10.1038/s41598-017-16217-4

Coppedè N, Tarabella G, Villani M, et al (2014) Human stress monitoring through an organic cotton-fiber biosensor. J Mater Chem B 2:5620–5626. https://doi.org/10.1039/C4TB00317A

Çorak BH, Okay FY, Güzel M, et al (2018) Comparative Analysis of IoT Communication Protocols. In: 2018 International Symposium on Networks, Computers and Communications (ISNCC). pp 1–6

Costa JM, Heuvelink E (2018) The global tomato industry. Tomatoes 1–26.

https://doi.org/10.1079/9781780641935.0001

Costa JM, Marques da Silva J, Pinheiro C, et al (2019) Opportunities and Limitations of Crop Phenotyping in Southern European Countries. Front Plant Sci 10:

Coulibaly S, Kamsu-Foguem B, Kamissoko D, Traore D (2022) Deep learning for precision agriculture: A bibliometric analysis. Intell Syst Appl 16:200102. https://doi.org/10.1016/j.iswa.2022.200102

Curtis OF (1926) What Is the Significance of Transpiration? Science 63:267–271. https://doi.org/10.1126/science.63.1628.267

Danton A, Roux J-C, Dance B, et al (2020) Development of a spraying robot for precision agriculture: An edge following approach. In: 2020 IEEE Conference on Control Technology and Applications (CCTA). pp 267–272

Davies WJ, Kudoyarova G, Hartung W (2005) Long-distance ABA Signaling and Its Relation to Other Signaling Pathways in the Detection of Soil Drying and the Mediation of the Plant's Response to Drought. J Plant Growth Regul 24:285–295. https://doi.org/10.1007/s00344-005-0103-1

de Menezes de Assis Gomes M, do Nascimento Siqueira L, Ferraz TM, et al (2023) Does abscisic acid and xylem sap pH regulate stomatal responses in papaya plants submitted to partial root-zone drying? Theor Exp Plant Physiol 35:185–197. https://doi.org/10.1007/s40626-023-00275-3

Deegan RD, Bakajin O, Dupont TF, et al (2000) Contact line deposits in an evaporating drop. Phys Rev E 62:756–765. https://doi.org/10.1103/PhysRevE.62.756

Dhanaraju M, Chenniappan P, Ramalingam K, et al (2022) Smart Farming: Internet of Things (IoT)-Based Sustainable Agriculture. Agriculture 12:1745. https://doi.org/10.3390/agriculture12101745

Dhondt S, Wuyts N, Inzé D (2013) Cell to whole-plant phenotyping: the best is yet to come. Trends Plant Sci 18:428–439. https://doi.org/10.1016/j.tplants.2013.04.008

Dimitriev OP, Grinko DA, Noskov YuV, et al (2009) PEDOT:PSS films—Effect of organic solvent additives and annealing on the film conductivity. Synth Met 159:2237–2239. https://doi.org/10.1016/j.synthmet.2009.08.022

Dix MJ, Aubrey DP (2021) Calibration approach and range of observed sap flow influences transpiration estimates from thermal dissipation sensors. Agric For Meteorol 307:108534. https://doi.org/10.1016/j.agrformet.2021.108534

Dobriyal P, Qureshi A, Badola R, Hussain SA (2012) A review of the methods available for estimating soil moisture and its implications for water resource management. J Hydrol 458–459:110–117. https://doi.org/10.1016/j.jhydrol.2012.06.021

Doebley JF, Gaut BS, Smith BD (2006) The Molecular Genetics of Crop Domestication. Cell 127:1309–1321. https://doi.org/10.1016/j.cell.2006.12.006

Enciso J, Avila CA, Jung J, et al (2019) Validation of agronomic UAV and field measurements for tomato varieties. Comput Electron Agric 158:278–283. https://doi.org/10.1016/j.compag.2019.02.011

Eshed Y, Zamir D (1995) An introgression line population of Lycopersicon pennellii in the cultivated tomato enables the identification and fine mapping of yield-associated QTL. Genetics 141:1147–1162. https://doi.org/10.1093/genetics/141.3.1147

FAO (2022a) FAO Strategy on Climate Change 2022–2031

FAO (2015) Climate change and food security: risks and responses

FAO (2022b) Tomato production in 2020. https://www.fao.org/faostat/en/#data/QCL. Accessed 12 Oct 2023

FAO (2009) HLEF2050_Global_Agriculture.pdf. https://www.fao.org/fileadmin/templates/wsfs/docs/Issues_papers/HLEF2050_Global_Agriculture.pdf. Accessed 31 Oct 2023

FAOSTAT (2010) Tomato | Land & Water | Food and Agriculture Organization of the United Nations | Land & Water | Food and Agriculture Organization of the United Nations. https://www.fao.org/land-water/databases-and-software/crop-information/tomato/en/. Accessed 22 Aug 2023

Farinon B, Picarella ME, Siligato F, et al (2022) Phenotypic and Genotypic Diversity of the Tomato Germplasm From the Lazio Region in Central Italy, With a Focus on Landrace Distinctiveness. Front Plant Sci 13:

Farooq MS, Riaz S, Abid A, et al (2020) Role of IoT Technology in Agriculture: A Systematic Literature Review. Electronics 9:319. https://doi.org/10.3390/electronics9020319

Fiorani F, Schurr U (2013) Future Scenarios for Plant Phenotyping. Annu Rev Plant Biol 64:267–291. https://doi.org/10.1146/annurev-arplant-050312-120137

Frary A, Doganlar S (2003) Comparative Genetics of Crop Plant Domestication and Evolution. Turk J Agric For 27:59–69. https://doi.org/-

Friedlein JT, Donahue MJ, Shaheen SE, et al (2016) Microsecond Response in Organic Electrochemical Transistors: Exceeding the Ionic Speed Limit. Adv Mater 28:8398–8404. https://doi.org/10.1002/adma.201602684

Fullana-Pericàs M, Conesa MÀ, Gago J, et al (2022) High-throughput phenotyping of a large tomato collection under water deficit: Combining UAVs' remote sensing with conventional leaf-level physiologic and agronomic measurements. Agric Water Manag 260:107283. https://doi.org/10.1016/j.agwat.2021.107283

Gamache KR, Giardino JR, Regmi NR, Vitek JD (2015) Chapter 12 - The Impact of Glacial Geomorphology on Critical Zone Processes. In: Giardino JR, Houser C (eds) Developments in Earth Surface Processes. Elsevier, pp 363–395

Garrett CGB, Brattain WH (1955) Physical Theory of Semiconductor Surfaces. Phys Rev 99:376–387. https://doi.org/10.1103/PhysRev.99.376

Gay C, Estrada F, Conde C, et al (2006) Potential Impacts of Climate Change on Agriculture: A Case of Study of Coffee Production in Veracruz, Mexico. Clim Change 79:259–288. https://doi.org/10.1007/s10584-006-9066-x

GCB (2023) The critical annual update revealing the latest trends in global carbon emissions. In: Glob. Carbon Budg. https://globalcarbonbudget.org. Accessed 4 Feb 2024

Gentile F, Vurro F, Janni M, et al (2022) A Biomimetic, Biocompatible OECT Sensor for the Real-Time Measurement of Concentration and Saturation of Ions in Plant Sap. Adv Electron Mater 8:2200092. https://doi.org/10.1002/aelm.202200092

Gentile F, Vurro F, Picelli F, et al (2020) A mathematical model of OECTs with variable internal geometry. Sens Actuators Phys 304:111894. https://doi.org/10.1016/j.sna.2020.111894

Ghini M, Curreli N, Camellini A, et al (2021) Photodoping of metal oxide nanocrystals for multi-charge accumulation and light-driven energy storage. Nanoscale 13:8773–8783. https://doi.org/10.1039/D0NR09163D

Giordano M, Petropoulos SA, Rouphael Y (2021) Response and Defence Mechanisms of Vegetable Crops against Drought, Heat and Salinity Stress. Agriculture 11:463. https://doi.org/10.3390/agriculture11050463

Giuliani MM, Gatta G, Cappelli G, et al (2019) Identifying the most promising agronomic adaptation strategies for the tomato growing systems in Southern Italy via simulation modeling. Eur J Agron 111:125937. https://doi.org/10.1016/j.eja.2019.125937

Goddard ME, Hayes BJ (2007) Genomic selection. J Anim Breed Genet Z Tierzuchtung Zuchtungsbiologie 124:323–330. https://doi.org/10.1111/j.1439-0388.2007.00702.x

Gosa, Bogale, Moschelion (2022) Diurnal stomatal apertures and density ratios affect whole-canopy

stomatal 2 conductance, water-use efficiency and yield. https://www.plant-ditech.com/images/pdf/Gosa%20et%20al%202022,%20bioRxiv.pdf. Accessed 20 Oct 2023

Gowdy J (2020) Our hunter-gatherer future: Climate change, agriculture and uncivilization. Futures 115:102488. https://doi.org/10.1016/j.futures.2019.102488

Grisso R, Thomason W, Holshouser D, Roberson GT (2011) Precision Farming Tools: Variable-Rate Application

Groenendaal L, Jonas F, Freitag D, et al (2000) Poly(3,4-ethylenedioxythiophene) and Its Derivatives: Past, Present, and Future. Adv Mater 12:481–494. https://doi.org/10.1002/(SICI)1521-4095(200004)12:7<481::AID-ADMA481>3.0.CO;2-C

Grossiord C, Buckley TN, Cernusak LA, et al (2020) Plant responses to rising vapor pressure deficit. New Phytol 226:1550–1566. https://doi.org/10.1111/nph.16485

Großkinsky DK, Svensgaard J, Christensen S, Roitsch T (2015) Plant phenomics and the need for physiological phenotyping across scales to narrow the genotype-to-phenotype knowledge gap. J Exp Bot 66:5429–5440. https://doi.org/10.1093/jxb/erv345

Gur A, Zamir D (2004) Unused Natural Variation Can Lift Yield Barriers in Plant Breeding. PLOS Biol 2:e245. https://doi.org/10.1371/journal.pbio.0020245

Habibullah MS, Din BH, Tan S-H, Zahid H (2022) Impact of climate change on biodiversity loss: global evidence. Environ Sci Pollut Res 29:1073–1086. https://doi.org/10.1007/s11356-021-15702-8

Hasan N, Choudhary S, Naaz N, et al (2021) Recent advancements in molecular marker-assisted selection and applications in plant breeding programmes. J Genet Eng Biotechnol 19:128. https://doi.org/10.1186/s43141-021-00231-1

Hasanagić D, Koleška I, Kojić D, et al (2020) Long term drought effects on tomato leaves: anatomical, gas exchange and antioxidant modifications. Acta Physiol Plant 42:121. https://doi.org/10.1007/s11738-020-03114-z

Haworth M, Marino G, Atzori G, et al (2023) Plant Physiological Analysis to Overcome Limitations to Plant Phenotyping. Plants 12:4015. https://doi.org/10.3390/plants12234015

He Y, A. Kukhta N, Marks A, K. Luscombe C (2022) The effect of side chain engineering on conjugated polymers in organic electrochemical transistors for bioelectronic applications. J Mater Chem C 10:2314–2332. https://doi.org/10.1039/D1TC05229B

Heslot N, Jannink J-L, Sorrells ME (2015) Perspectives for Genomic Selection Applications and Research in Plants. Crop Sci 55:1–12. https://doi.org/10.2135/cropsci2014.03.0249

Holme P, Rocha JC (2023) Networks of climate change: connecting causes and consequences. Appl Netw Sci 8:10. https://doi.org/10.1007/s41109-023-00536-9

Horii T, Li Y, Mori Y, Okuzaki H (2015) Correlation between the hierarchical structure and electrical conductivity of PEDOT/PSS. Polym J 47:695–699. https://doi.org/10.1038/pj.2015.48

Hosseini SZ, Ismaili A, Nazarian-Firouzabadi F, et al (2021) Dissecting the molecular responses of lentil to individual and combined drought and heat stresses by comparative transcriptomic analysis. Genomics 113:693–705. https://doi.org/10.1016/j.ygeno.2020.12.038

Hu D, Zhang W, Zhang Y, et al (2019) Reconstituting the genome of a young allopolyploid crop, Brassica napus, with its related species. Plant Biotechnol J 17:1106–1118. https://doi.org/10.1111/pbi.13041

Huang X-Y, Salt DE (2016) Plant Ionomics: From Elemental Profiling to Environmental Adaptation. Mol Plant 9:787–797. https://doi.org/10.1016/j.molp.2016.05.003

Iberdrola (2024) A smart farm.pdf. In: Iberdrolacom Smart-Farming-Precis.-Agric. https://www.iberdrola.com/documents/20125/40267/Infographic_SmartFarming.pdf/aed36b03-d538-0b0b-d2c4-c79e5f978bd3?t=1627038507160. Accessed 28 Jan 2024

Ilakiya T, Premalakshmi V, Arumugam T, Sivakumar T (2022) Variability analysis in tomato (Solanum lycopersicum L.) crosses under drought stress. J Appl Nat Sci 14:49–52. https://doi.org/10.31018/jans.v14iSI.3564

Ilyas M, Nisar M, Khan N, et al (2021) Drought Tolerance Strategies in Plants: A Mechanistic Approach. J Plant Growth Regul 40:926–944. https://doi.org/10.1007/s00344-020-10174-5

Impollonia G, Croci M, Ferrarini A (2022) Remote Sensing | Free Full-Text | UAV Remote Sensing for High-Throughput Phenotyping and for Yield Prediction of Miscanthus by Machine Learning Techniques. https://www.mdpi.com/2072-4292/14/12/2927. Accessed 29 Aug 2023

Islam A, Islam MS (2013) Electro-deposition Method for Platinum Nano- particles Synthesis. Eng Int 1:

Islam S, Hassan L, Hossain MA (2021) Breeding Potential of Some Exotic Tomato Lines: A Combined Study of Morphological Variability, Genetic Divergence, and Association of Traits. Phyton 91:97–114. https://doi.org/10.32604/phyton.2022.017251

IUCN (2023) The IUCN Red List of Threatened Species. In: IUCN Red List Threat. Species. https://www.iucnredlist.org/en. Accessed 3 Feb 2024

IUCN (2021) 1630480997-IUCN_RED_LIST_QUADRENNIAL_REPORT_2017-2020.pdf. https://nc.iucnredlist.org/redlist/resources/files/1630480997-

IUCN_RED_LIST_QUADRENNIAL_REPORT_2017-2020.pdf. Accessed 3 Feb 2024

Jaiswal AK, Mengiste TD, Myers JR, et al (2020) Tomato Domestication Attenuated Responsiveness to a Beneficial Soil Microbe for Plant Growth Promotion and Induction of Systemic Resistance to Foliar Pathogens. Front Microbiol 11:

Janni M, Claudia C, Federico B, et al (2021) Real-time monitoring of Arundo donax response to saline stress through the application of in vivo sensing technology. Sci Rep 11:18598. https://doi.org/10.1038/s41598-021-97872-6

Janni M, Coppede N, Bettelli M, et al (2019) In Vivo Phenotyping for the Early Detection of Drought Stress in Tomato. Plant Phenomics 2019:. https://doi.org/10.34133/2019/6168209

Janni M, Pieruschka R (2022) Plant phenotyping for a sustainable future. J Exp Bot 73:5085–5088. https://doi.org/10.1093/jxb/erac286

Jindo K, Evenhuis A, Kempenaar C, et al (2021) Review: Holistic pest management against early blight disease towards sustainable agriculture. Pest Manag Sci 77:3871–3880. https://doi.org/10.1002/ps.6320

Jócsák I, Végvári G, Vozáry E (2019) Electrical impedance measurement on plants: a review with some insights to other fields. Theor Exp Plant Physiol 31:359–375. https://doi.org/10.1007/s40626-019-00152-y

Johansen K, Morton MJL, Malbeteau Y, et al (2020) Predicting Biomass and Yield in a Tomato Phenotyping Experiment Using UAV Imagery and Random Forest. Front Artif Intell 3:

Johnsson A (2015) Oscillations in Plant Transpiration. In: Mancuso S, Shabala S (eds) Rhythms in Plants: Dynamic Responses in a Dynamic Environment. Springer International Publishing, Cham, pp 157–188

Kaliyaraj Selva Kumar A, Zhang Y, Li D, Compton RG (2020) A mini-review: How reliable is the drop casting technique? Electrochem Commun 121:106867. https://doi.org/10.1016/j.elecom.2020.106867

Kalyani Y, Collier R (2021) A Systematic Survey on the Role of Cloud, Fog, and Edge Computing Combination in Smart Agriculture. Sensors 21:5922. https://doi.org/10.3390/s21175922

Kar P (2013) Doping in Conjugated Polymers. John Wiley & Sons

Karami Z, Soleimani-Gorgan A, Vakili-Nezhaad GR, Roghabadi FA (2022) A layer-by-layer green inkjet printing methodology for developing indium tin oxide (ITO)-based transparent and conductive nanofilms. J Clean Prod 379:134455. https://doi.org/10.1016/j.jclepro.2022.134455

Kassim MRM (2020) IoT Applications in Smart Agriculture: Issues and Challenges. In: 2020 IEEE Conference on Open Systems (ICOS). pp 19–24

Keene ST, Fogarty D, Cooke R, et al (2019) Wearable Organic Electrochemical Transistor Patch for Multiplexed Sensing of Calcium and Ammonium Ions from Human Perspiration. Adv Healthc Mater 8:1901321. https://doi.org/10.1002/adhm.201901321

Kemp L, Xu C, Depledge J, et al (2022) Climate Endgame: Exploring catastrophic climate change scenarios. Proc Natl Acad Sci 119:e2108146119. https://doi.org/10.1073/pnas.2108146119

Khodagholy D, Rivnay J, Sessolo M, et al (2013) High transconductance organic electrochemical transistors. Nat Commun 4:2133. https://doi.org/10.1038/ncomms3133

Kim N, Petsagkourakis I, Chen S, et al (2019a) Electric Transport Properties in PEDOT Thin Films. In: Reynolds JR, Thompson BC, Skotheim TA (eds) Conjugated Polymers, 4th edn. CRC Press, pp 45–128

Kim T, Park S, Seo J, et al (2019b) Highly conductive PEDOT:PSS with enhanced chemical stability. Org Electron 74:77–81. https://doi.org/10.1016/j.orgel.2019.06.033

Knutti R, Rugenstein MAA (2015) Feedbacks, climate sensitivity and the limits of linear models. Philos Trans R Soc Math Phys Eng Sci 373:20150146. https://doi.org/10.1098/rsta.2015.0146

Kohli A, Frenken K, Spottorno C Disambiguation of water use statistics

Krishna KR (2017) Push Button Agriculture: Robotics, Drones, Satellite-Guided Soil and Crop Management. Apple Academic Press, New York

Kumar D, Kushwaha S, Delvento C, et al (2020) Affordable Phenotyping of Winter Wheat under Field and Controlled Conditions for Drought Tolerance. Agronomy 10:882. https://doi.org/10.3390/agronomy10060882

Kumar R, Hosseinzadehtaher M, Hein N, et al (2022) Challenges and advances in measuring sap flow in agriculture and agroforestry: A review with focus on nuclear magnetic resonance. Front Plant Sci 13:

Landi S, Punzo P, Nurcato R, et al (2023) Transcriptomic landscape of tomato traditional long shelf-life landraces under low water regimes. Plant Physiol Biochem 201:107877. https://doi.org/10.1016/j.plaphy.2023.107877

Lange AF, Peake J (2020) Precision Agriculture. In: Morton YTJ, Diggelen F, Spilker JJ, et al. (eds) Position, Navigation, and Timing Technologies in the 21st Century, 1st edn. Wiley, pp 1735–1747

Lenaerts B, Collard BCY, Demont M (2019) Review: Improving global food security through accelerated plant breeding. Plant Sci 287:110207. https://doi.org/10.1016/j.plantsci.2019.110207

Li L, Zhang Q, Huang D (2014) A Review of Imaging Techniques for Plant Phenotyping. Sensors 14:20078–20111. https://doi.org/10.3390/s141120078

Li Z, Creemers L, Zhang X (2022) Regenerative Medicine for Cartilage and Joint Repair. Frontiers Media SA

Liao J, Si H, Zhang X, Lin S (2019) Functional Sensing Interfaces of PEDOT:PSS Organic Electrochemical Transistors for Chemical and Biological Sensors: A Mini Review. Sensors 19:218. https://doi.org/10.3390/s19020218

Lifewire (2022) Is There a Limit to How Many Devices Can Connect to a Wi- Fi Network? In: Lifewire. https://www.lifewire.com/how-many-devices-can-share-a-wifi-network-818298. Accessed 22 Oct 2023

Liu W-C, Song R-F, Zheng S-Q, et al (2022) Coordination of plant growth and abiotic stress responses by tryptophan synthase β subunit 1 through modulation of tryptophan and ABA homeostasis in Arabidopsis. Mol Plant 15:973–990. https://doi.org/10.1016/j.molp.2022.04.009

Lu Y, Wang J-Y, Pei J (2021) Achieving Efficient n-Doping of Conjugated Polymers by Molecular Dopants. Acc Chem Res 54:2871–2883. https://doi.org/10.1021/acs.accounts.1c00223

Mahmud MSA, Abidin MSZ, Emmanuel AA, Hasan HS (2020) Robotics and Automation in Agriculture: Present and Future Applications. Appl Model Simul 4:130–140

Manfredi R, Vurro F, Janni M, et al (2023) Long-Term Stability in Electronic Properties of Textile Organic Electrochemical Transistors for Integrated Applications. Materials 16:1861. https://doi.org/10.3390/ma16051861

Marquez AV, McEvoy N, Pakdel A (2020) Organic Electrochemical Transistors (OECTs) Toward Flexible and Wearable Bioelectronics. Molecules 25:5288. https://doi.org/10.3390/molecules25225288

Mata-Nicolás E, Montero-Pau J, Gimeno-Paez E, et al (2020) Exploiting the diversity of tomato: the development of a phenotypically and genetically detailed germplasm collection. Hortic Res 7:66. https://doi.org/10.1038/s41438-020-0291-7

Meena A, Meena R, Meena A (2019) Use of Precision Agriculture for Sustainability and Environmental Protection. pp 1–22

Montanaro G, Dichio B, Xiloyannis C, Lang A (2012) Fruit transpiration in kiwifruit: environmental

drivers and predictive model. AoB PLANTS 2012:pls036. https://doi.org/10.1093/aobpla/pls036

Morice (2021) An Updated Assessment of Near-Surface Temperature Change From 1850: The HadCRUT5 Data Set. In: J. Geophys. Res. Atmospheres - Wiley Online Libr. https://agupubs.onlinelibrary.wiley.com/doi/full/10.1029/2019JD032361. Accessed 4 Feb 2024

Morisse M, Wells DM, Millet EJ, et al (2022) A European perspective on opportunities and demands for field-based crop phenotyping. Field Crops Res 276:108371. https://doi.org/10.1016/j.fcr.2021.108371

Moudgil A, Leong WL (2023) Highly Sensitive Transistor Sensor for Biochemical Sensing and Health Monitoring Applications: A Review. IEEE Sens J 23:8028–8041. https://doi.org/10.1109/JSEN.2023.3253841

Nankar AN, Tringovska I, Grozeva S, et al (2020) Tomato Phenotypic Diversity Determined by Combined Approaches of Conventional and High-Throughput Tomato Analyzer Phenotyping. Plants 9:197. https://doi.org/10.3390/plants9020197

Nelson CH (2021) Climate Change Patterns. In: Nelson CH (ed) Witness To A Changing Earth: A Geologist's Journey Learning About Natural and Human-caused Global Change. Springer International Publishing, Cham, pp 175–221

Nguyen N-T (2012) Chapter 4 - Fabrication technologies. In: Nguyen N-T (ed) Micromixers (Second Edition). William Andrew Publishing, Oxford, pp 113–161

Nikolou M, Malliaras GG (2008) Applications of poly(3,4-ethylenedioxythiophene) doped with poly(styrene sulfonic acid) transistors in chemical and biological sensors. Chem Rec 8:13–22. https://doi.org/10.1002/tcr.20133

NOAA (2021) Climate change impacts. https://www.noaa.gov/education/resource-collections/climate/climate-change-impacts. Accessed 9 Aug 2023

Nowak B (2021) Precision Agriculture: Where do We Stand? A Review of the Adoption of Precision Agriculture Technologies on Field Crops Farms in Developed Countries. Agric Res 10:515–522. https://doi.org/10.1007/s40003-021-00539-x

Ohayon D, Druet V, Inal S (2023) A guide for the characterization of organic electrochemical transistors and channel materials. Chem Soc Rev 52:1001–1023. https://doi.org/10.1039/D2CS00920J

OI Pomodoro da Industria Nord Italia OI Pomodoro da Industria Nord Italia. In: OI Pomodoro. https://oipomodoronorditalia.it/chi-siamo/. Accessed 14 Oct 2023

Ozeki K, Miyazawa Y, Sugiura D (2022) Rapid stomatal closure contributes to higher water use efficiency

in major C4 compared to C3 Poaceae crops. Plant Physiol 189:188–203. https://doi.org/10.1093/plphys/kiac040

Pagliarani C, Casolo V, Ashofteh Beiragi M, et al (2019) Priming xylem for stress recovery depends on coordinated activity of sugar metabolic pathways and changes in xylem sap pH. Plant Cell Environ 42:1775–1787. https://doi.org/10.1111/pce.13533

Pessoa HP, Dariva FD, Copati MGF, et al (2023) Uncovering tomato candidate genes associated with drought tolerance using Solanum pennellii introgression lines. PLOS ONE 18:e0287178. https://doi.org/10.1371/journal.pone.0287178

Pessoa HP, Rocha JR do AS de C, Alves FM, et al (2022) Multi-trait selection of tomato introgression lines under drought-induced conditions at germination and seedling stages. Acta Sci Agron 44:e55876. https://doi.org/10.4025/actasciagron.v44i1.55876

Pignone D, De Paola D, Rapanà N, Janni M (2015) Single seed descent: a tool to exploit durum wheat (Triticum durum Desf.) genetic resources. Genet Resour Crop Evol 62:1029–1035. https://doi.org/10.1007/s10722-014-0206-2

Pignone D, Hammer K (2013) Conservation, Evaluation, and Utilization of Biodiversity. In: Kole C (ed) Genomics and Breeding for Climate-Resilient Crops: Vol. 1 Concepts and Strategies. Springer, Berlin, Heidelberg, pp 9–26

Poonia A, Lakshmi D, Garg T, Vishnuvarthanan G (2023) A Comprehensive Study on Smart Farming for Transforming Agriculture Through Cloud and IoT. In: Convergence of Cloud Computing, AI, and Agricultural Science. IGI Global, pp 67–99

Powder KE (2020) Quantitative Trait Loci (QTL) Mapping. Methods Mol Biol Clifton NJ 2082:211–229. https://doi.org/10.1007/978-1-0716-0026-9_15

Prakash S (2021) IMPACT OF CLIMATE CHANGE ON AQUATIC ECOSYSTEM AND ITS BIODIVERSITY: AN OVERVIEW. Int J Biol Innov 03: https://doi.org/10.46505/IJBI.2021.3210

Purugganan MD (2019) Evolutionary Insights into the Nature of Plant Domestication. Curr Biol 29:R705–R714. https://doi.org/10.1016/j.cub.2019.05.053

Raj M, Gupta S, Chamola V, et al (2021) A survey on the role of Internet of Things for adopting and promoting Agriculture 4.0. J Netw Comput Appl 187:103107. https://doi.org/10.1016/j.jnca.2021.103107

Ranghetti L, Boschetti M, Nutini F, Busetto L (2020) “sen2r”: An R toolbox for automatically

downloading and preprocessing Sentinel-2 satellite data. Comput Geosci 139:104473. https://doi.org/10.1016/j.cageo.2020.104473

Rayhana R, Xiao G, Liu Z (2021) RFID Sensing Technologies for Smart Agriculture. IEEE Instrum Meas Mag 24:50–60. https://doi.org/10.1109/MIM.2021.9436094

Raza A, Razzaq A, Mehmood SS, et al (2019) Impact of Climate Change on Crops Adaptation and Strategies to Tackle Its Outcome: A Review. Plants 8:34. https://doi.org/10.3390/plants8020034

Rebetzke GJ, Jimenez-Berni J, Fischer RA, et al (2019) Review: High-throughput phenotyping to enhance the use of crop genetic resources. Plant Sci 282:40–48. https://doi.org/10.1016/j.plantsci.2018.06.017

Reynolds M, Atkin OK, Bennett M, et al (2021) Addressing Research Bottlenecks to Crop Productivity. Trends Plant Sci 26:607–630. https://doi.org/10.1016/j.tplants.2021.03.011

Rindos D (2013) The Origins of Agriculture: An Evolutionary Perspective. Academic Press

Ritchie H, Rosado P, Roser M (2022) Crop Yields. Our World Data

Ritchie H, Roser M (2017) Water Use and Stress. Our World Data

Rivnay J, Inal S, Salleo A, et al (2018) Organic electrochemical transistors. Nat Rev Mater 3:17086. https://doi.org/10.1038/natrevmats.2017.86

Romero P, Navarro JM, Ordaz PB (2022) Towards a sustainable viticulture: The combination of deficit irrigation strategies and agroecological practices in Mediterranean vineyards. A review and update. Agric Water Manag 259:107216. https://doi.org/10.1016/j.agwat.2021.107216

Rossi F, Manfrini L, Venturi M, et al (2022) Fruit transpiration drives interspecific variability in fruit growth strategies. Hortic Res 9:uhac036. https://doi.org/10.1093/hr/uhac036

Sadeghi-Tehran P, Sabermanesh K, Virlet N, Hawkesford M (2017) Automated Method to Determine Two Critical Growth Stages of Wheat: Heading and Flowering. Front Plant Sci 8:. https://doi.org/10.3389/fpls.2017.00252

Samantara K, Bohra A, Mohapatra SR, et al (2022) Breeding More Crops in Less Time: A Perspective on Speed Breeding. Biology 11:275. https://doi.org/10.3390/biology11020275

Sardaro MLS, Marmiroli M, Maestri E, Marmiroli N (2013) Genetic characterization of Italian tomato varieties and their traceability in tomato food products. Food Sci Nutr 1:54–62. https://doi.org/10.1002/fsn3.8

Sarić R, Nguyen VD, Burge T, et al (2022) Applications of hyperspectral imaging in plant phenotyping.

Trends Plant Sci 27:301–315. https://doi.org/10.1016/j.tplants.2021.12.003

Schaart JG, Van De Wiel CCM, Lotz LAP, Smulders MJM (2016) Opportunities for Products of New Plant Breeding Techniques. Trends Plant Sci 21:438–449. https://doi.org/10.1016/j.tplants.2015.11.006

Shafique K, Khawaja BA, Sabir F, et al (2020) Internet of Things (IoT) for Next-Generation Smart Systems: A Review of Current Challenges, Future Trends and Prospects for Emerging 5G-IoT Scenarios. IEEE Access 8:23022–23040. https://doi.org/10.1109/ACCESS.2020.2970118

Shamim F, Saqlan SM, Athar H-U-R, Waheed A (2014) SCREENING AND SELECTION OF TOMATO GENOTYPES/CULTIVARS FOR DROUGHT TOLERANCE USING MULTIVARIATE ANALYSIS

Sharma B, Molden D, Cook S (2015) Water use efficiency in agriculture: Measurement, current situation and trends

Shi H, Liu C, Jiang Q, Xu J (2015) Effective Approaches to Improve the Electrical Conductivity of PEDOT:PSS: A Review. Adv Electron Mater 1:1500017. https://doi.org/10.1002/aelm.201500017

Sikimić M, Amović M, Vujović V, et al (2020) An Overview of Wireless Technologies for IoT Network. In: 2020 19th International Symposium INFOTEH-JAHORINA (INFOTEH). pp 1–6

Simon DT, Gabrielsson EO, Tybrandt K, Berggren M (2016) Organic Bioelectronics: Bridging the Signaling Gap between Biology and Technology. Chem Rev 116:13009–13041. https://doi.org/10.1021/acs.chemrev.6b00146

Singh M, Vermaa A, Kumar V (2023) Chapter 3 - Geospatial technologies for the management of pest and disease in crops. In: Zaman Q (ed) Precision Agriculture. Academic Press, pp 37–54

Sonah H, Deshmukh RK, Sharma A, et al (2011) Genome-Wide Distribution and Organization of Microsatellites in Plants: An Insight into Marker Development in Brachypodium. PLOS ONE 6:e21298. https://doi.org/10.1371/journal.pone.0021298

Song P, Wang J, Guo X, et al (2021) High-throughput phenotyping: Breaking through the bottleneck in future crop breeding. Crop J 9:633–645. https://doi.org/10.1016/j.cj.2021.03.015

Srinivasa Rao K, Hamza Md, Ashok Kumar P, Girija Sravani K (2020) Design and optimization of MEMS based piezoelectric actuator for drug delivery systems. Microsyst Technol 26:1671–1679. https://doi.org/10.1007/s00542-019-04712-9

Stern DI, Kaufmann RK (2014) Anthropogenic and natural causes of climate change. Clim Change

122:257–269. https://doi.org/10.1007/s10584-013-1007-x

Strakosas X, Bongo M, Owens RM (2015) The organic electrochemical transistor for biological applications. J Appl Polym Sci 132:n/a-n/a. https://doi.org/10.1002/app.41735

Sun K, Zhang S, Li P, et al (2015) Review on application of PEDOTs and PEDOT:PSS in energy conversion and storage devices. J Mater Sci Mater Electron 26:4438–4462. https://doi.org/10.1007/s10854-015-2895-5

Swanson SJ, Choi W-G, Chanoca A, Gilroy S (2011) In Vivo Imaging of Ca2+, pH, and Reactive Oxygen Species Using Fluorescent Probes in Plants. Annu Rev Plant Biol 62:273–297. https://doi.org/10.1146/annurev-arplant-042110-103832

Takei H, Shirasawa K, Kuwabara K, et al (2021) De novo genome assembly of two tomato ancestors, Solanum pimpinellifolium and Solanum lycopersicum var. cerasiforme, by long-read sequencing. DNA Res 28:dsaa029. https://doi.org/10.1093/dnares/dsaa029

Tao H, Xu S, Tian Y, et al (2022) Proximal and remote sensing in plant phenomics: 20 years of progress, challenges, and perspectives. Plant Commun 3:100344. https://doi.org/10.1016/j.xplc.2022.100344

Tibbs Cortes L, Zhang Z, Yu J (2021) Status and prospects of genome-wide association studies in plants. Plant Genome 14:e20077. https://doi.org/10.1002/tpg2.20077

Trifilò P, Nardini A, Raimondo F, et al (2011) Ion-mediated compensation for drought-induced loss of xylem hydraulic conductivity in field-growing plants of Laurus nobilis. Funct Plant Biol 38:606. https://doi.org/10.1071/FP10233

Tyagi V, Nagargade M, Singh RK (2020) Agronomic Interventions for Drought Management in Crops. In: Rakshit A, Singh HB, Singh AK, et al. (eds) New Frontiers in Stress Management for Durable Agriculture. Springer Singapore, Singapore, pp 461–476

UNFCCC The Paris Agreement | UNFCCC. https://unfccc.int/process-and-meetings/the-paris-agreement. Accessed 27 Jan 2024a

UNFCCC What is the Kyoto Protocol? | UNFCCC. https://unfccc.int/kyoto_protocol. Accessed 27 Jan 2024b

UNFCCC UN Climate Change Conference - United Arab Emirates | UNFCCC. https://unfccc.int/cop28. Accessed 27 Jan 2024c

Varshney RK, Bohra A, Roorkiwal M, et al (2021) Fast-forward breeding for a food-secure world. Trends Genet 37:1124–1136. https://doi.org/10.1016/j.tig.2021.08.002

Venkateswarlu B, Shanker AK (2009) Climate change and agriculture: Adaptation and mitigation stategies. Clim CHANGE Agric 54:

Voss-Fels KP, Cooper M, Hayes BJ (2019) Accelerating crop genetic gains with genomic selection. Theor Appl Genet 132:669–686. https://doi.org/10.1007/s00122-018-3270-8

Vurro F, Janni M, Coppedè N, et al (2019) Development of an In Vivo Sensor to Monitor the Effects of Vapour Pressure Deficit (VPD) Changes to Improve Water Productivity in Agriculture. Sensors 19:4667. https://doi.org/10.3390/s19214667

Vurro F, Manfredi R, Bettelli M, et al (2023a) In vivo sensing to monitor tomato plants in field conditions and optimize crop water management. Precis Agric. https://doi.org/10.1007/s11119-023-10049-1

Vurro F, Marchetti E, Bettelli M, et al (2023b) Application of the OECT-Based In Vivo Biosensor Bioristor in Fruit Tree Monitoring to Improve Agricultural Sustainability. Chemosensors 11:374. https://doi.org/10.3390/chemosensors11070374

Wang C, Park MJ, Choo YW, et al (2023) Inkjet printing technique for membrane fabrication and modification: A review. Desalination 565:116841. https://doi.org/10.1016/j.desal.2023.116841

Wang T, Zhao R, Zhan K, et al (2021) Preparation of electro-reduced graphene oxide/copper composite foils with simultaneously enhanced thermal and mechanical properties by DC electro-deposition method. Mater Sci Eng A 805:140574. https://doi.org/10.1016/j.msea.2020.140574

Wang Y (2009) Research progress on a novel conductive polymer–poly(3,4-ethylenedioxythiophene) (PEDOT). J Phys Conf Ser 152:012023. https://doi.org/10.1088/1742-6596/152/1/012023

Watt M, Fiorani F, Usadel B, et al (2020) Phenotyping: New Windows into the Plant for Breeders. Annu Rev Plant Biol 71:689–712. https://doi.org/10.1146/annurev-arplant-042916-041124

Wikipedia (2006) File:Band gap comparison.svg - Wikipedia. https://commons.wikimedia.org/wiki/File:Band_gap_comparison.svg. Accessed 12 Jul 2023

Wohlfahrt G, Gu L (2015) The many meanings of gross photosynthesis and their implication for photosynthesis research from leaf to globe. Plant Cell Environ 38:2500–2507. https://doi.org/10.1111/pce.12569

Xiao Q, Bai X, Zhang C, He Y (2022) Advanced high-throughput plant phenotyping techniques for genome-wide association studies: A review. J Adv Res 35:215–230. https://doi.org/10.1016/j.jare.2021.05.002

Xie C, Yang C (2020) A review on plant high-throughput phenotyping traits using UAV-based sensors. Comput Electron Agric 178:105731. https://doi.org/10.1016/j.compag.2020.105731

Xu J, Gu B, Tian G (2022) Review of agricultural IoT technology. Artif Intell Agric 6:10–22. https://doi.org/10.1016/j.aiia.2022.01.001

Xu R, Li C (2022) A Review of High-Throughput Field Phenotyping Systems: Focusing on Ground Robots. Plant Phenomics 2022:. https://doi.org/10.34133/2022/9760269

Xu Y, Liu X, Fu J, et al (2020) Enhancing Genetic Gain through Genomic Selection: From Livestock to Plants. Plant Commun 1:100005. https://doi.org/10.1016/j.xplc.2019.100005

Yadav P, Jaiswal DK, Sinha RK (2021) 7 - Climate change: Impact on agricultural production and sustainable mitigation. In: Singh S, Singh P, Rangabhashiyam S, Srivastava KK (eds) Global Climate Change. Elsevier, pp 151–174

Yao L, van de Zedde R, Kowalchuk G (2021) Recent developments and potential of robotics in plant eco-phenotyping. Emerg Top Life Sci 5:289–300. https://doi.org/10.1042/ETLS20200275

Yolcu S, Alavilli H, Lee B (2020) Natural Genetic Resources from Diverse Plants to Improve Abiotic Stress Tolerance in Plants. Int J Mol Sci 21:8567. https://doi.org/10.3390/ijms21228567

Yong KT, Yong PH, Ng ZX (2023) Tomato and human health: A perspective from post-harvest processing, nutrient bio-accessibility, and pharmacological interaction. Food Front. https://doi.org/10.1002/fft2.299

Yoo CY, Pence HE, Hasegawa PM, Mickelbart MV (2009) Regulation of Transpiration to Improve Crop Water Use. Crit Rev Plant Sci 28:410–431. https://doi.org/10.1080/07352680903173175

Zandalinas SI, Rivero RM, Martínez V, et al (2016) Tolerance of citrus plants to the combination of high temperatures and drought is associated to the increase in transpiration modulated by a reduction in abscisic acid levels. BMC Plant Biol 16:105. https://doi.org/10.1186/s12870-016-0791-7

Zhang Y, Liu J, Singh M, et al (2020a) Superionic Conductivity in Ceria-Based Heterostructure Composites for Low-Temperature Solid Oxide Fuel Cells. Nano-Micro Lett 12:178. https://doi.org/10.1007/s40820-020-00518-x

Zhang Z, Kayacan E, Thompson B, Chowdhary G (2020b) High precision control and deep learning-based corn stand counting algorithms for agricultural robot. Auton Robots 44:1289–1302. https://doi.org/10.1007/s10514-020-09915-y

Coating Technique - an overview | ScienceDirect Topics. https://www.sciencedirect.com/topics/engineering/coating-technique. Accessed 19 Jul 2023

Acknowledgements

I want to thanks the ALSIA Metapontum for funding my PhD and most of all I want to sincerely thanks my family, which always supported me leading to overcome every difficulty. Thanks, it would have been nothing without you! Another big support came from my colleagues, who made fancy and smarter every day.